POLITECNICO DI MILANO

Facoltà di Ingegneria Industriale e dell'Informazione

Corso di Laurea Specialistica in Ingegneria Nucleare

ASYMPTOTIC TIME BEHAVIOUR OF NUCLEAR SYSTEMS: A MONTE CARLO APPROACH

Relatore: PADOVANI Enrico

Correlatore: ZOIA Andrea

Tesi di Laurea di:

EPIFANO Enrica, matricola 787486

Anno Accademico 2013-2014

Ai miei nipotini,

Francesco e Alessia

Abstract

In recent years, concerns about reactor safety have increased the need for computational methods that can provide accurate information about time-evolving scenarios, such as those occurring by design (transients, start-up, etc.) or by accident (rod ejection, for instance). In this respect, the attention has been directed to the Monte Carlo methods, which are very accurate since introduce a minimal amount of approximations. Monte Carlo methods including the time dependence have been recently proposed: the Dynamic Monte Carlo methods, which allow assessing the complete time evolution of the neutron population. However, a non-negligible drawback is that these methods suffer from slow convergence and are very time-consuming. If one is interested in the asymptotic (long time) behaviour of the system, instead of the full time dynamics, a possible solution is to resort to the α-static Monte Carlo method, which is very accurate and less time-consuming than dynamic methods. This latter is the subject of this thesis.

We will show that the α-static Monte Carlo method allows determining the asymptotic time behaviour of the neutron population by transforming the time-dependent Boltzmann equation into an eigenvalue problem (the so called α eigenvalue). The mathematical theory at the basis of this method and the properties of the α-eigenvalue spectrum of the Boltzmann operator

will be explained; in particular, we will show that the asymptotic time behaviour of the neutron population is dominated by the algebraically largest eigenvalue, named the fundamental eigenvalue. Then, we will present a Monte Carlo algorithm to solve the eigenvalue problem.

Finally, we will address the diffusion of neutrons in moderating materials and we will assess the asymptotic time behaviour of the system by using the α-static method. To this aim, during the work of this thesis, we have developed a Monte Carlo α-static code, based on the algorithm proposed, which provides the fundamental eigenvalue α_0 and the associated eigenfunction. We have also developed a dynamic Monte Carlo code, which can be used as reference to assess the time behaviour of the system. Finally, we have developed a deterministic solver, which provides a picture of the entire α-eigenvalue spectrum.

The key results of the simulations performed will be presented with a double aim: to validate the α static methods and to explore some interesting physical properties of moderators.

Sommario

Negli ultimi anni, la crescente attenzione verso la sicurezza dei reattori nucleari ha evidenziato la necessità di metodi computazionali che possano fornire informazioni accurate sulla dinamica degli scenari dipendenti dal tempo, sia quelli previsti *by design* (avvio del reattore, transitori di potenza, etc.) sia quelli incidentali, per esempio l'espulsione di una barra di controllo. In questo contesto, è naturale che l'attenzione si sia rivolta ai metodi Monte Carlo, nei quali le approssimazioni introdotte sono minime e, pertanto, sono molto accurati. Recentemente sono stati proposti dei metodi Monte Carlo che includono la dipendenza dal tempo: i metodi Monte Carlo dinamici, che permettono di stimare l'intera evoluzione temporale della popolazione neutronica. Tuttavia, questi metodi hanno un innegabile svantaggio: è necessario un considerevole tempo di calcolo per ottenere dati statisticamente validi. In alcune situazioni, può capitare che non sia necessario conoscere la dinamica completa del sistema considerato, ma che sia sufficiente il solo comportamento asintotico: in questo caso, una possibile soluzione consiste nel ricorrere al metodo Montecarlo α-statico che, pur essendo molto accurato, richiede tempi di calcolo decisamente inferiori rispetto ai metodi dinamici. Questa tesi è incentrata proprio sul metodo α-statico.

Nel seguito, verrà mostrato come il metodo α-statico, trasformando l'equazione

di Boltzmann dipendente dal tempo in un problema agli autovalori, consenta di trovare il comportamento asintotico nel tempo della popolazione neutronica. Nella tesi verranno descritte la teoria matematica alla base di tale metodo e le proprietà dello spetto degli autovalori α associati all'operatore di Boltzmann; in particolare, verrà dimostrato che il comportamento asintotico della popolazione neutronica è dominato dal più grande tra gli autovalori: l' autovalore fondamentale α_0. Successivamente, presenteremo un algoritmo Monte Carlo per risolvere il problema agli autovalori.

Infine, tratteremo la diffusione dei neutroni nei materiali moderatori e cercheremo il comportamento asintotico del sistema usando il metodo α-statico. A tale scopo, durante questo lavoro di tesi, è stato sviluppato un codice Monte Carlo α-statico, basato sull'algoritmo proposto, capace di trovare l'autovalore fondamentale α_0 e l'autofunzione a questo associata. Abbiamo sviluppato anche un codice Monte Carlo dinamico, il quale fornisce la completa evoluzione temporale del sistema; i dati forniti da questo secondo codice possono essere considerati i risultati di riferimento per valutare la correttezza delle informazioni fornite dal codice α-statico. Infine, abbiamo sviluppato anche un solver deterministico, che fornisce l'intero spetto degli autovalori α. I risultati più importanti delle simulazioni effettuate verranno presentati con un duplice obiettivo: la validazione dei metodi α-statici e lo studio di alcune interessanti proprietà fisiche dei moderatori.

Contents

List of Figures

Chapter 1

Introduction

This thesis represents the final project for the Master of Science program in Nuclear Engineering of the Politecnico di Milano (Italy) and is the result of a six months internship at the Service d'Etudes des Réacteurs et de Mathématiques Appliquées (SERMA) of CEA/Saclay.

The aim of the SERMA is the modelisation of nuclear systems, in particular in the field of reactor physics and radiation shielding. My work has been carried out at the Laboratoire du Transport Stochastique et Déterministe (LTSD), which conceives mathematical and numerical algorithms and develops computer codes aimed at simulating radiation transport. In particular, the LTSD laboratory is in charge of developing the 3-dimensional continuous-energy Monte Carlo code TRIPOLI-4 ®.
Monte Carlo methods allow evaluating neutron and photon flux (i.e, solving the Boltzmann linear transport equation) by simulating the stochastic trajectories of neutrons and photons in phase space.

For historical reasons, also due to the limited computer power available at the time these methods were first introduced, Monte Carlo is mainly adopted to determine the stationary solution of the Boltzmann equation, where the time evolution can be safely neglected (the so called "static" calculations). In particular, in the context of radiation shielding Monte Carlo methods are typically used to solve for fixed-source problems, whereas in reactor physics they are typically used to determine the effective multiplication factor (k_{eff}) of the system and for this reason take the name of *k-static methods*. Generally speaking, Monte Carlo methods are very accurate, because they introduce a minimal amount of approximations, but they suffer from slow convergence and are thus more time-consuming than deterministic methods. In this respect, Monte Carlo simulation is typically adopted for performing reference calculations, against which the results of the faster (but approximated) deterministic solvers are then validated.

In recent years, concerns about reactor safety have increased the need for computational methods that can provide accurate information about time-evolving scenarios, such as those occurring by design (transients, start-up, etc.) or by accident (rod ejection, for instance). In the context of Monte Carlo simulation, current research trends focus on *dynamic methods*, which follow the particles along their time evolution. Unfortunately, these methods demand an even larger computer time than static methods.

An intermediate bridge between static Monte Carlo and dynamic Monte Carlo is represented by the so-called *α-static Monte Carlo*. This method actually allows the prompt and delayed reactor period to be determined by transforming the time-dependent Boltzmann equation into a static eigen-

value problem (the so called α or time eigenvalue). In this respect, α-static methods are ideally suited so as to assess the asymptotic time behaviour of the system.

A Monte Carlo algorithm to find the α-eigenvalue has been recently developed at the LTSD laboratory and implemented in the development version of the TRIPOLI-4 ® code.
The aim of this work is to verify and validate these new methods. The α-static Monte Carlo has been applied to the study of some simple physical systems: the outcomes of Monte Carlo simulations have been compared to reference results, coming either from exact analytical solutions (when available), or from independent numerical codes. By virtue of this analysis, the strengths and the weaknesses of the α-static algorithm have been put in evidence, and an improved understanding of the method has been achieved.

This document is structured in five chapters:

1. In the first chapter, we shall familiarize with:
    - time dependent problems concerning nuclear systems;
    - the time dependent Boltzmann equation and its stationary form;
    - the state-of-art numerical methods to solve the Boltzmann equation.
2. In the second chapter, we shall focus on the α-static methods:
    - the basic mathematical theory;
    - the algorithm implemented in TRIPOLI-4 ®;

- the physical meaning of the fundamental discrete eigenvalue and some issues about its existence.

3. In the third chapter, we shall present some physical systems of interest and we will revisit the knowledge present in literature concerning their time behaviour, i.e. their α-eigenvalues spectrum.

4. In the fourth chapter, we shall show the results of our simulations. In particular, we shall compare the results of the α-static code to those coming from a dynamic Monte Carlo code and a deterministic solver.

5. Finally, in the last chapter, we shall explain our conclusions about the potentialities and the drawbacks of the α-static methods.

Chapter 2

Numerical methods for nuclear systems

In this chapter, we shall introduce the Boltzmann equation governing the time-dependent neutron transport. We shall briefly discuss the numerical methods (deterministic and Monte Carlo) usually adopted to solve the stationary form of this equation. Then, we will address the additional difficulties arising from explicitly considering the time dependence. Finally, we will evaluate the potentialities and the drawbacks of the recently proposed Monte Carlo methods for dealing with time-dependent systems: the dynamic Monte Carlo and the α static Monte Carlo.

2.1 The Boltzmann equation

Consider the statistical behaviour of a large population of neutrons in a bounded domain, under transient or steady state conditions. We define the particle density $n(\vec{r}, v, \hat{\Omega}, t)$ as the average number of neutrons present in

the infinitesimal volume of the six-dimensional *phase space* ($\vec{r} \div \vec{r} + \mathrm{d}\vec{r}, v \div v + \mathrm{d}v, \hat{\Omega} \div \hat{\Omega} + \mathrm{d}\hat{\Omega}$) at time t. Starting from a given initial condition, the time evolution of the neutron density $n(\vec{r}, v, \hat{\Omega}, t)$ in a system is provided by the time-dependent linear Boltzmann equation, possibly coupled with the equations for the precursors concentrations $c(\vec{r}, t)$ [3]. In neutron transport, it is reasonable to suppose the absence of particle-particle interactions (due to the weak neutron density as compared to that of the nuclei of the traversed medium [3]) and this implies that the equations are linear. The derivation of such equations is based on the principle of *particle conservation in the phase space* [3, 17, 20].

The linear Boltzmann equation for the neutron density reads

$$\frac{\partial}{\partial t} n(\vec{r}, v, \hat{\Omega}, t) + L\, n(\vec{r}, v, \hat{\Omega}, t) = F_p\, n(\vec{r}, v, \hat{\Omega}, t) + \sum_{i,j} \frac{\chi_d^{i,j}(\vec{r}, v)}{4\pi} \lambda_{i,j} c_{i,j}(\vec{r}, t) \tag{2.1}$$

where we have defined the linear transport operator

$$L\, f = v\hat{\Omega} \cdot \nabla f + v\Sigma_t f - \int_0^\infty \int_{4\pi} \Sigma_s(\vec{r}, v' \to v, \hat{\Omega}' \to \hat{\Omega}) v' f(\vec{r}, v', \hat{\Omega}') \mathrm{d}\hat{\Omega}'\, \mathrm{d}v' \tag{2.2}$$

and the prompt fission operator

$$F_p\, f = \frac{\chi_p(\vec{r}, v)}{4\pi} \int_0^\infty \int_{4\pi} \nu_p \Sigma_f(\vec{r}, v') v' f(\vec{r}, v', \hat{\Omega}') \mathrm{d}\hat{\Omega}'\, \mathrm{d}v' \tag{2.3}$$

Here notation is as follows: v is the neutron speed, $\vec{r}$ is the position vector and $\hat{\Omega}$ is the angular direction vector, Σ_t is the total cross-section, Σ_s is the differential scattering cross-section, χ_p is the normalized speed spectrum for prompt fission neutrons, ν_p is the average number of prompt fission neutrons, Σ_f is the fission cross-section, $\chi_d^{i,j}$ is the normalized spectrum of delayed neutrons emitted from precursor family j of isotope i, $\lambda_{i,j}$ is the decay constant of precursor family j of isotope i and the double sum is extended over all

fissile isotopes i in the system and over all precursor families j for each fissile isotope.

The Boltzmann equation for the neutron density is then coupled to the equation for the evolution of the precursor concentration, which reads

$$\frac{\partial}{\partial t}c_{i,j}(\vec{r},t) = \int_0^\infty \int_{4\pi} \nu_d^{i,j}\Sigma_f^i v' n(\vec{r},v',\hat{\Omega}',t)\,\mathrm{d}\hat{\Omega}'\,\mathrm{d}v' - \lambda_{i,j}c_{i,j}(\vec{r},t), \tag{2.4}$$

where $\nu_d^{i,j}$ is the average number of delayed fission neutrons of precursor family j of isotope i.

The equations above are completed by assigning the proper initial and boundary conditions for n and $c_{i,j}$.

For very short time scales $t \ll \lambda_{ij}^{-1}$, the impact of delayed neutrons can be safely neglected, so that we would have

$$\frac{\partial}{\partial t}n(\vec{r},v,\hat{\Omega},t) + L\,n(\vec{r},v,\hat{\Omega},t) = F_p\,n(\vec{r},v,\hat{\Omega},t), \tag{2.5}$$

but this is not the case for observation times t comparable to the decay lifetimes $\lambda_{i,j}^{-1}$ of the precursors [3]. Furthermore, we have assumed here that all physical parameters (such as cross-sections, energy spectra, and so on) are time-independent: this amounts to taking t shorter than the typical time scale of thermal-hydraulic and Doppler feedback [24, 1]. If N fissile isotopes are present, each associated to M precursors families, equations (2.1) and (2.4) form a system of $1 + N \times M$ equations to be solved simultaneously. In the following we will address this issue.

2.2 Stationary problems

For customary problems emerging in reactor physics and radiation shielding, we are only interested in determining the steady-state of a system and we

can eliminate the time dependence from our equations. This can be achieved by resorting to two different approaches, depending on the physical situation we are dealing with.

The first approach emerges in radiation shielding calculations, where a *fixed source* Q is typically imposed. In this case, we simply integrate in time from zero to infinity in order to eliminate the time dependence.
By observing that we have $\partial_t n = \partial_t c = 0$, combing equations (2.1) and (2.4) yields

$$L\, n(\vec{r}, v, \hat{\Omega}) = (F_p + F_d) n(\vec{r}, v, \hat{\Omega}) + Q(\vec{r}, v, \hat{\Omega}) \tag{2.6}$$

where $n(\vec{r}, v, \hat{\Omega})$ is the stationary neutron density and

$$F_d\, f = \sum_{i,j} \frac{\chi_d^{i,j}(\vec{r}, v)}{4\pi} \int_0^\infty \int_{4\pi} \nu_d^{ij} \Sigma_f(\vec{r}, v') v' f(\vec{r}, v', \hat{\Omega}') \mathrm{d}\hat{\Omega}'\, \mathrm{d}v' \tag{2.7}$$

Eq. (2.6) is again a balance equation: the total net disappearances (due to absorptions or leakage, minus scattering, which preserves the particle number) must be balanced by the total productions (prompt and delayed fissions, if any) plus the contribution of the source.

The second approach emerges in reactor physics calculations, in which we are interested in finding the *critical* (i.e., stationary) core configuration. In this case, one tries to make the system time-independent by balancing the lack or the excess of neutrons through a "control coefficient", named *effective multiplication factor* k_{eff}. Conceptually, k_{eff} can be defined as a scalar such that, if the number of neutrons generated by each prompt and delayed fission interaction is scaled by this number, the reactor is then artificially critical.
Therefore, by setting the time-derivative to zero and introducing k_{eff}, Eq. (2.1)

becomes [3]

$$L\, n(\vec{r}, v, \hat{\Omega}) = \frac{1}{k_{eff}}(F_p + F_d)n(\vec{r}, v, \hat{\Omega}) \tag{2.8}$$

where we have again collected the prompt and delayed fission terms. Remark that in this case we require $F_p + F_d > 0$. Eq. (2.8) is formally an eigenvalue problem for the eigenvalue-eigenfunction pair $\{k, n\}$ [8]. It can be shown that Eq. (2.8) admits an infinite number of discrete eigenvalues k under mild conditions about geometry, boundary conditions and cross sections [3, 17]; the corresponding eigenfunctions $n = n_k(\vec{r}, v, \hat{\Omega})$ are referred to as k-modes. The multiplication factor k_{eff} is the largest k-eigenvalue whose associated k-mode is everywhere non-negative (the so-called fundamental mode).

Since Eq. (2.8) has been made stationary by artificially introducing k_{eff} as a population control acting on the number of fission, the shape of the fundamental k-mode is not expected represent any real neutron density except when the reactor is exactly critical, i.e., $k_{\text{eff}} = 1$. In other words, if we are dealing with a system that is far from critical and we solve Eq. (2.8) for this system, the obtained k-modes do not carry any physical meaning.

The main aim of Eq. (2.8) is to provide information concerning the value of k_{eff} for a given reactor configuration. If $k_{\text{eff}} > 1$ the reactor is supercritical, if $k_{\text{eff}} < 1$ the reactor is subcritical, and if $k_{\text{eff}} = 1$ the reactor is exactly critical. The system reactivity can be obtained as $\rho = (k - 1)/k$.

There are two methods for solving equations (2.6) and (2.8): the so-called *deterministic* approach, which basically consists in discretizing the solution in the space, energy and angle variables and solving the resulting linear system as a set of equations where the unknown is the vector containing the discretized solution; and the so-called *stochastic* approach, which consists in solving the equation by resorting to Monte Carlo methods. In the following, we will deal with the latter.

2.2.1 Monte Carlo transport theory

It can be shown [41] that the integro-differential equation (2.6) can be equivalently written in integral form:

$$\psi(\vec{r}, v, \hat{\Omega}) = \int_{\Gamma} \psi(\vec{r'}, v', \hat{\Omega'}) K(\vec{r'} \to \vec{r}, v' \to v, \hat{\Omega'} \to \hat{\Omega}) d\vec{r'} dv' d\hat{\Omega'} + S(\vec{r}, v, \hat{\Omega}), \tag{2.9}$$

where:

$\psi = v\Sigma_t(\vec{r}, v) n(\vec{r}, v, \hat{\Omega})$ is the *collision density*, i.e., the average number of particles interacting with the matter at point $(\vec{r}, v, \hat{\Omega})$ of the phase space;

$K(\vec{r'} \to \vec{r}, v' \to v, \hat{\Omega'} \to \hat{\Omega}) = C(v' \to v, \hat{\Omega'} \to \hat{\Omega}, \vec{r}) T(\vec{r'} \to \vec{r}, v, \hat{\Omega})$ is the *transport kernel*, which represents the particle density traveling from point $(\vec{r'}, v', \hat{\Omega'})$ of the phase space Γ and reaching point $(\vec{r}, v, \hat{\Omega})$;

$S(\vec{r}, v, \hat{\Omega})$ represents the *first collision source* and is equal to $S = \int T(\vec{r'} \to \vec{r}, v, \hat{\Omega}) Q(\vec{r'}, v, \hat{\Omega}) d\vec{r'}$, i.e., the average number of particles coming from the physical source $Q(\vec{r'}, v, \hat{\Omega})$ and having their first collision at point $(\vec{r}, v, \hat{\Omega})$.

The *transfer kernel* T may be characterized by stating that, for a particle leaving a collision at point $(\vec{r'}, v, \hat{\Omega})$, the expected number of next collisions in the spatial volume V_r is:

$$\int_{V_r} T(\vec{r'} \to \vec{r}, v, \hat{\Omega}) d\vec{r}. \tag{2.10}$$

If V_r represents an infinite medium, the integral must give 1, meaning that the event of a particle leaving position $\vec{r'}$ and having a collision somewhere in a infinite medium is a *certain event*.

The transfer kernel T reads

$$T(\vec{r'} \to \vec{r}, v, \hat{\Omega}) = \Sigma_t(\vec{r}, v) \exp[- \int_0^{\hat{\Omega}\cdot(\vec{r}-\vec{r'})} \Sigma_t(\vec{r'} + s\hat{\Omega}, v) ds]. \tag{2.11}$$

The *collision kernel* is defined so that, for a particle entering a collision at point $(\vec{r}, v', \hat{\Omega}')$, the expected number of particles leaving the collision in the speed-direction volume V_E is:

$$\int_{V_E} C(v' \to v, \hat{\Omega}' \to \hat{\Omega}, \vec{r}) dv d\hat{\Omega}. \tag{2.12}$$

The collision kernel reads

$$C(v' \to v, \hat{\Omega}' \to \hat{\Omega}, \vec{r}) = \sum_i^I p_i(v', \vec{r'}) y_i(v') f_i(v' \to v, \hat{\Omega}' \to \hat{\Omega}, \vec{r}), \tag{2.13}$$

where:

$p_i(v', \vec{r'})$ is the probability of undergoing reaction i out of a set of I possible reactions; it is represented by

$$p_i = \frac{\Sigma_i(v', \vec{r'})}{\Sigma_t(v', \vec{r'})}, \tag{2.14}$$

i.e., the ratio between the reaction cross section Σ_i and the total cross section Σ_t;

$y_i(v')$ is the multiplicity of secondary neutrons leaving reaction i;

$f_i(v' \to v, \hat{\Omega}' \to \hat{\Omega}, \vec{r})$ is the normalized distribution in the speed-direction space of secondary neutrons.

The sum of p_i and the integral of the distribution function over the whole energy space are normalized to one. The multiplicity term $y_i(v')$ depends on the reaction (it can be zero for absorption, one for scattering, or larger for other reactions).

Observe that we are assuming that the only transported particles are neutrons. The coupling with other particles, such as for instance photons, will be neglected.

The Monte Carlo method for solving Eq. (2.9) (or equivalently Eq. (2.6)) consists in generating a large number of neutron *random walks* in the phase space so that their ensemble average converges to ψ (or n). Each random walk can be seen as the physical random trajectory of the transported particle, which travels along straight lines according to the transfer kernel T, separated by collisions with the nuclei, described by the collision kernel C. The *random walks* start from the source Q, have k collisions in the viable space and are eventually lost from boundaries or absorbed. Such random walks are defined by the set of coordinates in the phase space reached by the particles (for the sake of simplicity, from now on the coordinates in the phase space will be denoted by the point $P = (\vec{r}, v, \hat{\Omega})$).
The construction of the random walk is the basic step to be performed in order to simulate the transport of particles. Once the particle is created from the source Q, it travels through the phase space via the $K(P, P')$ kernel. Assuming full knowledge of the kernels at each point of the viable phase space, the random walks can be then generated by:

- sampling the traveled distance from the continuous density function of the transfer kernel T;
- sampling the reaction event from the discrete probability function p_i;
- sampling the energy and the direction of the secondary particle after the collision from the continuous distribution function f_i associated to the sampled reaction.

The topic of sampling techniques will be not approached in the following. Once an ensemble (i.e., a large collection) of random walks has been sampled, the purpose of a Monte Carlo simulation is in general to define the appropriate *random variable* $\xi(\alpha)$ associated to the *random walk* α whose expected value provides an estimate for the quantity:

$$E[\xi(\alpha)] \equiv \left\langle n(\vec{x}) \middle| g(\vec{x}) \right\rangle = \int_{\Gamma} n(\vec{x}) g(\vec{x}) d\vec{x}, \tag{2.15}$$

which represents the inner product of the particle density $n(\vec{x})$ times a general test function $g(\vec{x})$ on a defined volume of the phase space. The function $g(\vec{x})$ is precisely the *score* that is desired, and $\langle n|g\rangle$ represents the *density-averaged* score over the volume of interest. The quantity $\xi(\alpha)$, which must be properly chosen so to ensure the convergence $E(\xi) = \langle n|g\rangle$, takes the name of Monte Carlo estimator [41]. The expected value of an ensemble of N random walks can be computed as:

$$E[\xi(\alpha)] = \frac{\sum_n \xi(\alpha_n)}{N}, \tag{2.16}$$

where α_n is the $n-th$ random walk and $\xi(\alpha_n)$ is the associated random variable. It can be shown [41] that convergence of the estimator as a function of the number of simulated random walks goes with the square root of N.

The first kind of estimator is the so-called *collision* estimator, defined as:

$$\xi_{coll}(\alpha) = \sum_m \frac{g(\vec{x}_m)}{\Sigma_t(v_m) v_m}, \tag{2.17}$$

If we are interested in evaluating a score in a portion V of the phase space, the test function must be zero everywhere but in V; in other words, the test function must be multiplied by the *marker function* $\chi_V(\vec{x})$:

$$\chi_V(\vec{x}) = \begin{cases} 1 & \text{if} \quad \vec{x} \in V \\ 0 & \text{if} \quad \vec{x} \notin V \end{cases}$$

By progressively reducing the dimensions of such volume V, we can obtain the value of the score evaluated at a single point of the phase space. On the other hand, the smaller the volume, the smaller is the probability to obtain a sample of the event in that position. Special techniques exist to obtain an estimate of the pointwise distribution of a physical quantity in the phase space (the so-called point-flux estimation: here we will not address this issue). Observe that we have here considered density-averaged scores: more often, quantities of interests in reactor physics require averages over the neutron flux $\phi = nv$. The corresponding flux estimator of collision type can be constructed as

$$\xi_{coll}(\alpha) = \sum_{m} \frac{g(\vec{x}_m)}{\Sigma_t(v_m)}, \tag{2.18}$$

which is such that $E(\xi) = \langle \phi | g \rangle$.
As an alternative to the *collision estimator*, the *track estimator* allows obtaining a better estimation of density-averaged scores in small volumes. It is defined as [41]:

$$\xi_{track}(\alpha) = \sum_{m=1}^{k} g(\vec{x}_m) t_m, \tag{2.19}$$

where t_m is the time spent by the $m-th$ particle in the volume V of the phase space. For flux-averaged scores, we can then define

$$\xi_{track}(\alpha) = \sum_{m=1}^{k} g(\vec{x}_m) d_m, \tag{2.20}$$

where d_m is the track of the m-th particle in the volume V.

It can be shown [41] that, for any given g, we have $\xi_{track}(\alpha) \equiv \xi_{coll}(\alpha)$, which implies that the two estimators converge to each other when $N \to \infty$, i.e., they are unbiased.

The variance associated to the estimators depends on the problem we want to solve. In general, the **collision** estimator (Eq. 2.17) works better in large volumes, whereas the **track** estimator (Eq. 2.19) is better suited for small volumes. We will make use of both in our simulations.

2.2.2 Monte Carlo power iteration

The Monte Carlo method for solving criticality problems, which are described by Eq. (2.8), is slightly different from the one just shown. In fact, in this case, we do not have a source distribution from which starting the particle random walks. However, Eq. (2.8) describes a linear eigenvalue problem that can be solved by power iteration method [26].

We can begin with a guess neutron distribution $n_0(\vec{r}, v, \hat{\Omega})$, called *generation zero*.

Then, we obtain the generation-one neutron density by applying a proper integral transport operator to the previous neutrons

$$n_1(\vec{r}, v, \hat{\Omega}) = K\, n_0(\vec{r}, v, \hat{\Omega}). \tag{2.21}$$

and we find the first estimate of the k factor, which is given by the ratio

$$k_1 = \frac{|n_1|}{|n_0|}. \tag{2.22}$$

In order to avoid that neutron population goes to zero or diverges, we have to apply a population control, by dividing n_1 for k_1, so that we start the next generation with the same number of particles. We simulate the next generation, starting the particle stories from the fission positions of the previous generation and we iterate this procedure for a large number M of neutron generations:

$$n_{i+1}(\vec{r}, v, \hat{\Omega}) = K\, n_i(\vec{r}, v, \hat{\Omega}). \tag{2.23}$$

In the limit of $M \to \infty$, $k_i \to k_{eff}$ and the limit neutron density $n_i(\vec{r}, v, \hat{\Omega})$ is the eigenfunction associated to k_{eff} [26].

2.3 Time-dependent problems

In chapter 2.2, we have seen how to solve the steady-state transport Boltzmann equation by Monte Carlo methods. We now move to consider the full time-dependent Boltzmann equation.

Assessing the time behaviour of neutron transport is important in several situations of interest in nuclear engineering: reactor start-up, reactivity measurement, safety calculations, kinetics of accelerator-driven systems (ADS), only to name a few. In fact, the knowledge of the reactor kinetics is fundamental both for normal scenarios (start-up, power transients) and accidental situations (rod ejection). Moreover, some reactor designs, such as the Accelerator Driven Subcritical system (ADS), intrinsically work at non-steady-state. The ADS has been investigated in the last decades as a promising tool to incinerate actinides and to transmute long-lived radioactive wastes. The nuclear fuel configuration is subcritical and an external neutron source (driven by an accelerator) is used to sustain the chain reaction. The time behaviour of such a system is subject to several transients and knowledge of the neutron dynamics is therefore needed [22].

In order to assess the reactor kinetics, we have to solve the time-dependent Boltzmann equation, which is a daunting task and demands special numerical methods so as to cope with the complexity of the involved system of equations.

2.3.1 Deterministic methods

Until now, the analysis of transient dynamics of a neutron population has been mainly carried out by resorting to deterministic methods. Here, for the sake of completeness we briefly recall some of the basic deterministic methods [8, 22].

The *direct method* is a straightforward way to solve a time-dependent equation [8]. The time interval of interest is divided in small time sub-intervals $[t_j, t_{j+1}]$, and for every sub-interval a stationary Boltzmann equation is solved, by means of the usual numerical techniques (spatial discretization, multigroup energy approximations and so on). The direct method is complicated by the presence of very different time scales, which makes the Boltzmann equations a "stiff" system: indeed, an extremely fine time step is required to accurately describe the prompt-neutron behaviour ($t \approx \mu$s) and a large number of time steps is required to represent the delayed-neutron behaviour ($t \approx s$). Therefore, this method is seldom used.

The *space-time factorization method* is based on the idea of factorizing the neutron density into two parts: $n(\vec{r}, \vec{v}, t) = T(t)n_0(\vec{r}, \vec{v}, t)$ (for shortness, we have represented the angular dependence in the velocity vector), where the *amplitude* T depends only on time and the *shape function* n_0 varies slowly in time. Under this assumption, we can accurately obtain n_0 even adopting large time-steps. Suppose now that the shape function is known. It can be shown [8] that, if we substitute the factorized density into Eq. (2.1) and Eq. (2.4) and we integrate over the space and energy domain weighting for

the adjoint flux, we obtain the point-reactor kinetics equations:

$$\frac{dT(t)}{dt} = \frac{\rho(t) - \beta(t)}{\Lambda(t)} T(t) + \lambda c(t) \tag{2.24}$$

$$\frac{dc(t)}{dt} = \frac{\beta(t)}{\Lambda(t)} T(t) - \lambda c(t) \tag{2.25}$$

where $\rho(t)$, $\beta(t)$ and $\Lambda(t)$ are the *kinetics parameters* defined in terms of the shape function n_0 integrated in space and energy (therefore the only left dependence is on time). In particular, $\beta(t)$ is the *effective delayed-neutron fraction*, $\Lambda(t)$ is the *neutron mean generation time* and $\rho(t)$ is the *reactivity* of the system, each depending on the time step. The actual implementation of the space-time factorization method is based on an iterative scheme. The shape function is first approximated by a known function in a large time step (*shape step*). With the approximated n_0, the kinetics parameters $\beta(t)$, $\rho(t)$ and $\Lambda(t)$ are calculated within the shape step. Equations (2.24) and (2.25) are then solved for the amplitude function $T(t)$ with fine time steps (*amplitude steps*). Usually, the shape steps are several times larger than amplitude steps.

The *modal expansion method* is based on the hypothesis of total separation between time dependence and space-energy dependence [8]. The approximated time-dependent solutions is written as

$$n(\vec{r}, \vec{v}, t) = \sum_n A_n(t) n_n^\alpha(\vec{r}, \vec{v}) \tag{2.26}$$

$$c(\vec{r}, t) = \sum_n A_n(t) c_n^\alpha(\vec{r}) \tag{2.27}$$

where n_n^α and c_n^α are (precomputed) space-energy dependent expansion functions, the so-called α-modes and $A_n(t)$ is the expansion coefficient for the $n^{th}\alpha$-mode. The modes n_n^α and c_n^α can be obtained by plugging (2.26)

and (2.27) into equations (2.1) and (2.4) and solving the resulting equations.

All such methods, even the direct method, introduce several approximations, which are intrinsically due to the nature of deterministic solvers. Sometimes, it is desirable to have a higher-fidelity method for transient analysis. In this respect, Dynamic Monte Carlo methods have been recently proposed to solve the time-dependent Boltzmann equation [22].

2.3.2 Dynamic Monte Carlo

The basic ideas behind Monte Carlo theory simulation have been recalled in chapter 2.2 as far as the solution of the stationary problems is concerned. As remarked, Monte Carlo methods solve the Boltzmann equation by simulating particle histories, therefore introduce as few approximations as possible. The accuracy and the general applicability of these methods represent some of the reasons why many researchers and designers choose Monte Carlo simulation, which is typically used as the reference for deterministic codes. A non-negligible drawback is that Monte Carlo in most practical cases turns out to be much slower than deterministic solvers. It is tempting to apply Monte Carlo methods also to transient calculations, which goes under the name of *dynamic Monte Carlo method*.

There are several new problems that need to be addressed in order to perform kinetic calculations with Monte Carlo codes [22]. First of all, the time factor, i.e., $\frac{\partial n}{\partial t}$, is explicitly present, so that when sampling random walks we not only have to record the position in the phase space $(\vec{r}, \vec{v})$ but also the time instants of birth, interaction and death of the particles. For

this reason, we have to split the time domain into bins and tally the scores of each event per bin. Moreover, a serious issue comes from the delayed neutron population. As we said, the time scale of delayed neutrons is much larger than that of prompt neutrons. In fact, while prompt neutrons are (almost) instantaneously emitted at fission events, the delayed neutrons come from the beta decay of precursors. Therefore, the probability density that a delayed neutron is emitted obeys the exponential decay law:

$$P(t) = \lambda_i e^{-\lambda_i t} \tag{2.28}$$

where λ is the specific decay constant of the i^{th} precursor. In principle, when a Monte Carlo simulation is performed, it is possible to sample ν_p prompt neutrons at the time of fission event t_f ans sample ν_d delayed neutrons at time $t = t_f + t_d$, where t_d is drawn from Eq. (2.28). This method mimics what actually happens in the physical system, but it would create too much variance, due to the very different time scales of the two populations [22]. Indeed, for a Monte Carlo calculation it is important to have enough statistics per tally bin. A possible remedy is therefore to force the precursors to generate a delayed neutron in each time bin; then, in order to obtain an unbiased score, we have to attribute to this neutron a modified statistical weight [22].
This algorithm is named *forced precursors decay*. With this method, all precursors are stored, in order to have a decay in each time interval subsequent to the precursor appearance in the system. This implies that the total number of precursors increases continuously. Therefore, population control is needed, not only for neutrons as customary, but also for precursors.

The precise details of the algorithm can be found in [22]. This preliminary discussion suggests that the explicit time dependence makes Monte

Carlo simulation much more complex than for static calculations. As a general rule, dynamic Monte Carlo methods demand an even larger simulation time than static simulations.

Despite all these drawbacks, dynamic Monte Carlo methods are quite appealing for the reactor physics, and are going to be implemented in the development version of the Monte Carlo code TRIPOLI-4 ®. This future version of the code will make possible to compute reactor power transients in regular operation as well as in accidents, and eventually integrate the feedback coming from thermal-hydraulic codes.

2.3.3 Alpha static methods

In many practical situations, the knowledge of the full time dynamics of the system is not needed, and only the asymptotic (long time) behaviour is sought for. This is the case, for instance, of pulsed-neutron experiments or reactivity measures, where one is interested in determining the *asymptotic relaxation* of the system, following a given initial burst of neutrons at $t = 0$ [3, 17].

Asymptotic relaxation phenomena do not involve the solution of the full time-dependent Boltzmann equation, and can be dealt with by resorting to a different approach. The idea is similar to the modal expansion method, in which the neutron density is decomposed in a separated-variable form as

$$n(\vec{r}, \vec{v}, t) = \sum_n A_n(t) n_n^{\alpha}(\vec{r}, \vec{v}). \tag{2.29}$$

Indeed, in the analysis of asymptotic time relaxation, it is postulated that the neutron population obeys

$$n(\vec{r}, \vec{v}, t) = \sum_{\alpha} n_{\alpha}(\vec{r}, \vec{v}) e^{\alpha t} \tag{2.30}$$

so that for long times we have

$$n(\vec{r},\vec{v},t) \approx n_{\alpha_0}(\vec{r},\vec{v})e^{\alpha_0 t}, \tag{2.31}$$

where α_0 is the algebraically largest value among all α of the expansion.
In other words, we are assuming that the neutron population at long times will grow or decay in an exponential fashion, with asymptotic period given by α_0. As for the space and velocity behaviour, Eq. (2.31) implies that at long times the functional shape of n will not change anymore, and will be given by $n \approx n_{\alpha_0}(\vec{r},\vec{v})$. As for the precursor population, it is similarly demanded that

$$c(\vec{r},t) = \sum_{\alpha} c_\alpha(\vec{r})e^{\alpha t}. \tag{2.32}$$

If we are interested in knowing the complete time behaviour of $n(\vec{r},v,\hat{\Omega},t)$ and $c(\vec{r},t)$, we should replace the full expansions (2.30) and (2.32) into the Boltzmann equation and explicitly solve the resulting equations. However, due to the postulated exponential nature of the neutron and precursor populations, after a transient, only the term with the algebraically largest coefficient α_0 will survive. Therefore, in order to assess the asymptotic neutron and precursor behaviour, we are led to consider only the dominant frequency α_0.
By replacing $n = n_\alpha e^{\alpha t}$ and $c = c_\alpha e^{\alpha t}$ into Eq. (2.1) and Eq. (2.4) respectively, we get a set of coupled equations

$$\alpha n_\alpha(\vec{r},v,\hat{\Omega}) + L\, n_\alpha(\vec{r},v,\hat{\Omega}) = +F_P\, n_\alpha(\vec{r},v',\hat{\Omega}') + \sum_{i,j} \frac{\chi_d^{i,j}(\vec{r},v)}{4\pi}\lambda_{i,j}c_\alpha^{i,j}(\vec{r}) \tag{2.33}$$

and

$$\alpha c_\alpha^{i,j}(\vec{r}) = \int_0^\infty \int_{4\pi} \nu_d^{i,j}\Sigma_f^i(\vec{r},v')v n_\alpha(\vec{r},v',\hat{\Omega}')\,\mathrm{d}\hat{\Omega}'\,\mathrm{d}E' - \lambda_{i,j}c_\alpha^{i,j}(\vec{r}), \tag{2.34}$$

which are formally a system of eigenvalue equations, whose dominant eigenvalue is precisely α_0 [3]. Equations (2.33) and (2.34) do not depend on time anymore and therefore look like static equations (in a sense that will be made clear in the following chapter). Due to the presence of the α term, eqs. (2.33) and (2.34) take the name of α-static equations: the next chapter will be devoted to the specific Monte Carlo methods conceived to assess the asymptotic time behaviour of nuclear systems by solving the α-static equations.

We conclude by observing that approximating the full expansion (2.30) with the fundamental mode $n_{\alpha_0}e^{\alpha_0 t}$ is formally equivalent to adopting the space-time factorization with a time-independent shape function: $n(\vec{r},\vec{v},t) = T(t)n_0(\vec{r},\vec{v})$. In this case, the kinetics parameters previously introduced, namely ρ, Λ and β, are all constant. Therefore, equations (2.24) and (2.25) simply become the *point kinetic equations*:

$$\frac{dT(t)}{dt} = \frac{\rho-\beta}{\Lambda}T(t) + \lambda c(t) \tag{2.35}$$

$$\frac{dc(t)}{dt} = \frac{\beta}{\Lambda}T(t) - \lambda c(t). \tag{2.36}$$

Chapter 3

The α static methods

In the previous chapter, we have introduced the α-static method. In this chapter we shall make clear the mathematical basis of this method and then we shall introduce the algorithm developed in TRIPOLI-4 ®.

3.1 The mathematical theory

The full time behaviour of the neutron density in a system is provided by the time-dependent Boltzmann equation

$$\frac{\partial}{\partial t} n(\vec{r}, v, \hat{\Omega}, t) + L\, n(\vec{r}, v, \hat{\Omega}, t) = F_p\, n(\vec{r}, v, \hat{\Omega}, t) + \sum_{i,j} \frac{\chi_d^{i,j}(\vec{r}, v)}{4\pi} \lambda_{i,j} c_{i,j}(\vec{r}, t) \tag{3.1}$$

coupled with the precursor equation (2.4)

$$\frac{\partial}{\partial t} c_{i,j}(\vec{r}, t) = \int_0^\infty \int_{4\pi} \nu_d^{i,j} \Sigma_f^i v' n(\vec{r}, v', \hat{\Omega}', t)\, \mathrm{d}\hat{\Omega}'\, \mathrm{d}v' - \lambda_{i,j} c_{i,j}(\vec{r}, t). \tag{3.2}$$

When the long-time (asymptotic) behaviour is sufficient so as to characterize the system evolution [3, 17], an exponential relaxation of the kind

$$n(\vec{r}, v, \hat{\Omega}, t) = n_\alpha(\vec{r}, v, \hat{\Omega}) e^{\alpha t} \tag{3.3}$$

and

$$c_{i,j}(\vec{r}, t) = c_\alpha^{i,j}(\vec{r}) e^{\alpha t} \tag{3.4}$$

is postulated for both the neutron flux and the precursors concentrations, where the parameter α (carrying the units of the inverse of a time) plays the role of the inverse of the asymptotic relaxation time scale [3, 17]. Equations (3.3) and (3.4) formally stem from imposing the separation of variables in Eqs. (3.1) and (3.2), and can be more rigorously justified by resorting to Laplace transform analysis or equivalently to spectral analysis [17]. Yet, proving the feasibility of such exponential relaxation is highly non-trivial in general, and precise (although not very restrictive) conditions are required on the geometry of the domain and on the material cross-sections [3, 17, 28]. We shall discuss this issue later.

Replacing Eqs. (3.3) and (3.4) into Eqs. (3.1) and (3.2), respectively, yields the so-called α-static equations

$$\alpha n_\alpha(\vec{r}, v, \hat{\Omega}) + L\, n_\alpha(\vec{r}, v, \hat{\Omega}) = + F_P\, n_\alpha(\vec{r}, v', \hat{\Omega}') + \sum_{i,j} \frac{\chi_d^{i,j}(\vec{r}, v)}{4\pi} \lambda_{i,j} c_\alpha^{i,j}(\vec{r}), \tag{3.5}$$

$$\alpha c_\alpha^{i,j}(\vec{r}) = \int_0^\infty \int_{4\pi} \nu_d^{i,j} \Sigma_f^i(\vec{r}, v') v n_\alpha(\vec{r}, v', \hat{\Omega}')\, \mathrm{d}\hat{\Omega}'\, \mathrm{d}E' - \lambda_{i,j} c_\alpha^{i,j}(\vec{r}), \tag{3.6}$$

which form a stationary, coupled system, formally representing an eigenvalue problem. Finally, solving with respect to n_α results into the (nonlinear) eigenvalue problem [3, 43, 9, 19]

$$\alpha n_\alpha(\vec{r}, v, \hat{\Omega}) + L\, n_\alpha(\vec{r}, v, \hat{\Omega}) = F_p\, n_\alpha(\vec{r}, v, \hat{\Omega}) + \sum_{i,j} \frac{\lambda_{i,j}}{\lambda_{i,j} + \alpha} F_d^{i,j}\, n_\alpha(\vec{r}, v, \hat{\Omega}), \tag{3.7}$$

where α is the eigenvalue and n_α the associated eigenmode, and we have defined

$$F_d^{i,j}\, f = \frac{\chi_d^{i,j}(\vec{r}, v)}{4\pi} \int_0^\infty \int_{4\pi} \nu_d^{i,j} \Sigma_f^i(\vec{r}, v') f(\vec{r}, v', \hat{\Omega}')\, \mathrm{d}\hat{\Omega}'\, \mathrm{d}v'. \tag{3.8}$$

In principle, Eq. (3.7) has $1 + N \times M$ sets of eigenvalues (one prompt and $N \times M$ delayed eigenvalues) associated to each eigenmode n_α [3, 9, 19]. In order to determine the asymptotic time behaviour of the system, Eq. (3.7) must be solved for the algebraically largest eigenvalue α, so that the corresponding fundamental mode $n_\alpha(\vec{r}, E, \hat{\Omega})$ will provide the asymptotic space, angle and energy shape of the neutron flux at long times. We shall treat the problems of the prompt and delayed behaviour separately.

3.1.1 The *prompt* behaviour

When delayed contributions can be neglected (i.e., $F_d^{i,j} n_\alpha = 0$), α is called the *prompt time eigenvalue*: the mathematical properties of the resulting (linear) eigenvalue equation

$$\alpha n_\alpha(\vec{r}, v, \hat{\Omega}) + L\, n_\alpha(\vec{r}, v, \hat{\Omega}) = F_p\, n_\alpha(\vec{r}, v, \hat{\Omega}) \tag{3.9}$$

and the numerical schemes for assessing the dominant eigenvalue have been the subject of considerable research efforts (see for instance the comprehensive works [3, 17, 28, 2] about theoretical aspects and [21, 6, 15, 39, 45, 34, 48] concerning numerical methods).

Knowledge of the spectrum $\sigma(A)$ of the Boltzmann operator

$$A\,f = (-L + F_p)f = -v\hat{\Omega}\cdot\nabla f - v\Sigma_t f + \int_0^\infty\int_{4\pi}\Sigma_s(\vec{r}, v' \to v, \hat{\Omega}' \to \hat{\Omega})v' f(\vec{r}, v', \hat{\Omega}')\mathrm{d}\hat{\Omega}'\,\mathrm{d}v' + \frac{\chi_p(\vec{r}, v)}{4\pi}\int_0^\infty\int_{4\pi}\nu_p\Sigma_f(\vec{r}, v')v' f(\vec{r}, v', \hat{\Omega}')\mathrm{d}\hat{\Omega}'\,\mathrm{d}v' \quad (3.10)$$

is fundamental so as to determine the properties of Eq. (3.9) and in particular of its dominant eigenvalue and eigenmode.

3.1.1.1 Finite spatial domain

An exhaustive analysis of the spectrum $\sigma(A)$ of the Boltzmann operator A has been provided by Larsen and Zweifel in [28] for a broad class of collision kernels and geometries. Here, we recall the main results [28] for the eigenvalue problem

$$A\,n_\alpha = \alpha n_\alpha.$$

We define A in an $L_1(D \times V)$ space, where D is the bounded spatial domain and V is the velocity domain, i.e., $v_0 < v < v_1$, where $v_0 < v_1 < c$, c being the speed of light. First, we consider the *streaming and removal operator* T, defined as

$$T = -[\vec{v}\cdot\nabla_{\mathbf{r}} + v\Sigma_T(\vec{r}, v)]. \quad (3.11)$$

Let us denote v_0 the minimum allowed neutron speed. It can be then shown that [28]:

- If $v_0 > 0$, then the spectrum $\sigma(T)$ consists solely of the point at infinity: $\sigma(T) = \{\infty\}$.

- If $v_0 = 0$, then the spectrum $\sigma(T)$ consists of the complex half plane: $\sigma(T) = \{\alpha \mid \mathrm{Re}\{\alpha\} \leq \alpha^*\}$, where $\alpha^* = -\lim_{v\to 0} v\Sigma_T(v)$.

The spectrum $\sigma(T)$ of the operator T may then contain a continuum portion. The limiting value α^* takes the name of Corngold limit and physically represents the minimum collision frequency. We consider now a *one-speed transport operator* A_0, defined as

$$A_0 = T + K_0, \tag{3.12}$$

where K_0 is a collision operator that does not change the neutron speed. This operator describes a *purely elastic* or *Bragg scattering* and has the form

$$K_0\, f = \int_{v'} k_0(\vec{r}, v', \hat{\Omega}' \to \hat{\Omega})\delta(v' \to v) f(v')dv' \tag{3.13}$$

Therefore, the operator A_0 does not change the neutron speed and depends only parametrically upon v. It can be shown [28] that the one-speed operator A_0 has a spectrum $\sigma(A_0)$ entirely formed by isolated eigenvalues, for fixed v. The eigenvalues depend parametrically upon the neutron speed. In general, as v varies between v_0 and v_1, some of the eigenvalues will remain stationary and some will shift and trace out curves. Thus, the spectrum $\sigma(A_0)$ will consist of isolated points and curved lines. As in the previous case, if we allow $v_0 = 0$ there will be also a continuum half-plane in the α-spectrum.

Finally, we consider the general case where the transport operator A is

$$A = T + K, \tag{3.14}$$

where K is the *scattering operator*, physically corresponding to fission, slowing down, thermal scattering and Bragg scattering.
It can be shown [28] that the eigenvalue spectrum $\sigma(T + K)$ differs from the

spectrum $\sigma(T + K_0)$ only by the addition of a point spectrum.

Summarizing, the collision terms of the Boltzmann operator contribute to the α-spectrum $\sigma(A)$ with discrete eigenvalues and (Bragg scattering) curves. The streaming operator may induce (under the assumption of $v_0 = 0$) the presence of a continuum half-plane in the spectrum. If this is the case, a question of utmost importance concerns the existence of a simple dominant eigenvalue, i.e., a simple eigenvalue α_0 whose real part is larger than any other α in the spectrum, and whose associated eigenfunction n_α is non-negative. In fact, if a continuum portion is present in the spectrum $\sigma(A)$, the neutron density expansion (2.30) must be written in the more general form

$$n(\vec{r}, \vec{v}, t) = \sum_{\alpha} n_\alpha(\vec{r}, \vec{v}) e^{\alpha t} + \int_{-\infty}^{\alpha^*} G(\alpha) n_\alpha(\vec{r}, \vec{v}) e^{\alpha t} d\alpha, \tag{3.15}$$

where $G(\alpha)$ are weight functions expressing the amplitude density of each continuum eigenfunction. If the fundamental eigenvalue exists (i.e., if the discrete sum in Eq. (3.15) is not empty), the asymptotic behaviour will be dominated by the exponential term with $\alpha = \alpha_0$. If $\alpha_0 \leq \alpha^*$, the discrete spectrum disappears into the continuum and the sum in Eq. (3.15) is empty. In this case, the asymptotic behaviour of the neutron density will be dominated by the continuum and it will not be possible to extract a single dominant exponential decay [17]. It can be shown that α_0 disappears into the continuum if the radius of the domain D is smaller than a critical value, which is typically of the order of a mean free path [32, 44].

3.1.1.2 Infinite spatial domain

We now discuss the behaviour of the spectrum $\sigma(A)$ for infinite spatial domains. An analysis of this case has been provided by Duderstadt [17] and

Corngold [13]. We have again an eigenvalue problem of the type:

$$A\, n_\alpha = \alpha n_\alpha. \tag{3.16}$$

Maintaining the same notation, the operator A is given by $A = T + K$. In this case, the streaming and removal operator T is simply

$$T = -v\Sigma_T(v) \tag{3.17}$$

and K is the scattering kernel. Note that, under the assumption of infinite and homogeneous medium, the angle and position dependencies have been eliminated by integrating over these variables.

The spectral analysis of Duderstadt [17], carried out under the hypothesis of allowing $v_0 = 0$, shows that the spectrum $\sigma(A)$ of the Boltzmann operator A for an infinite medium is composed by:

- a continuum unidimensional set $\sigma_c(A) = \{\alpha : \alpha = -v\Sigma_t(v), v \in [0, \infty)\}$
- a real discrete set of eigenvalues $\alpha \geq \alpha^*$, where $\alpha^* = -\lim_{v\to 0} v\Sigma_T(v)$.

Corngold has shown [13] that the properties of the discrete set depend on the scattering kernel considered, i.e., on the diffusion properties of the medium. For example, for incoherent solids, the discrete eigenvalues are finite in number. Ordinarily, only few discrete α exist, or sometimes only the fundamental α_0 exists. It is also possible, by introducing an absorption rate $\Sigma_a(v)v$ which increases sufficiently strongly with v, to have an empty discrete set. On the contrary, for gases, we find an infinite set of discrete eigenvalues, with α^* appearing as a limit point of this set. In this case, the possibility of an empty point spectrum, by introducing an absorption rate strongly increasing with v, is not realistic.

3.1.2 The α-problem with delayed neutrons

The full Eq. (3.7)

$$\alpha n_\alpha(\vec{r}, v, \hat{\Omega}) + L\, n_\alpha(\vec{r}, v, \hat{\Omega}) = F_p\, n_\alpha(\vec{r}, v, \hat{\Omega}) + \sum_{i,j} \frac{\lambda_{i,j}}{\lambda_{i,j} + \alpha}\, F_d^{i,j}\, n_\alpha(\vec{r}, v, \hat{\Omega})$$

including delayed contributions (in which case α is called the delayed time eigenvalue, and physically represents the inverse of the reactor period) has received comparatively less attention (see for instance [3, 9, 19, 23] for a survey) but has recently attracted renewed attention [22, 7, 40, 31] in view of the practical applications in reactor kinetics. Indeed, integrating Eq. (3.7) over all phase space variables leads to the reactor inhour equation [3]

$$\rho_0 = \alpha\Lambda_0 + \sum_{i,j} \frac{\alpha}{\lambda_{i,j} + \alpha} \beta_0^{i,j} \tag{3.18}$$

where $\rho_0 = (k_0 - 1)/k_0$ is the reactivity, with

$$k_0 = \frac{\langle 1, F_p\, \phi_\alpha + \sum_{i,j} F_d^{i,j}\, \phi_\alpha \rangle}{\langle 1, L\, \phi_\alpha \rangle}, \tag{3.19}$$

Λ_0 is the mean generation time

$$\Lambda_0 = \frac{\langle 1, \frac{1}{v} \phi_\alpha \rangle}{\langle 1, F_p\, \phi_\alpha + \sum_{i,j} F_d^{i,j}\, \phi_\alpha \rangle}, \tag{3.20}$$

and $\beta_0^{i,j}$ are the flux-averaged delayed fractions

$$\beta_0^{i,j} = \frac{\langle 1, F_d^{i,j}\, \phi_\alpha \rangle}{\langle 1, F_p\, \phi_\alpha + \sum_{i,j} F_d^{i,j}\, \phi_\alpha \rangle}, \tag{3.21}$$

with $\sum_{i,j} \beta_0^{i,j} = \beta_0$. In the equations (3.19), (3.20), and (3.21), the importance function has been chosen equal to 1. From Eq. (3.18) it is apparent that α plays the role of the reactor period in the inhour equation.

3.2 The proposed algorithm

We present now a Monte Carlo method to find the dominant eigenvalue α_0. We begin with the algorithm for prompt eigenvalue (the equation without delayed contributions) and then extend it so as to cover the full Eq (3.7). The fundamental eigenvalue α_0 can be estimated via Monte Carlo methods by adapting the power iteration algorithm for k static criticality calculations (described in Chapter 2). The method is then called α-k *power iteration* algorithm and its specific details depend on the sign of the dominant eigenvalue α [21, 6, 15, 48]. In the following, we sketch the structure of the algorithm by considering supercritical ($\alpha > 0$) and subcritical ($\alpha < 0$) configurations separately.

3.2.1 Positive dominant eigenvalue, $\alpha > 0$

When $F_d^{i,j} n_\alpha = 0$ and $\alpha > 0$, Eq. (3.7) can be identically rewritten as [21, 6]

$$L_\alpha \, n_\alpha(\vec{r}, v, \hat{\Omega}) = \frac{1}{k} \, F_p \, n_\alpha(\vec{r}, v, \hat{\Omega}), \tag{3.22}$$

where $L_\alpha = L + \Sigma_\alpha$ is a modified transport operator, $\Sigma_\alpha = \alpha$ and α is to be determined such that the fictitious parameter $k = 1$ in Eq. (3.22) . By remarking that the positive term Σ_α can be interpreted as an additional sterile capture cross-section added to the total cross section, the usual α-k power iteration algorithm is applied as follows: we start from a tentative distribution n_α^0 (zero-th iteration) for the neutrons and provide a guess value for α^0. Then, we search for the corresponding k eigenvalue by standard power iteration, which will depend on the current value of α. On the basis of k, we will then adjust the value of α for the next generation (for instance, one can take $\alpha^{j+1} = k\alpha^j$). This procedure is iterated until k converges to $k = 1$: the

corresponding value of α will provide the fundamental prompt eigenvalue, and the associated n_α the fundamental eigenmode.

The *delayed* contributions can be included [50] by rewriting

$$L_\alpha\, n_\alpha(\vec{r}, v, \hat{\Omega}) = \frac{1}{k}\left[F_p\, n_\alpha(\vec{r}, v, \hat{\Omega}) + \sum_{i,j} \frac{\lambda_{i,j}}{\lambda_{i,j}+\alpha}\, F_d^{i,j}\, n_\alpha(\vec{r}, v, \hat{\Omega})\right], \quad (3.23)$$

where the factor

$$\gamma_{i,j} = \lambda_{i,j}/(\lambda_{i,j}+\alpha) > 0 \quad (3.24)$$

in front of the $F_d^{i,j}$ terms acts as a population control tool to be applied to each delayed neutron coming from delayed fission. This means that the weight of delayed neutrons is first multiplied by a factor $\gamma_{i,j}$ and then divided by a factor k before being assigned to the next generation.

3.2.2 Negative dominant eigenvalue, $\alpha < 0$

When $F_d^{i,j} n_\alpha = 0$ and $\alpha < 0$, the standard α-k power iteration algorithm applied to Eq. (3.7) is known to be numerically unstable and usually leads to abnormal code termination [21]. In reference [48] an improved algorithm for negative α has been provided and shown to be numerically stable. The key ingredient consists in rewriting Eq. (3.7) as follows

$$L_{\alpha,\eta}\, n_\alpha(\vec{r}, v, \hat{\Omega}) = \frac{1}{k}\left[F_p\, n_\alpha(\vec{r}, v, \hat{\Omega}) + F_{\alpha,\eta}\, n_\alpha(\vec{r}, v, \hat{\Omega})\right], \quad (3.25)$$

where $L_{\alpha,\eta} = L + \Sigma_{\alpha,\eta}$, $\Sigma_{\alpha,\eta} = -\eta\alpha$ (η being an arbitrary positive constant) and we have formally defined the creation operator

$$F_{\alpha,\eta}\, f = \int_0^\infty \int_{4\pi} \nu_\eta \delta(v - v')\delta(\hat{\Omega} - \hat{\Omega}')\Sigma_{\alpha,\eta} f(\vec{r}, v', \hat{\Omega}') v'\, \mathrm{d}\hat{\Omega}'\, \mathrm{d}v' \quad (3.26)$$

with $\nu_\eta = (\eta + 1)/\eta > 0$.

The term $\Sigma_{\alpha,\eta}$ acts here as an additional creation cross-section, whose associated creation operator $F_{\alpha,\eta}$ appears at the right hand side of the equation (with a delta-spectrum in energy and angle). Then, Eq. (3.25) can be solved by applying the power iteration similarly as done above. Observe in particular that Eq. (3.25) holds also for moderating materials, where $F_p\,\phi_\alpha$ vanishes: in this case, neutrons are promoted to the next generation of the power iteration algorithm only via the creation operator $F_{\alpha,\eta}$ [48].

Including *delayed* contributions [50] leads to

$$L_{\alpha,\eta}\,n_\alpha = \frac{1}{k}\left[F_p\,n_\alpha + F_{\alpha,\eta}\,n_\alpha + \sum_{i,j}\gamma_{i,j}\,F_d^{i,j}\,n_\alpha\right], \tag{3.27}$$

where again the factor $\gamma_{i,j} = \lambda_{i,j}/(\lambda_{i,j} + \alpha)$ in front of the $F_d^{i,j}$ terms acts as a population control tool. Observe however that now $\gamma_{i,j}$ introduces singularities in Eq. (3.27) at the values $\alpha = -\lambda_{i,j}$, α being negative. If we restrict our search to the dominant α eigenvalue, this implies that α must be found in the interval $-\lambda_\alpha < \alpha < 0$, where $\lambda_\alpha = \min_{i,j}\lambda_{i,j}$ is the smallest decay constant over all fissile isotopes and over all precursors families. Bearing this consideration in mind, the treatment of delayed neutrons proceeds as above, i.e., the weight of delayed neutrons is first multiplied by a factor $\gamma_{i,j}$ and then divided by a factor k before being assigned to the next generation.

3.3 Verification tests

The Monte Carlo method discussed above has just been recently implemented in the development version of the Monte Carlo code TRIPOLI-4 ®. Preliminary validation and verification tests have been satisfactory [42, 50].

The aim of this work is to verify and validate the α-k power iteration algorithm in some specific situations. We have seen in paragraph 3.1 that, under the hypothesis of minimum neutron speed $v_0 = 0$, the α spectrum contains a continuum half-plane. We have also seen that all discrete eigenvalue might disappear into the continuum, so that a fundamental α eigenvalue does not exist anymore, and the asymptotic decay is not exponential.
Then, what is the behaviour of the α-static code in this particular situation? Does it converge to any value and, if this is the case, can we associate a physical meaning to this value? What is the shape of the associated eigenfunction, if any? We shall try to answer these questions.

Actually, a word of caution is necessary here. As we said, the presence of a continuum portion in the spectrum $\sigma(A)$ intrinsically depends on the minimum neutron velocity v_0 being allowed to vanish, i.e., $v_0 = 0$. In industrial Monte Carlo codes, such as TRIPOLI-4 ®, this can not happen in practice: the tabulated continuous-energy cross sections typically assume that $E_0 \sim 10^{-5} eV$, whence $v_0 \sim 44\ m/s$. Then, v_0 being small but non-vanishing, a dominant eigenvalue surely exists and the questions above can not be simply answered within the code. For this reason, we have developed a specific (and simplified) α-static Monte Carlo code for testing the $\alpha - k$ algorithm. This allows also simple hypotheses and transport models to be checked separately, without being hindered by the full complexity of the TRIPOLI-4 ® code. The results of our α-static code have been verified against exact or numerical solutions, when available. Also, an analog dynamic Monte Carlo code has been developed, with the aim of performing dynamic simulations by following neutrons in time: this latter code has been used so as to validate the α-static algorithm. This work will be detailed in the following.

Chapter 4

Physical models for neutron transport in moderating materials

Our aim being the verification and validation of the α-static method, we look for reasonably simple nuclear systems where analytical or numerical solutions are easily available and can therefore be used as a reference. Starting from the full time-dependent Boltzmann equation, we will introduce a series of simplifications that will allow reaching our goal, yet retaining the key physical features of the systems at hand.
Under these assumptions, we will recall here the key results concerning the fundamental time eigenvalue and the associated fundamental eigenmode for such systems. Only moderating configurations will be examined. The results obtained in this chapter will be used in Chapter 5 to validate our α-static code.

We begin by considering the simplest possible case of neutron transport,

namely, the diffusion of *thermal neutrons* through a medium when multiplication (fission) is neglected.
Such situation occurs in the analysis of *asymptotic relaxation phenomena* in *neutron thermalization* [44, 17] . For instance, one may be interested in injecting a burst of neutrons in a sample,and measuring the subsequent decay of the neutron population as a function of time. Such pulsed-neutron experiments provide information about the neutron transport parameters (such as the diffusion coefficient) and have been extensively performed in the sixties so as to characterize various moderating materials, such as water or graphite [13].

We begin our analysis by considering the diffusion of one-speed neutrons in an infinite medium. Then, we take into account finite-size effects by introducing the simplest possible leakage model, the so-called *rod model*. Next we address the thermalization of continuous-energy neutrons in two different kinds of moderators: the hydrogen-based moderators and the crystalline moderators. Finally, we treat the case of *fast neutrons* transport.

4.1 One-speed neutron diffusion

4.1.1 Infinite medium

In the case of one-speed transport in an infinite homogeneous medium, cross sections are constant and Eq. 2.1 simplifies to:

$$\frac{\partial}{\partial t}n(t) + \Sigma_t v n(t) = \Sigma_s v n(t), \tag{4.1}$$

where $n(t) = \int_{4\pi} n(\hat{\Omega}, t)\mathrm{d}\hat{\Omega}$ is the neutron density integrated over directions. Note also that, in this simple case, the cross sections become constants. The one-speed transport model is quite trivial, yet provides a rough idea of the

asymptotic time behaviour of a moderating system.

Recalling equation 4.1, and observing that $\Sigma_t = \Sigma_s + \Sigma_a$, we simply have

$$n(t) = n_0 e^{-\Sigma_a v t}, \tag{4.2}$$

where $n_0 = n(t = 0)$ is the initial condition for the neutron density. Neutrons disappear from the system with a decay constant equal to the absorption rate: this means that $\alpha_0 = -\Sigma_a v$, which provides a first elementary check for α-static methods.

4.1.2 The rod model

In order to go a step further in our analysis, we must include finite-size effects due to spatial boundaries. To simplify the matter, we will consider the so-called rod model. Neutrons move on a 1-dimensional interval [0,L], where only two directions are allowed (forward and backward). Moreover, we assume that scattering is isotropic. The system has been extensively used in reactor physics [17, 30, 46, 48, 49] because it is rather easily amenable to analytical solutions and yet retains the key mechanisms of leakages from the boundaries.

The Boltzmann equation for rod model degenerates in two coupled linear differential equations for the two components of the angular density, namely,

$$\frac{\partial}{\partial t} n^+(x,t) + \Sigma_t v n^+(x,t) + v \frac{\partial}{\partial x} n^+(x,t) = \frac{1}{2} \Sigma_s v [n^+(x,t) + n^-(x,t)] \tag{4.3}$$

$$\frac{\partial}{\partial t} n^-(x,t) + \Sigma_t v n^-(x,t) - v \frac{\partial}{\partial x} n^-(x,t) = \frac{1}{2} \Sigma_s v [n^+(x,t) + n^-(x,t)] \tag{4.4}$$

where $n^+(x,t) = n(x, \hat{\Omega} = +, t)$, $n^-(x,t) = n(x, \hat{\Omega} = -, t)$ and x is the spatial coordinate oriented in the forward direction.

Considering leakage, we can impose the boundary conditions:

$$n^+(0,t) = 0 \tag{4.5}$$

$$n^-(L,t) = 0 \tag{4.6}$$

Observe that we have here used the hypothesis of isotropy for the scattering term: half of the neutrons coming from a collision are re-emitted in the forward direction, and half in the backward direction, whence the 1/2 factor appearing in front of the diffusion cross-section.

We seek then separate-variable solutions of the form $n^{\pm}(x,t) = n^{\pm}(x)e^{\alpha t}$. Replacing this functional form into equations (4.3) and (4.4), we obtain the system

$$+ v\frac{\partial}{\partial x}n^+(x) + \Sigma_t v n^+(x) + \alpha n^+(x) = \frac{1}{2}\Sigma_s v(n^+(x) + n^-(x)) \tag{4.7}$$

$$- v\frac{\partial}{\partial x}n^-(x) + \Sigma_t v n^-(x) + \alpha n^-(x) = \frac{1}{2}\Sigma_s v(n^+(x) + n^-(x)). \tag{4.8}$$

Montagnini and Pierpaoli [30] have shown that the α eigenvalue spectrum of the one-speed isotropic rod model is composed of a finite, non-void set of real eigenvalues and an infinite set of pairs of complex conjugates eigenvalues (falling in pairs). It is actually possible to find a dispersion relation $\Lambda(\alpha) = 0$ whose roots are the discrete α-eigenvalues [46] by solving the system of equations 4.7 and 4.8.

Equations 4.7 and 4.8 are homogeneous, so that the trivial solutions $n^+ = n^- = 0$ are possible and satisfy the boundary conditions. Searching for non-trivial solutions, and imposing boundary conditions, leads to a determinant equation for the α-eigenvalues, in the form $\Lambda(\alpha) = 0$, i.e., a dispersion relation [48]. Carrying out the calculations leads to

$$\cosh\left(L\Sigma_t\sqrt{\frac{\alpha}{v\Sigma_t}\left(\frac{\alpha}{v\Sigma_t}-1\right)}\right)+\frac{\left(\frac{\alpha}{v\Sigma_t}-\frac{1}{2}\right)\sinh\left(L\Sigma_t\sqrt{\frac{\alpha}{v\Sigma_t}\left(\frac{\alpha}{v\Sigma_t}-1\right)}\right)}{\sqrt{\frac{\alpha}{v\Sigma_t}\left(\frac{\alpha}{v\Sigma_t}-1\right)}}=0, \tag{4.9}$$

whose numerical roots are precisely the α-eigenvalues of our system.
Eq. (4.9) relates the physical parameters of the system to the α-eigenvalues. Based on physical considerations, the dominant α must be negative: the neutron population comes to extinction because of leakage and absorption. The full α-eigenvalue spectrum can be easily obtained by either numerically searching for the roots of Eq. (4.9), or discretizing Eqs. (4.7) and (4.8) and finding the eigenvalues of the corresponding matrix. A qualitative picture of the spectrum is shown in figure 4.1.

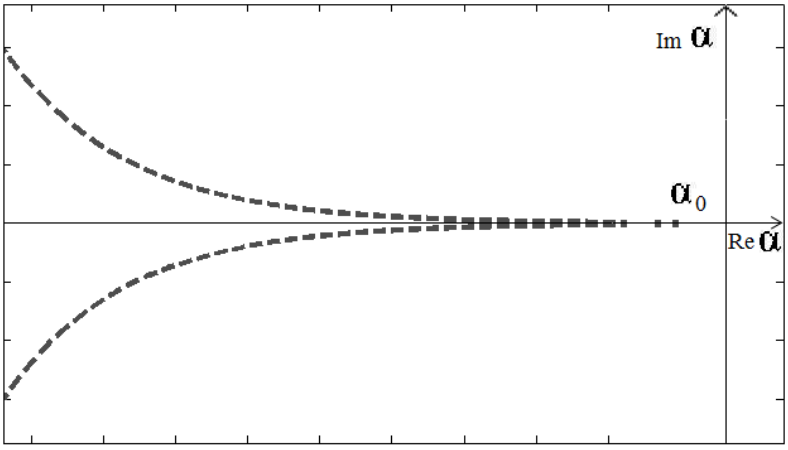

Fig. 4.1: α-eigenvalue spectrum of the rod model for one-speed neutron transport

The one-speed rod model has been successfully used in [46] for the verification of the α-static method.

4.2 Neutron thermalization

We move now to the more realistic case of neutron thermalization, where particles are allowed to change their speed at each collision with the surrounding nuclei. In this case, the neutron density depends on speed, and cross sections are also (generally speaking) speed-dependent. We will use in this paragraph the functional forms for the cross sections and the scattering kernel that are characteristic of the hydrogen-based moderators.

4.2.1 Infinite medium

We begin by considering the neutron thermalization in an infinite medium. Recalling Eq. (2.1) and making use of the hypothesis of isotropic scattering allows integrating $n(x, v, \hat{\Omega})$ over all directions, which yields

$$\frac{\partial}{\partial t} n(v,t) + v\Sigma_t(v) n(v,t) = \int_0^\infty v'\Sigma_s(v' \to v) n(v',t) \mathrm{d}v' \tag{4.10}$$

Since we consider a pulsed source at $t = 0$, the source term does not explicitly appears in Eq. (4.10) and is present only in the initial condition. As customary, we look for solutions of the form $n(t) = n_0(v)e^{\alpha t}$: by replacing this functional form in Eq. (4.10), we obtain:

$$\alpha n(v) + v\Sigma_t(v) n(v) = \int_0^\infty v'\Sigma_s(v' \to v) n(v') \mathrm{d}v'. \tag{4.11}$$

This equation can be rewritten in a compact form as:

$$\alpha n(v) = L\, n(v), \tag{4.12}$$

where L is the Boltzmann operator for neutron transport in an infinite

medium, in the absence of multiplication, namely,

$$L = -v\Sigma_t(v) + \int_0^\infty v'\Sigma_s(v' \to v)\mathrm{d}v'. \tag{4.13}$$

Equation (4.12) is formally an eigenvalue problem of the same kind studied in Chapter 3. The general features of the eigenvalue spectrum can be inferred by resorting to the analysis of the operator L, as discussed in Chapter 3. Here we recall some useful properties: the spectrum of the Boltzmann operator is composed of:

- a set of real discrete eigenvalues in the interval $(\alpha^*, 0]$, where $\alpha^* = -\min_{v\epsilon[0,\infty)}[v\Sigma_t(v)]$;
- a continuous spectrum $\mathrm{C} = (-\infty, \alpha^*]$.

A qualitative picture of the spectrum is shown in figure 4.2.

The discrete eigenvalues are associated to regular eigenfunctions that actually correspond to a form of neutron density $n(v,t)$ that is separable in velocity and time. When the discrete set is not empty, the larger of these eigenvalues is the inverse of the fundamental time constant of the system and the associated eigenfunction will provide the asymptotic time behaviour of the neutron density. We have seen that the smallest possible value for a discrete eigenvalue is equal to $-\min_{v\epsilon[0,\infty)}[v\Sigma_t(v)]$, that is the opposite of the minimum collision frequency. This intuitively means that the neutron distribution can not decay faster than the infinitesimal group of neutrons with the smallest possible collision rate [13]. Usually, this value is attained for $v \to 0$.

The precise details of the eigenvalue spectrum, in particular of the discrete set, depend on the explicit form of the scattering kernel. If we restrict

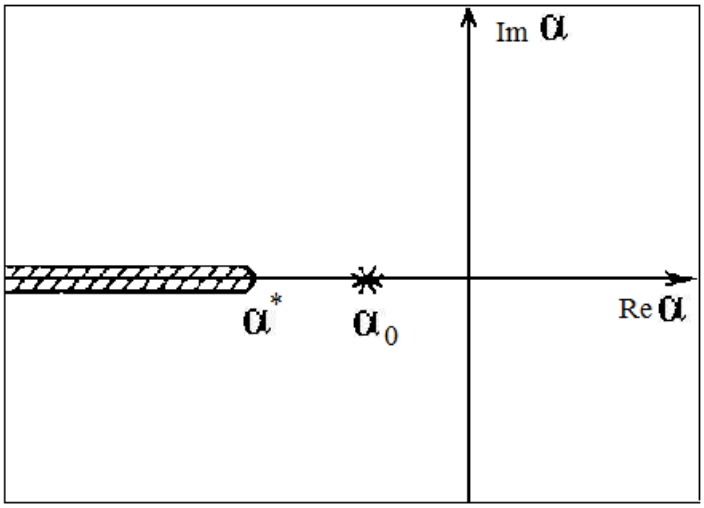

Fig. 4.2: α-eigenvalue spectrum for the neutron thermalization in an infinite moderating medium

our attention to the thermalization process, i.e., the interaction between the neutrons and the nuclei at thermal equilibrium, the scattering kernel must satisfy the detailed balance:

$$vM(v)\Sigma_s(v \to v') = v'M(v')\Sigma_s(v' \to v), \tag{4.14}$$

where $M(v)$ is the Maxwell-Boltzmann distribution with most probable speed v_T

$$M(v) = \frac{4}{\sqrt{\pi}v_T^3}v^2e^{-v^2/v_T^2} \tag{4.15}$$

and $\Sigma_s(v \to v')$ depends on the structural properties of the nuclei in the traversed medium.

Corngold and Kuscer [13] have thoroughly examined how the different correlation functions for a gas, a liquid and a solid are reflected in the behaviour of the differential cross sections $\Sigma_s(v \to v')$ at low energy, and their impact

on the eigenvalue spectrum. We summarize here their results:

- *Non-absorbing material.* When the absorbing cross section vanishes (Σ_a=0), it is possible to show that the only solution to Eq. (4.11) is just the Maxwell-Boltzmann distribution $M(v)$ at the temperature T of the host medium.

  The corresponding fundamental eigenvalue is simply $\alpha = 0$. Neutron density does not evolve in time, in the absence of leakages and absorptions.

- $1/v$ *absorption.* If the absorption cross section is of the kind $\Sigma_a(v) \propto 1/v$ over all speeds, the absorption rate $\Sigma_a(v)v$ is constant. Then, it can be shown [3] that the Maxwellian distribution is still a solution of Eq. (4.11), and the fundamental discrete eigenvalue is equal to $\alpha = -v\Sigma_a(v)$. After a possible transient, the neutron density asymptotically approaches a Maxwell Boltzmann distribution, whose amplitude decreases exponentially in time, with a time constant equal to the absorption rate:

$$n(v,t) = e^{-\Sigma_a(v)vt} M(v). \tag{4.16}$$

- *Non-*$1/v$ *absorption.* When the absorption rate is not constant, the discrete eigenvalue set can significantly change and it is even possible for the discrete set to be empty. The shape of the spectrum is related to the particular properties of the scattering kernel, which in turn depend on the type of material:

  - *Gaseous moderator.* For a gaseous moderator, it has been shown [13] that there exists an infinite set of discrete decay constants, accumulating towards the lower limit α^*. In theory, it is possible to have an empty set, but only by introducing an absorption section

differing violently from the $1/v$ law in the small-v range. This in practice never happens for gases.

– *Solid moderator.* For a solid moderator, the decay constants are finite in number (usually, only a few α_j or sometimes just the fundamental eigenvalue). Moreover, by introducing an absorption rate that increases sufficiently strongly with v, the discrete eigenvalue set can be empty.

These results show that the loss of discrete eigenvalues is caused by absorption rates increasing with speed. When this is the case, fast neutrons disappear from the system sooner than the slow neutrons: the neutron density undergoes an *absorption cooling* [10]. Usually, the competition between the thermalization process and the absorption cooling eventually leads to an asymptotic speed distribution (the fundamental eigenmode). However, if the fast neutron absorption is too strong, the thermalization process is not able to compete with absorption cooling and the neutron distribution degenerates into a singular mode (containing a $\delta(v)$ term) where a finite fraction of the population is to be found at $v = 0$.
We are going now to introduce a particular scattering kernel that makes possible to explicitly observe the disappearance of discrete constant decay due to absorption cooling [10].

The analysis of the spectrum of the Boltzmann operator for moderating materials is made simpler if we introduce a separable scattering kernel of the form [17]:

$$\Sigma_s(v' \to v) = \beta v \Sigma_s(v) M(v) \Sigma_s(v'), \tag{4.17}$$

where β is a normalization constant defined as $\beta^{-1} = \int_0^\infty v\Sigma_s(v)M(v)\mathrm{d}v$. The kernel of equation (4.17) does not correspond to any physical model but

it has the useful property of giving the correct total cross section and of satisfying detailed balance [17, 44]. This kernel is sometimes known as the *amnesia kernel* because the scattering probability $p(v' \to v)$ is independent of the initial velocity of the neutron and thus the scattering spectrum has no knowledge of how it was produced [44].
If we replace (4.17) into Eq. (4.11), we obtain

$$[\alpha + v\Sigma_t(v)]n(v) = \beta v\Sigma_s(v)M(v)\int_0^\infty v'\Sigma_s(v')n(v')\mathrm{d}v' \tag{4.18}$$

If we search for the discrete eigenvalues, we know that the term $[\alpha + v\Sigma_t(v)]$ is not zero [17]. We can divide (4.18) by this term, then multiply by $[v\Sigma_s(v)]$ and integrate over all velocity values. We find that the discrete time constants must satisfy the dispersion relation [17]:

$$\Lambda(\alpha) = 1 - \beta\int_0^\infty \frac{[v\Sigma_s(v)]^2 M(v)}{\alpha + v\Sigma_t(v)}\mathrm{d}v = 0. \tag{4.19}$$

The dispersion relation allows to find the discrete eigenvalues, by analytic or numerical methods. We will make an extensive use of this relation for our verification tests in the next chapter .

4.2.2 Bounded medium

We now turn our attention to the more general problem of neutron diffusion in a finite non-multiplying medium. Specific geometries, such as spheres, slabs, and so on, have been extensively considered in literature [32]. Before proceeding to the analysis of the rod-model geometry, we begin by recalling some general results concerning the eigenvalue spectrum of the Boltzmann

operator in three dimensions.

We rewrite the Boltzmann equation for the finite homogeneous case:

$$\frac{\partial}{\partial t}n(\vec{r},v,\hat{\Omega},t)+v\hat{\Omega}\cdot\nabla n(\vec{r},v,\hat{\Omega},t)+v\Sigma_t(v)n(\vec{r},v,\hat{\Omega},t)= \int_0^\infty\int_{4\pi}\Sigma_s(v'\to v,\hat{\Omega}'\to\hat{\Omega})v'n(\vec{r},v',\hat{\Omega}',t)\,\mathrm{d}\hat{\Omega}'\,\mathrm{d}v'. \quad (4.20)$$

Eq. 4.20 depends on the space variable and we must also include the boundary conditions. For the transport equation, it is common to impose the free-surface boundary conditions: this means that neutrons can not re-enter from the system boundaries.

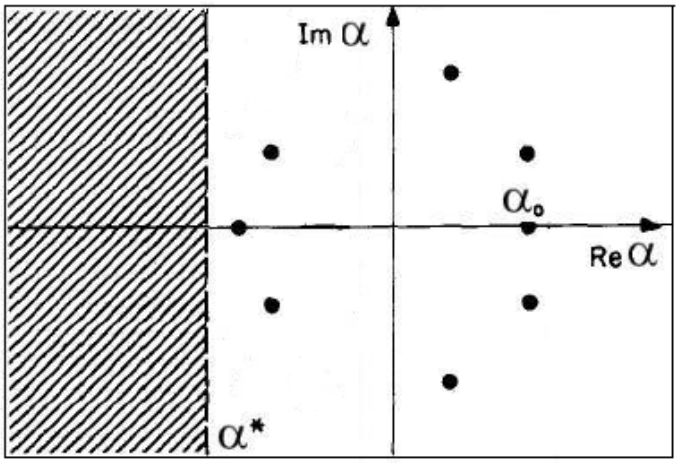

Fig. 4.3: α-eigenvalue spectrum for the neutron thermalization in a bounded moderating medium

The streaming term $\hat{\Omega}\cdot\nabla$ in the equation makes the analysis of the spectrum much more difficult. A qualitative representation of this spectrum

is reported in figure 4.3. It can be shown [3, 44] that the smallest discrete eigenvalue α_0 must lie in the region

$$\alpha_0 \geq -\lim_{v\to 0}[v\Sigma_t(v)]. \tag{4.21}$$

Although this condition has a different origin from the one discussed above for the infinite case, for typical moderators, the behaviour of cross-sections in the small-v range is such that this condition coincides with that of infinite domains, namely :

$$\min_{v\epsilon[0,\infty)}[v\Sigma_t(v)] = \lim_{v\to 0}[v\Sigma_t(v)]. \tag{4.22}$$

However, while the minimum collision frequency is a physical bound for the discrete dominant eigenvalue for infinite domains, in the case of finite domains the discrete spectrum can be empty. Indeed, it can be shown that the discrete dominant eigenvalue decreases monotonically with the system dimension, if the other physical parameters are left unchanged. Therefore, there must exist a *critical dimension* of the system where

$$\alpha_0 = -\lim_{v\to 0}[v\Sigma_t(v)]. \tag{4.23}$$

If the system size is further reduced below this limit, the discrete eigenvalue disappears into the continuum. This has been confirmed by rigorous analysis of scattering models in both solids and gases.

In the previous section, we have seen that the disappearance of the fundamental mode can occur in an infinite medium because of a non-constant absorption rate, which leads to a cooling of the speed spectrum. The leakage term is actually responsible for a similar effect: in fact, the neutrons with larger speed may escape more easily from the medium. This effect is known as *diffusion cooling*, because the net result of this preferential leakage is to shift the neutron spectrum towards energies lower than those of a

Maxwellian distribution at the temperature of moderator. There is again a competition between two opposite effects: leakage and energy transfer. The former cools down the neutron spectrum, whereas the latter one tends to restore the Maxwellian distribution. When an equilibrium between these two phenomena is reached, a fundamental mode exists, with an associated dominant time decay constant. On the contrary, if the escape rate is too strong, the equilibrium is broken and no discrete eigenvalue exists.

4.2.3 The minimum neutron speed

Before concluding the discussion about the pure thermalization case, we have to make some clarifications about the continuum part of the spectrum.
Until now, we have implicitly assumed that the minimum possible neutron speed is zero, e.g. the Maxwellian energy distribution is defined between zero and infinity. If we impose a cut-off on the minimum neutron speed $v_0 > 0$, it can be demonstrated [28] that the continuum spectrum part does not exist any more.
We have understood that the possible disappearance of the fundamental mode must be due to the zero-speed neutrons. It seems that, when the faster neutrons quickly disappear from the system (diffusion or absorption cooling), the existence of zero-speed neutrons, whose flight time is very long (possibly infinite) , generates a sort of conflict, which leads to the loss of a regular behaviour.
However, we have to remember that the limit of zero neutron velocity does not satisfy the conditions for the applicability of the transport equation [32]. In fact, the Boltzmann equation can be used only to describe the motion of classical particles; but, in the zero velocity limit, the De Broglie wavelenght for neutrons is no more negligible. Hence, we should include quantum me-

chanic calculation in transport theory [32].

The scientific literature is divided on this point. Larsen [28] asserts that a theory with a cut off on the minimum possible velocity is closer to the physical reality. On the contrary, Nelkin [32] says that including the uncertainty principle would not change the results previously discussed. The fact that the disappearance of an exponential time behaviour has been observed [44] in some experiments bring us to agree with the physical analysis of Nelkin.

4.2.4 The rod model equations

For the case of the one-dimensional rod model, Eq. 4.20 greatly simplifies. In fact, as shown before, the term $\hat{\Omega} \cdot \nabla$ can be split into two simple spatial derivatives: $\pm\frac{\partial}{\partial x}$. Moreover, with the hypothesis of isotropic separable scattering kernel previously introduced, the equations become

$$\frac{\partial}{\partial t}n^+(x,v,t) + v\Sigma_t n^+(x,v,t) + v\frac{\partial}{\partial x}n^+(x,v,t) = \beta v\Sigma_s(v)M(v)\int_0^\infty \frac{1}{2}v'\Sigma_s(v')(n^+(x,v',t)+n^-(x,v',t))\mathrm{d}v' \quad (4.24)$$

$$\frac{\partial}{\partial t}n^-(x,v,t) + v\Sigma_t n^-(x,v,t) - v\frac{\partial}{\partial x}n^-(x,v,t) = \beta v\Sigma_s(v)M(v)\int_0^\infty \frac{1}{2}v'\Sigma_s(v')(n^+(x,v',t)+n^-(x,v't))\mathrm{d}v', \quad (4.25)$$

together with the boundary conditions:

$$n^+(0,v,t) = 0 \quad (4.26)$$

$$n^-(L,v,t) = 0 \quad (4.27)$$

We search for separate-variable solutions of the type $n(x,v,t) = n(x,v)e^{\alpha t}$. Then, substituting this functional form into equations 4.24 and 4.25 we find

$$+ v\frac{\partial}{\partial x}n^+(x,v) + v\Sigma_t n^+(x,v) + \alpha n^+(x,v) = \frac{\beta}{2}v\Sigma_s(v)M(v)\int_0^\infty v'\Sigma_s(v')(n^+(x,v') + n^-(x,v'))\mathrm{d}v'. \quad (4.28)$$

$$- v\frac{\partial}{\partial x}n^-(x,v) + v\Sigma_t n^-(x,v) + \alpha n^-(x,v) = \frac{\beta}{2}v\Sigma_s(v)M(v)\int_0^\infty v'\Sigma_s(v')(n^+(x,v') + n^-(x,v'))\mathrm{d}v'. \quad (4.29)$$

The simple form of equations 4.28 and 4.46 allows explicit results concerning the eigenvalue spectrum to be derived.

4.3 Neutron thermalization and Bragg scattering

In section 4.2.1, we have shown two important features concerning the discrete eigenvalue set of a bounded system:

- the greatest discrete eigenvalue can not be smaller than the Corngold limit α^*;
- there exists a minimum system size L^* such that no discrete eigenvalues exist for systems smaller that the critical size; this implies that the asymptotic time behaviour of neutron flux is not exponential in these small systems.

However, some pulsed neutron experiments in polycrystalline moderators have shown a discrepancy between theory and experiments. In fact, some experimental works have found, for very small systems, a good exponential decay with decay constant smaller than $|\alpha^*|^{-1}$. A considerable amount of theoretical work has been motivated by this apparent lack of coherence.

Conn and Corngold [10, 11] have found a good explanation for the experimental results using the *asymptotic reactor theory*, which is a good approximation only for systems whose dimensions are much larger than a mean free path (as it would be clear in a while) but has turned out to be a successful tool to study moderators with Bragg scattering.
The asymptotic reactor theory supposes a separable solution of the form

$$n(\vec{r}, v, \hat{\Omega}, t) = n_B(v, \hat{\Omega}, t)e^{i\vec{B}\cdot\vec{r}}, \tag{4.30}$$

where $|\vec{B}|$ is a fixed, real number. The idea behind the asymptotic reactor theory is to expand the solution in a Fourier series of spatial modes, each indexed by a different B. In practice, however, one makes the hypothesis that a single value of B suffices to characterize the spatial shape of the fundamental eigenmode [17, 44]. This particular value of B takes the name of *geometrical buckling* and satisfies: $|\vec{B}| \approx \pi/L$, where L is a characteristic dimension of the system.

If we applied this theory to the study of moderators with *regular* scattering kernel, like those analyzed in chapter 4.2, we would find a *critical buckling* B^* in correspondence of the critical size L^*. The Corngold theorem [12, 13] asserts that no discrete eigenvalues exist for systems characterized by a buckling larger than B^*; notice that the theorem is equivalent to the condition on the critical size discussed in chapter 4.2.1.

Returning to polycrystalline moderators, the experiments seem to prove that the *maximum B theorem* is not valid: a particular elastic coherent scattering occurring in crystalline materials, the *Bragg scattering* is responsible for the discrepancy between theory and experiments.

The Bragg scattering cross section has a step behaviour and vanishes below a characteristic speed, the Bragg cut-off v_b. In this interaction, the neutron does not change its speed. Therefore, in the hypothesis of isotropic Bragg scattering, we have to add to the scattering kernel a term of the type

$$\hat{S_B} = \int_0^\infty \delta(v - v')v'\Sigma_b(v')\mathrm{d}v' \tag{4.31}$$

where $\Sigma_b(v')$ is defined only for $v \geq v_B$.

The real behaviour of this scattering cross sections is quite complicated because it exhibits a series of finite discontinuities. We are going to use a simpler description of this interaction, like Conn and Corngold did [10, 11].

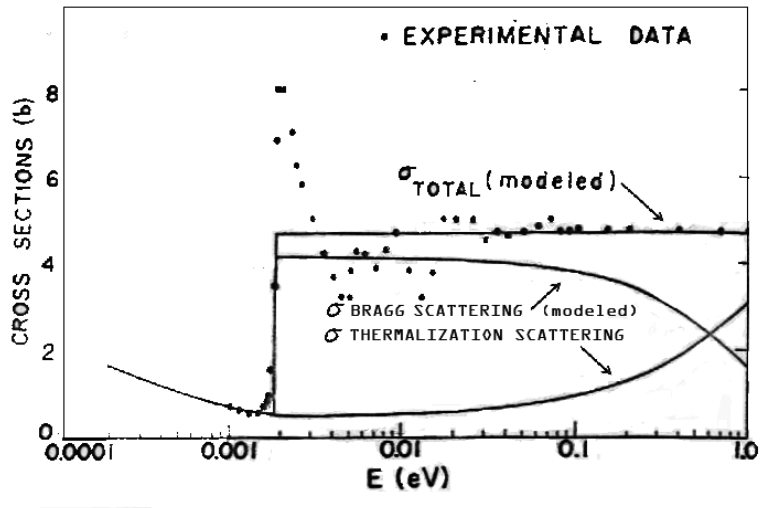

Fig. 4.4: Cross-sections modeling for crystalline moderators

The thermalization kernel is modeled with the simple separable kernel previously introduced 4.17 and a simple model of Bragg scattering is introduced. The scattering cross-section used are illustrated in Figure 4.4. As indicated, the total cross section is assumed constant above the Bragg cut-off while the Bragg cross section tends to zero at high energies. The thermalization cross section is of type $1/v$ at low energies and slowly re-increases at high energies.

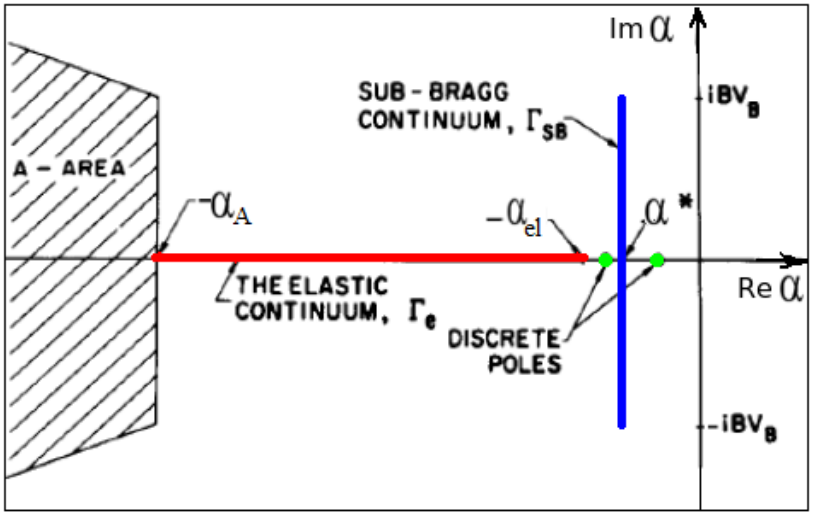

Fig. 4.5: The α-eigenvalue spectrum for crystalline moderators

Summarizing, for a three-dimensional bounded polycrystalline medium, the equation becomes:

$$\frac{\partial}{\partial t}n(\vec{r},v,\hat{\Omega},t) = (S + S_B - A - L)n(\vec{r},v,\hat{\Omega},t) \tag{4.32}$$

where S_B is the Bragg scattering operator. If we suppose a solution of the form $n(\vec{r},v,\hat{\Omega},t) = n_B(v,\hat{\Omega},t)e^{i\vec{B}\cdot\vec{r}}$, substitute it into the equation and use Laplace transform technique [10], we can find that the α plane structure is

similar to that of figure 4.5.

We find:

- The area to the left of $\alpha_A = -\min_{v\epsilon[v_b^+,\infty)}[v\Sigma_T(v)]$ is the set defined by

$$\alpha + v\Sigma_T(v) + iBv\mu = 0 \tag{4.33}$$

(where μ is the cosine between the buckling vector and the velocity) for $v > v_B$. It reflects the nature of $\Sigma_T(v)$ above the Bragg cutoff. This area can become fragmented if we account for the small discontinuities in $\Sigma_T(v)$ caused by higher order Bragg reflections.

- The vertical line cut at $\alpha^* = -\min_{v\epsilon[0,\infty)}[v\Sigma_T(v)]$ is a result of the constant collision frequency below the Bragg cutoff. It is therefore called the *sub-Bragg continuum*, Γ_{SB}. It is also defined by Eq. 4.33 for $0 \leqslant v \leqslant v_B$ and it is disjoint from the area because $\Sigma_T(v)$ is discontinuous at v_B. If we abandon the hypothesis of constant collision frequency below the Bragg cutoff, the line is expanded into a narrow area, extending along the real axis from α^* to $Re\{\alpha\} = -v_B[\Sigma_s(v_B) + \Sigma_a(v_B)]$ (where Σ_s does not include the Bragg scattering).

- The horizontal line defined by

$$1 - \frac{\Sigma_B(v)}{B}\tan^{-1}\frac{Bv}{\alpha + v\Sigma_T(v)} = 0 \tag{4.34}$$

is the *elastic continuum* Γ_e. The maximum value of this set is $\alpha_{el} = -\min_{v\epsilon[v_B^+,\infty)}\alpha(B^2, v_B)$ and it is obtained when $\Sigma_T(v)$ and $\Sigma_B(v)$ are evaluated just above the Bragg cutoff. Note that, for fixed v, Eq. 4.34 has the form of the one-velocity dispersion law and proves the one-speed nature of Bragg-scattered neutrons.

- A set of discrete eigenvalues that must be real and negative but are not necessarily bounded by α^*. By examining figure 4.5, we see it is as usual possible for discrete eigenvalues to exist between the origin and α^* and, as well, in the gap between Γ_{SB} and Γ_e. Those in the gap will have magnitude greater than α^* and be bounded by the edge of the elastic continuum, $\alpha_{el}(B^2)$.

The final statement contradicts the maximum B theorem, but this is not really shocking because in order to prove it we need to assume some cross sections features; these features are not respected by Bragg cross section because of its discontinuity. The appearance of gaps makes the statement of the theorem a little different. There is now a critical buckling B^{*2} , such that, if $B^2 > B^{*2}$, an exponential can be observed and any discrete eigenvalue which exists is $\alpha < \alpha^*$, and a critical buckling B^{**2}, such that if $B^2 > B^{**2}$, no discrete eigenvalues exist. However, even when isolated discrete eigenvalues exist for $B^2 > B^{*2}$, the exponential behaviour is no longer dominant at long times. It can be shown [10] that the eigenfunction associated with a discrete eigenvalue $< \alpha^*$ cannot be everywhere positive and thus cannot dominate the solution at long times. The asymptotic behavior of the neutron density cannot be described by this eigenfunction alone: there must be a continuum contribution.

We can now compare the theoretical eigenvalues and the experimental measured time decay constants α_0:

- When $\alpha_0 > \alpha^*$, the exponential behaviour observed in the laboratory may be immediately associated with the fundamental eigenvalue.

- When $\alpha_{el} < \alpha_0 < \alpha^*$, an exponential decay could be observed in lab-

oratory but its interpretation is not so simple. We have now to take into account three contributions: the discrete eigenvalue, the sub-Bragg continuum contribution, the elastic continuum contribution (the area continuum contribution can be neglected because it vanishes much too rapidly). If $B^2 \gtrsim B^{*2}$, α_0 is "far" from α_{el} and the decay is well represented by the contributions of the discrete pole and Γ_{SB}. In this case, it can be observed an exponential decay but it is followed, at very long times, by non-exponential behaviour, due to Γ_{SB}.
As the size of system is reduced, both α_0 and $\alpha_e l$ become more negative, but their difference vanishes. The contribution of the discrete eigenvalue becomes less important, until a "mode-switching" occurs and the decay is described by the contributions from Γ_e and Γ_{SB}.

- If the system size is too small, no more exponential behaviour is observed. It means that the discrete eigenvalue has disappeared and the spectrum is made of only continuous sets.

The unexpected results of diffusion experiments in poly-crystals have been explained with the asymptotic reactor theory. We should now ask if these conclusions are still valid including the correct boundary conditions. There are a lot of discussions about this point in the scientific literature [28, 16, 27, 5, 4]. In fact, the construction of a rigorous transport theory turns out to be quite insidious as depending on the existence domain chosen for the eigenfunctions. Generally speaking, the results found for transport theory are similar to those obtained in the asymptotic approximation [4].

4.4 Slowing down and thermalization

A very important class of transport phenomena involves the slowing down of fast particles as they move through a host medium. If the energy of the particles is much larger than thermal energy of the host material, it is fair to ignore the microscopic motion of the particles comprising the host and to treat all interactions as if the energetic particles collided with particles which are at rest. In such interactions the energetic particles can only lose energy and the upscattering in energy can be ignored. Such *superthermal* particle transport problems arise in a variety of applications such as the slowing down of fission neutrons (with initial energy of $10^6\ eV$), but also the transport of energetic charged particles through matter and the thermalization of energetic particles in gases or plasmas.
The simplification of ignoring the motion of the background atoms considerably changes the mathematical nature of the appropriate form of the transport equation from that we encountered in thermalization problems. In particular, the neglect of microscopic motion in the host material greatly simplifies the form of the scattering kernel. Indeed, on occasion it even allows for an analytical treatment of the transport process.

We now introduce the new operators of fission and slowing down. The transport equation describing fast neutrons moving in a three dimensional bounded system is

$$\frac{\partial}{\partial t}n + v\hat{\Omega}\cdot\nabla n + v\Sigma_t(v) = S\,n + S_{SD}\,n \tag{4.35}$$

where $n(\vec{r}, v, \hat{\Omega}, t)$ depends on space, direction, velocity and time, S is the usual thermalization scattering operator and S_{SD} is the *slowing down* scat-

tering operator.

Because of the lack of upscattering, the integral slowing down operator is of the form:

$$S_{SD} = \int_v^\infty K(v, v')dv'$$

and so it differs from S for the extremes of integration: the lower bound is no more zero. Nicolaenko [33] has proven that this operator has the following properties:

- it is completely continuous, therefore possessing no continuous spectrum
- it has no eigenvalue spectrum except for the point at infinity.

We can give a physical explanation for these properties [17]. The existence of eigenvalues, that is, of nontrivial solutions f for the problem $S_{SD}\, n_\alpha = \alpha n_\alpha$ implies physically that the scattering operator is able to *regenerate* or *preserve* the energy spectrum of $n(v)$. But the absence of upscattering implies that S_{SD} always generates an energy spectrum with a lower average energy. Hence the slowing down kernel in the fast regime is incapable of maintaining an equilibrium energy spectrum; that is, the corresponding scattering operators have an empty point eigenvalue spectrum.
In our models, we will use a slowing down scattering operator of the form

$$S_{SD} = v\Sigma_{sd} \int_v^\infty \frac{const}{v'} dv' \tag{4.36}$$

which takes into account:

- the absence of upscattering;
- a cross section Σ_{sd} constant in the slowing down range;

- an uniform energy distribution after scattering. It means that a neutron with an initial energy E', after a scattering, will have a new energy E between $0 \leq E \leq E'$, with equal probability. We have to clarify that this is exactly correct only for scattering with hydrogen: the neutron can lose its whole energy ($E = 0$) with a single collision only if the target has its same mass (mass number $A \simeq 1$). We rewrite this condition in term of the velocity probability density:

$$p(E' \to E)dE = p(v' \to v)dv, \tag{4.37}$$

$$p(v' \to v) = p(E' \to E)\frac{dE}{dv} = \frac{1}{E'}\frac{dE}{dv}$$

Substituting $E = \frac{1}{2}mv^2$, we finally obtain:

$$p(v' \to v) = \frac{2v}{v'^{\,2}}$$

Under these hypothesis, the slowing down scattering operator

$$S_{SD} = \int_v^\infty \Sigma_s v' p(v' \to v)dv'$$

assumes the form of Eq. (4.36) with $const = 2$.

We recall here the form of the thermalization scattering operator has the form:

$$S = \beta v \Sigma_s(v) M(v) \int_0^\infty \Sigma_s(v')v'dv' \tag{4.38}$$

Note that the thermalization scattering operator can provide both a *downscattering* and an *upscattering* mechanism. The latter can *regenerate* the energy spectrum and create point eigenvalues, as seen in paragraph 4.2.

We shall rewrite the Eq. (4.35) for an infinite medium and for the rod model.

4.4.1 Infinite medium

We begin by consider the fast neutron transport in an infinite medium. Recalling Eq. (4.35), the form of scattering operators previously introduced and making use of the hypothesis of isotropic scattering allows integrating $n(\vec{r}, v, \hat{\Omega}, t)$ over all directions, which yields:

$$\frac{\partial}{\partial t} n(v,t) + v\Sigma_t(v) n(v,t) = \\ = 2v\Sigma_{sd} \int_v^\infty \frac{n(v',t)}{v'} dv' + \beta v \Sigma_s(v) M(v) \int_0^\infty \Sigma_s(v') v' n(v',t) dv'. \quad (4.39)$$

Since we consider a pulsed source at $t = 0$, the source term does not explicitly appear in Eq. (4.39) and is included in the initial condition. As customary, we look for solutions of the form $n(v,t) = n(v)e^{\alpha t}$: by replacing this functional form in Eq. (4.39), we obtain:

$$[\alpha + v\Sigma_t(v)] n(v) = 2v\Sigma_{sd} \int_v^\infty \frac{n(v')}{v'} dv' + \beta v \Sigma_s(v) M(v) \int_0^\infty \Sigma_s(v') v' n(v',t) dv'. \quad (4.40)$$

4.4.2 The rod model

We direct now our attention to the one-dimensional rod model. As usual, Eq. (4.35) greatly simplifies: the term $\hat{\Omega} \cdot \nabla$ can be split into two simple derivatives: $\pm \frac{\partial}{\partial x}$. Adding the slowing down operator, the rod model equations become:

$$\frac{\partial}{\partial t}n^+(x,v,t) + v\Sigma_t n^+(x,v,t) + v\frac{\partial}{\partial x}n^+(x,v,t) = v\Sigma_{sd}\int_v^\infty \frac{n^+(x,v',t)+n^-(x,v',t)}{v'}dv' + \beta v\Sigma_s(v)M(v)\int_0^\infty \frac{1}{2}v'\Sigma_s(v')(n^+(x,v',t)+n^-(x,v',t))\mathrm{d}v' \quad (4.41)$$

$$\frac{\partial}{\partial t}n^-(x,v,t) + v\Sigma_t n^-(x,v,t) - v\frac{\partial}{\partial x}n^-(x,v,t) = v\Sigma_{sd}\int_v^\infty \frac{n^+(x,v',t)+n^-(x,v',t)}{v'}dv' + \beta v\Sigma_s(v)M(v)\int_0^\infty \frac{1}{2}v'\Sigma_s(v')(n^+(x,v',t)+n^-(x,v',t))\mathrm{d}v', \quad (4.42)$$

together with the usual boundary conditions:

$$n^+(0,v,t) = 0 \quad (4.43)$$

$$n^-(L,v,t) = 0 \quad (4.44)$$

We search again for separate-variable solutions of the type $n^\pm(x,v,t) = n^\pm(x,v)e^{\alpha t}$. Then, substituting this functional form into equations 4.41 and 4.42 we find

$$+v\frac{\partial}{\partial x}n^+(x,v)+v\Sigma_t n^+(x,v)+\alpha n^+(x,v) = v\Sigma_s\int_v^\infty \frac{n^+(x,v')+n^-(x,v')}{v'}dv' + \beta v\Sigma_s(v)M(v)\int_0^\infty \frac{1}{2}v'\Sigma_s(v')(n^+(x,v')+n^-(x,v'))\mathrm{d}v' \quad (4.45)$$

$$-v\frac{\partial}{\partial x}n^+(x,v)+v\Sigma_t n^-(x,v)+\alpha n^-(x,v) = v\Sigma_s\int_v^\infty \frac{n^+(x,v')+n^-(x,v')}{v'}dv' + \beta v\Sigma_s(v)M(v)\int_0^\infty \frac{1}{2}v'\Sigma_s(v')(n^+(x,v')+n^-(x,v'))\mathrm{d}v'. \quad (4.46)$$

Chapter 5

Assessing the properties of moderators with α-static methods

In the previous chapters we have discussed the mathematical theory of the *alpha*-static methods and the details of the algorithm at the base of the Monte Carlo α-static code that we have developed. We have also introduced in chapter 4 some physical models of interest for moderating materials. We shall proceed now to present some results of the simulations performed by our code with a double aim:

- the verification and validation of the α static methods;
- exploring the physical properties of moderators and the asymptotic time relaxation of the neutrons in these materials.

The **α-static Monte Carlo code** used for the simulations has been developed in C++ language; it is based on the algorithm presented in chapter 3 and it is able to simulate the transport of neutrons with a velocity distribu-

tion in infinite media or bounded one-dimensional media. The *alpha*-static code results will be compared to reference results:

- analytical solutions, coming from literature or directly obtained in this work;
- independent numerical codes. In particular, we have developed:
  - a **dynamic Monte Carlo code**, in C++ language; this code is a valuable tool because, as we have discussed in chapter 2, dynamic Monte Carlo methods reproduce the real physics of a process in time and can be used as reference for the other numerical methods;
  - a **deterministic solver**, in Matlab; this code finds the eigenvalues of the Boltzmann stationary equation by discretizing the space and energy domains. Even if deterministic methods give an approximated solution, as seen in chapter 2, this solver is useful because it finds *all* the eigenvalues of the Boltzmann operator and so provides a picture of the entire spectrum.

5.1 Preliminary tests: one-speed transport

We briefly present as a first check the simulation results for the simplest case discussed in paragraph 4.1: the one-speed neutron transport in moderating media.

We have seen in paragraph 4.1.1 that, in the case of an infinite medium, if we inject a burst of neutrons at $t = 0$, the fundamental eigenvalue α_0 characterizing the neutron decay is equal to the opposite of the absorption

rate, namely, $\alpha_0 = -\Sigma_a v$. We summarize the data utilized for the simulation in the following table:

L	infinite
Σ_s	1.0 cm^{-1}
Σ_a	0.5 cm^{-1}
v	1.0 $cm\ s^{-1}$

For this case, with these parameters, we run the α-static code and we obtain the α convergence as function of generations; we can see in figure 5.1 the result of the simulation. The α_0 eigenvalue averaged over the last 50 generations (after discarding the first 50) is plotted as a green line of figure 5.1 and we see that it is in very good agreement with the value given by theory (purple line of figure 5.1).

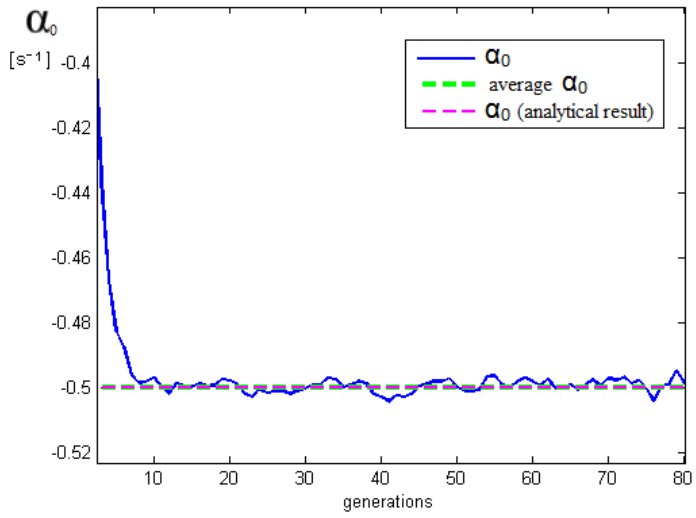

Fig. 5.1: Diffusion of one-speed neutrons in an infinite medium: the fundamental eigenvalue α_0 provided by the α-static code plotted as a function of the generations.

We pass now to the rod model presented in paragraph 4.1.2. We have seen

that the discrete α eigenvalues can be found by solving the dispersion relation of Eq. (4.9). We proceed by simulating a pulsed-neutron experiment: we inject a burst of neutrons in the center of the rod and simulate their transport. The parameters adopted here are:

L	3.0 cm
Σ_s	0.9 cm^{-1}
Σ_a	0.2 cm^{-1}
v	1 cms^{-1}

Using Eq. (4.9), we find that the fundamental eigenvalue is $\alpha_0 \simeq -0.7698\ s^{-1}$ (plotted as a purple line in figure 5.2). We run the *alpha*-static code and we obtain the α convergence as a function of the generations, shown in figure 5.2. After discarding the first 50 generations, we compare the α_0 averaged over the last 50 generations (the green line in figure 5.2) and compare this value to that computed by using the Eq. (4.9): we find again a very good agreement between the analytic and numerical result.

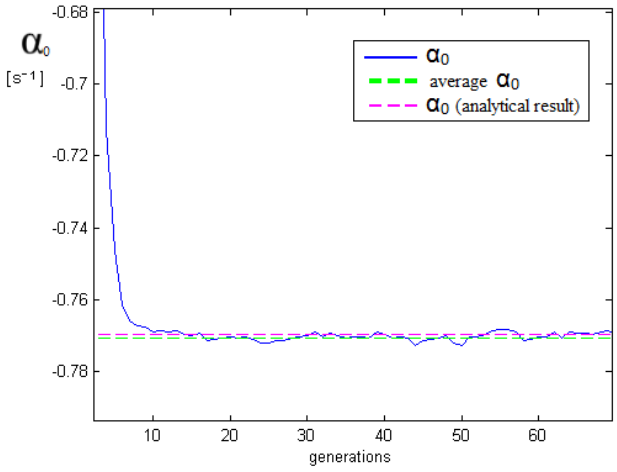

Fig. 5.2: Diffusion of one-speed neutrons in a bounded medium: the fundamental eigenvalue α_0 provided by the α-static code plotted as a function of the generations.

5.2 Neutron thermalization simulations

We shall focus now on the problem of the neutron thermalization analyzed in paragraph 4.2. Before discussing the results for the infinite medium and for the rod model, we summarize some modeling parameters that are common to both systems:

- the source used for the simulations is a burst of one-speed neutrons ($v = 1\ cm/s$) injected at $t = 0$;
- the scattering and absorption cross sections are of the kind $1/v$ plus a constant:
$$\Sigma_s(v) = \frac{\Sigma_s}{v} + \Sigma_s^0 \quad , \quad \Sigma_a(v) = \frac{\Sigma_a}{v} + \Sigma_a^0. \tag{5.1}$$
Their qualitative behaviour is represented in figure 5.3
- the scattering kernel is the *amnesia* kernel of Eq.(4.17): a single shock is sufficient to thermalize the neutron;
- the most probable speed of the Maxwellian distribution is $v_T = 1$.

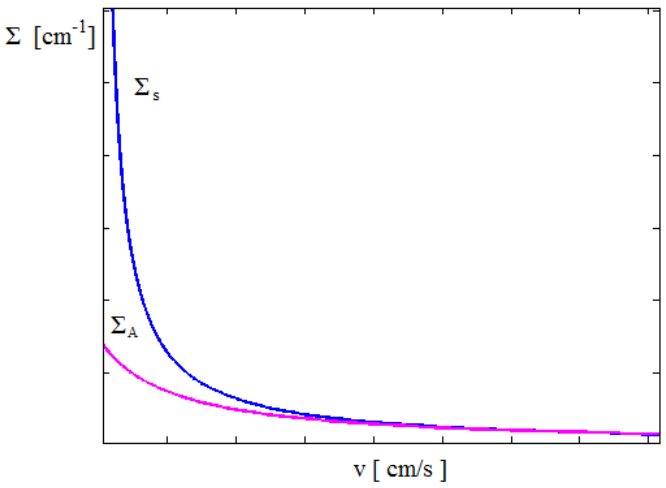

Fig. 5.3: Absorption and scattering cross-sections modeling

5.2.1 Infinite medium

We have discussed the α spectrum features of an infinite moderating system in paragraph 4.2.1. We recall the most important results:

1. the spectrum is composed of real discrete eigenvalues in the interval $(\alpha^*, 0]$ and of a continuum spectrum $C = (-\infty, \alpha^*]$; see figure 4.2;

2. the limit of the continuum set α^* is the opposite of the minimum reaction rate; considering the cross sections introduced above, we have:

$$\alpha^* = -\min_{v\epsilon[0,\infty)}[v\Sigma_t(v)] = -[v(\frac{\Sigma_s}{v} + \Sigma_s^0 + \frac{\Sigma_a}{v} + \Sigma_a^0)]_{v=0} = -(\Sigma_s + \Sigma_a); \tag{5.2}$$

3. the discrete eigenvalues are the solutions of the dispersion relation [17] that we recall here:

$$\Lambda(\alpha) = 1 - \beta \int_0^\infty \frac{[v\Sigma_s(v)]^2 M(v)}{\alpha + v\Sigma_t(v)} \mathrm{d}v = 0, \tag{5.3}$$

   where β is the normalization constant defined as $\beta^{-1} = \int_0^\infty v\Sigma_s(v)M(v)\mathrm{d}v$;

4. the disappearance of discrete eigenvalues can occur in the presence of an absorption rate that increases strongly enough with v because of the *absorption cooling* [13] discussed in 4.2.1.

Considering an absorption cross section of the type $\Sigma_a(v) = \frac{\Sigma_a}{v} + \Sigma_a^0$, it follows that the absorption rate increases with increasing Σ_a^0. We have been able to find the *critical* value $\Sigma_a^{0\,*}$ corresponding to the disappearance of discrete eigenvalues by substituting $\alpha = \alpha^* + \epsilon$ into Eq.(5.3) and taking the limit for $\epsilon \to 0$. If our system is characterized by a $\Sigma_a^0 < \Sigma_a^{0\,*}$, at least

one discrete eigenvalue exists; on the contrary, if $\Sigma_a^0 > \Sigma_a^{0\,*}$ there are no discrete eigenvalues in the Boltzmann operator spectrum. By carrying out the explicit calculation, we find

$$\Sigma_a^{0\,*} = \frac{(\frac{\Sigma_s}{v_T})^2 + \frac{\Sigma_s}{\bar{v}}\Sigma_s^0}{\Sigma_s(\bar{v})}, \tag{5.4}$$

where $\bar{v}$ is the average velocity of the Maxwell-Boltzmann distribution

$$\bar{v} = \frac{2}{\sqrt{\pi}} v_T. \tag{5.5}$$

We shall discuss two simulations: in the former, we shall choose $\Sigma_a^0 < \Sigma_a^{0\,*}$ and we expect to find at least one discrete eigenvalue; in the latter, on the contrary, we shall choose $\Sigma_a^0 > \Sigma_a^{0\,*}$ in order to test the behaviour of the α-static code in the absence of discrete eigenvalues.

Simulation 1 ($\Sigma_a^0 < \Sigma_a^{0\,*}$)

We summarize the parameters used for the simulation in the following table:

L	infinite
Σ_s	1.0 s^{-1}
Σ_s^0	0.1 cm^{-1}
Σ_a	0.5 s^{-1}
Σ_a^0	0.8 cm^{-1}
v_T	1.0 $cm\ s^{-1}$

Considering these data, using equations (4.21) and (5.4), we find that the continuum limit is characterized by:

α^*	-1.5 s^{-1}
Σ_a^0 *	$\simeq$ 1.1038 cm^{-1}

Thanks to the deterministic solver that we have developed, we can find the eigenvalue spectrum of this case, which is shown in figure 5.4. The spectrum has been obtained by using an energy discretization with M meshes; increasing M, the interval of the spectrum to the left of α^* is progressively *filled*: this shows that the interval $(-\infty, \alpha^*]$ is actually a continuum, in agreement with the theory. Indeed, the spectrum obtained by our deterministic solver is similar to that one of figure 4.2 discussed in 4.2.1. We can observe in figure 5.4 that there is a single discrete eigenvalue behind the continuum region.

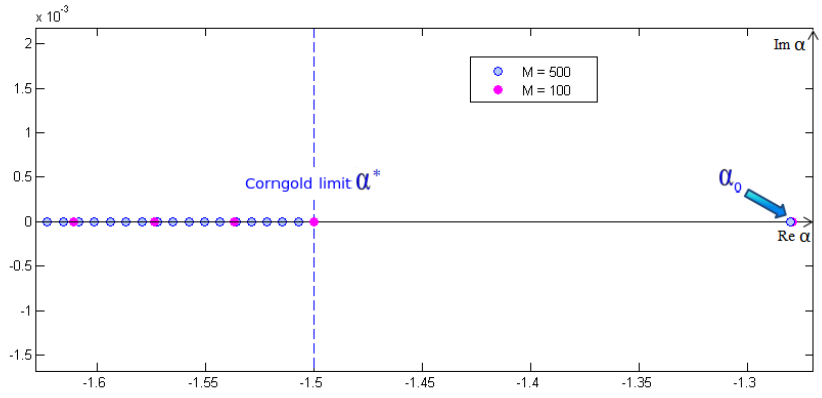

*Fig. 5.4: α-eigenvalue spectrum (obtained by the deterministic solver) for the neutron thermalization in an infinite moderating medium with $\Sigma_a^0 < \Sigma_a^0$ *.*

Following this analysis of the spectrum, we run the α-static code for this case and we obtain the α convergence as a function of the generations; we can see in figure 5.5 the result of the simulation. We see that the α_0 averaged over the last 50 generations (plotted as a green line of figure 5.5) is in very good agreement with the single discrete eigenvalue of the spectrum of figure

5.4 given by the deterministic solver.

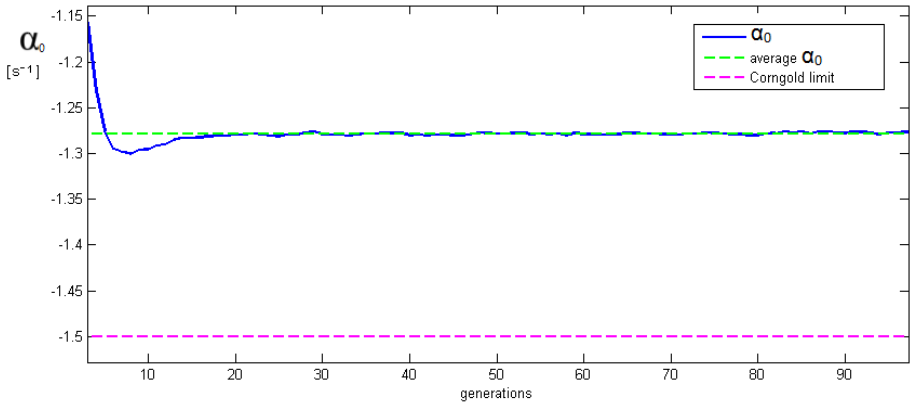

Fig. 5.5: Neutron thermalization in an infinite medium with $\Sigma_a^0 < \Sigma_a^{0\,*}$: the fundamental eigenvalue α_0 provided by the α-static code plotted as a function of the generations.

The existence of a discrete eigenvalue means that, after a transient, the neutron density $n(v,t)$ can be represented by the separable form

$$n(v,t) = n_0(v)e^{\alpha_0 t},$$

where $n_0(v)$ is the eigenfunction associated to α_0 and physically represents the asymptotic velocity distribution of the neutrons. To assess the behaviour of the neutron population in time, we run the dynamic Monte Carlo code (used as a reference simulation). Then, we compare the asymptotic time behaviour ($e^{\alpha_0 t}$) and the neutron density $n(v)$ provided by the *alpha*-static code to the reference results of the dynamic Monte Carlo code.

In figure 5.6(a), we can observe that the behaviour of the neutron population with respect to time (green curve), after a transient, is well fitted by an exponential decay with rate α_0. There is a good agreement also in the neutron velocity distribution provided by the static (blue curve) and dynamic (green

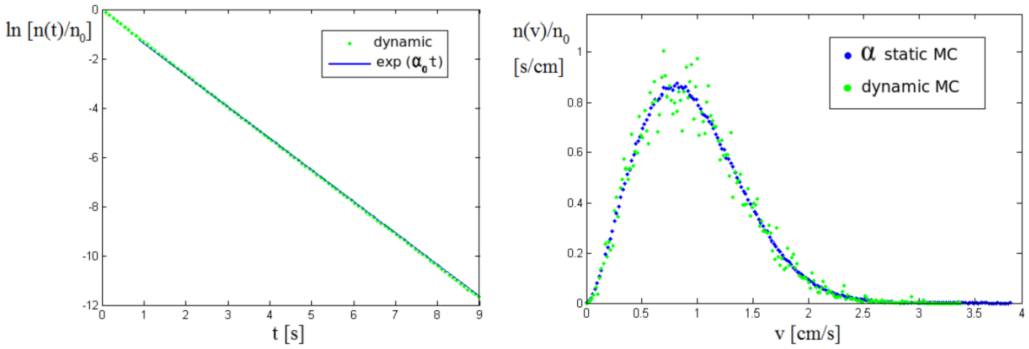

(a) The time decay of the neutron population in an infinite medium with $\Sigma_a^0 < \Sigma_a^{0\,*}$.

(b) The asymptotic velocity distribution of the neutron population in an infinite medium with $\Sigma_a^0 < \Sigma_a^{0\,*}$.

Fig. 5.6: The α-static results (blue) compared to the Dynamic Monte Carlo results (green).

curve) codes, as shown in figure 5.6(b). Furthermore, we notice that the velocity distribution of the α static code is much less *dispersed* than that of the dynamic code: as we mentioned in chapter 2, dynamic codes need a very large number of simulated particles to achieve good statistics. On the contrary, α-static codes need a relatively smaller number of simulated particles.

Simulation 2 ($\Sigma_a^0 > \Sigma_a^{0\,*}$)

We summarize the parameters adopted for the second simulation in the following table:

L	infinite
Σ_s	1.0 s^{-1}
Σ_s^0	0.1 cm^{-1}
Σ_a	0.5 s^{-1}
Σ_a^0	1.4 cm^{-1}
v_T	1.0 $cm\ s^{-1}$

Summarizing, the only parameter changed with respect to the previous simulation is the constant part of the absorption cross section (so that α^* is unchanged). We use our deterministic solver to compute the eigenvalue spectrum for this latter case and we show it in figure 5.7. We see that the only difference with respect to the previous spectrum of figure 5.4 is the absence of discrete eigenvalues, as expected.

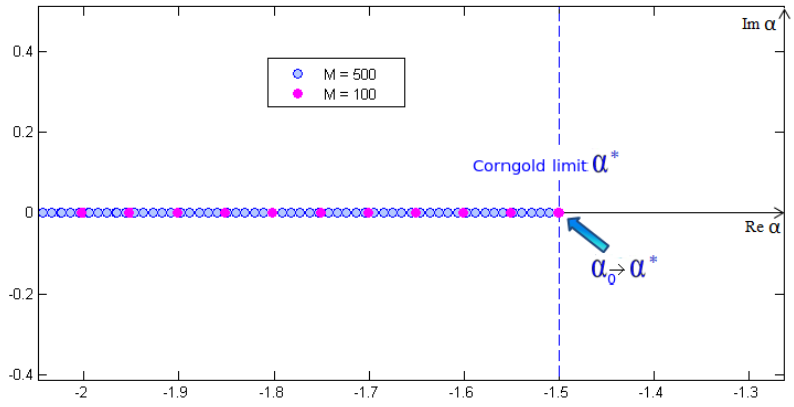

*Fig. 5.7: α-eigenvalue spectrum (obtained by the deterministic solver) for the neutron thermalization in an infinite moderating medium with $\Sigma_a^0 > \Sigma_a^0$ *.*

Then, we run the α-static code for this latter case and we plot the the α convergence as a function of the generations in figure 5.8; we note that the

code still converges to a value: the Corngold limit α^*. However, we see that convergence is quite slow. In fact, convergence is achieved after almost 2000 generations. This difficulty is due to an "attraction" toward lower values of α, that is toward the continuum part of the spectrum.

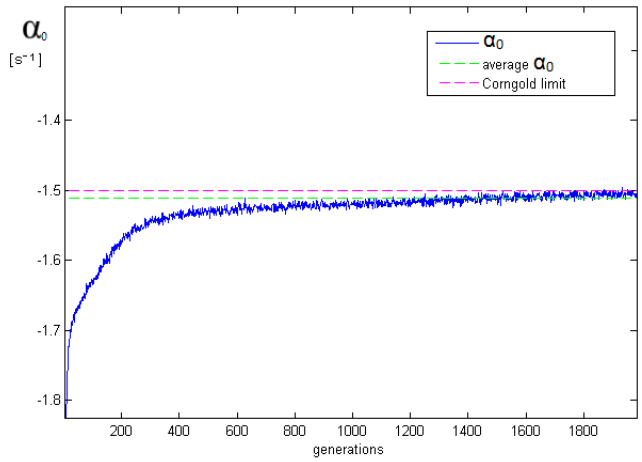

Fig. 5.8: Neutron thermalization in an infinite medium with $\Sigma_a^0 > \Sigma_a^{0\,*}$: the fundamental eigenvalue α_0 provided by the α-static code plotted as a function of the generations.

Does the convergence of the α-static code imply that the neutron density $n(v,t)$ has a separable form with an exponential time behaviour characterized by a rate α^*? To answer this question, we have to investigate the time behaviour of the neutron population and for this reason we run the dynamic Monte Carlo code. In figure 5.6(a) we compare the reference neutron time decay obtained by the dynamic Monte Carlo code (green) to an exponential function with rate α_0 given by the α-static code (blue). The two curves in figure 5.6(a) do not have the same slope. Moreover, in figure 5.6(b), we see that the neutron velocity distribution given by the α-static code (blue) is different from the neutron velocity distribution given by the dynamic Monte Carlo code (green).

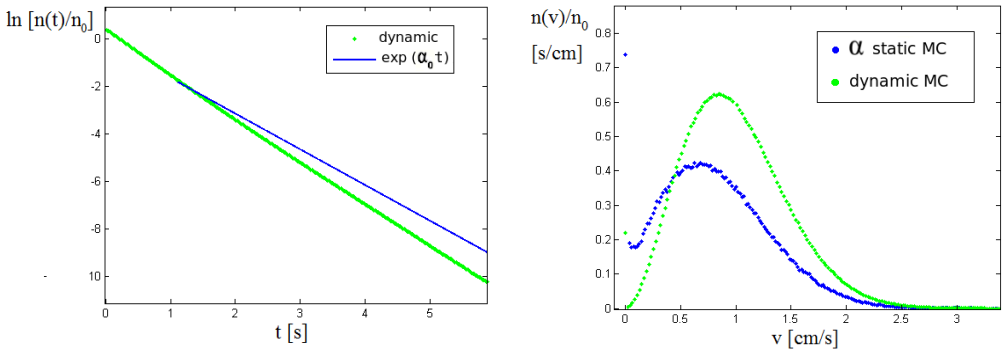

(a) The time decay of the neutron population in an infinite medium with $\Sigma_a^0 > \Sigma_a^{0\,*}$

(b) The asymptotic velocity distribution of the neutron population in an infinite medium with $\Sigma_a^0 > \Sigma_a^{0\,*}$

Fig. 5.9: The α-static results (blue) compared to the Dynamic Monte Carlo results (green).

Therefore, for this choice of the physical parameters, we can conclude that the results provided by the α-static code are not representative of the asymptotic time behaviour. This is not surprising, because the hypothesis of variable separation is no more valid when a discrete eigenvalue is missing, as learned in chapter 4. Actually, as expected from theory [12], the disappearance of discrete eigenvalues corresponds to singular velocity distribution, i.e. with a $\delta(v)$ term. In other words, a finite fraction of neutrons has $v = 0$; this is confirmed also by Monte Carlo simulations (both static and dynamic), as shown by the peaks at zero velocity in figure 5.9(b).

The conclusion about the α-static code unreliability in this case is not really troubling. In fact, the situation analyzed is quite *pathological*: like we have said in paragraph 4.2.1, absorption rates so high are not common.

5.2.2 The rod model

In paragraph 4.2.2, we have discussed the α spectrum features of a bounded three-dimensional medium. We summarize the basic results:

1. the spectrum is composed of real discrete eigenvalues in the interval $(\alpha^*, 0]$ and of a continuous planar spectrum $C = (-\infty, \alpha^*]$, as qualitatively shown in figure 4.3;

2. the continuum limit or Corngold limit is

$$\alpha^* = -\lim_{v \to 0}[v\Sigma_t(v)]; \tag{5.6}$$

3. the discrete dominant eigenvalue decreases monotonically with the system dimension, if the other physical parameters are left unchanged. Therefore, there must exist a *critical dimension* of the system where $\alpha_0 = \alpha^*$; if the system size is further reduced below this limit, the discrete eigenvalue disappears into the continuum. This is due to the *diffusion cooling* discussed in paragraph 4.2.1.

For a bounded one-dimensional system we still expect a discrete eigenvalue set and a continuum interval, separated by the Corngold limit. However, what can be said about the continuum region? Has it the same planar structure? To answer this question, we resort to the deterministic solver, which computes the spectrum by solving the eigenvalue problem. The solution provided by the deterministic solver depends on the number of space (N) and energy (M) discretization meshes: the exact spectrum would be obtained by increasing N and M to infinity.
In figure 5.10 we plot two spectra obtained with different N and M: in figure 5.10(a), N is fixed ($N = 40$) and M changes ($M = 20$ for the green spectrum,

$M = 30$ for the blue spectrum and $M = 40$ for the purple spectrum). In figure 5.10(b), on the contrary, M is fixed ($M = 40$) and N changes ($N = 20$ for the green spectrum, $N = 30$ for the blue spectrum and $N = 40$ for the purple spectrum).

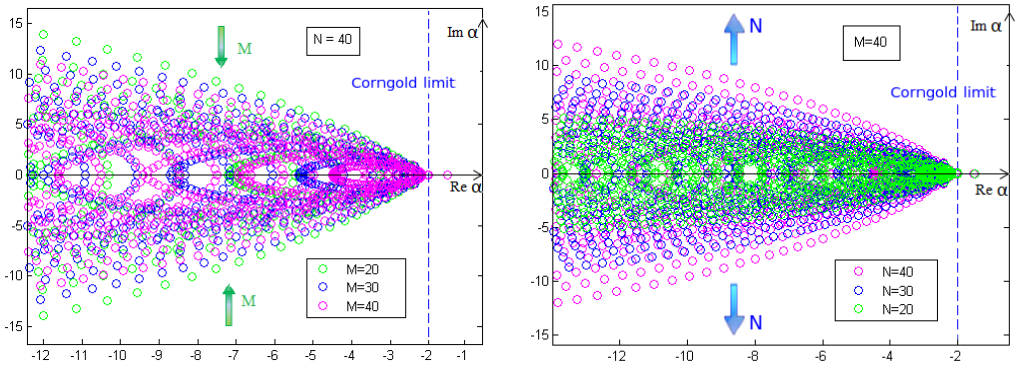

(a) Spectrum obtained with N (space discretization meshes) fixed and M (energy discretization meshes) increasing

(b) Spectrum obtained with M (energy discretization meshes) fixed and N (space discretization meshes) increasing

Fig. 5.10: α-eigenvalue spectrum (obtained by the deterministic solver) for the neutron thermalization in a one-dimensional bounded moderating medium

The continuous form is not so obvious: it seems a bullet-shape but we notice that the spectrum considerably changes with the discretization. In fact, increasing the energy mesh number, the continuum is *filled* (like in the infinite case) but also slightly pushed toward the real axis; on the contrary, increasing the space mesh number, the continuum grows, filling a plane. This latter effect seems to be dominant: we conjecture that the continuous interval structure of the one-dimensional medium is planar as in the three-dimensional case.

In analogy with the three-dimensional case, we suppose that the fundamental discrete eigenvalue disappears in the continuum for a critical length L^* of the rod; we search now for an analytic expression for L^*. We recall the stationary equations (4.28) and (4.46) for the rod:

$$+ v\frac{\partial}{\partial x}n^+(x,v) + v\Sigma_t n^+(x,v) + \alpha n^+(x,v) = \frac{\beta}{2}v\Sigma_s(v)M(v)\int_0^\infty v'\Sigma_s(v')[n^+(x,v') + n^-(x,v')]\mathrm{d}v'$$

$$- v\frac{\partial}{\partial x}n^-(x,v) + v\Sigma_t n^-(x,v) + \alpha n^-(x,v) = \frac{\beta}{2}v\Sigma_s(v)M(v)\int_0^\infty v'\Sigma_s(v')[n^+(x,v') + n^-(x,v')]\mathrm{d}v'$$

together with the boundary conditions:

$$n^+(0,v) = 0 \tag{5.7}$$

$$n^-(L,v) = 0. \tag{5.8}$$

We suppose that the constant part of the scattering and absorption cross sections is zero:

$$\Sigma_s(v) = \frac{\Sigma_s}{v} \quad , \quad \Sigma_a(v) = \frac{\Sigma_a}{v}; \tag{5.9}$$

under this hypothesis, the Corngold limit is

$$\alpha^* = -(\Sigma_s + \Sigma_a). \tag{5.10}$$

Recalling the expression of the Maxwell-Boltzmann distribution (Eq.(4.15))

$$M(v) = \frac{4}{\sqrt{\pi}v_T^3}v^2 e^{-v^2/v_T^2}$$

with the cross sections just defined, the normalization factor β is simply

$$\beta^{-1} = \int_0^\infty v\Sigma_s(v)M(v)\mathrm{d}v = \Sigma_s. \tag{5.11}$$

Substituting this β value, replacing $\alpha = \alpha^*$ into the stationary rod equations and dividing by v, we obtain

$$\frac{\partial}{\partial x}n^+(x,v) = \frac{1}{2}\frac{M(v)}{v}\int_0^\infty v'\Sigma_s[n^+(x,v') + n^-(x,v')]\mathrm{d}v' \tag{5.12}$$

$$-\frac{\partial}{\partial x}n^-(x,v) = \frac{1}{2}\frac{M(v)}{v}\int_0^\infty v'\Sigma_s[n^+(x,v') + n^-(x,v')]\mathrm{d}v'. \tag{5.13}$$

If we integrate over velocity, defining $n(x) = \int_0^\infty n(x,v)\mathrm{d}v$, the equations become:

$$\frac{\mathrm{d}}{\mathrm{d}x}n^+(x) = \Gamma[n^+(x) + n^-(x)] \tag{5.14}$$

$$-\frac{\mathrm{d}}{\mathrm{d}x}n^-(x) = \Gamma[n^+(x) + n^-(x)] \tag{5.15}$$

where Γ is a constant equal to

$$\Gamma = \frac{\Sigma_s}{v_T\sqrt{\pi}} = \frac{\Sigma(v_T)}{\sqrt{\pi}}. \tag{5.16}$$

Equations (5.14) and (5.15) form a system of two coupled ordinary differential equations. Solving the system with the boundary conditions (5.23) (5.24) leads to an analytic formulation for L^*:

$$L^* = \frac{\sqrt{\pi}}{\Sigma_s(v_T)}, \tag{5.17}$$

which is of the order of the mean scattering free path and does not depend on the absorption cross section. This is not surprising, because, the existence of

a critical dimension is due to the *diffusion cooling*, which is related to leakage alone.

We shall now discuss two simulations: in the former, we shall choose a rod length greater than L^*, expecting to find at least one discrete eigenvalue; in the latter, on the contrary, we shall choose a rod dimension smaller than L^*, in order to test the behaviour of the α-static code in the absence of discrete eigenvalues.

Simulation 1 ($L > L^*$)

We summarize the parameters adopted for the simulation in the following table:

L	2 cm
Σ_s	1.0 s^{-1}
Σ_s^0	0 cm^{-1}
Σ_a	1.0 s^{-1}
Σ_a^0	0 cm^{-1}
v_T	1.0 $cm\ s^{-1}$

Considering these data, using equations (5.10) and (5.17) we find that the continuum limit is characterized by:

α^*	-2.0 s^{-1}
L^*	$\simeq$ 1.7725 cm

In figure 5.11, we display the eigenvalue spectrum obtained by the deterministic solver, using an energy discretization with M meshes and a space discretization with N meshes. We observe that there exists a discrete eigenvalue.

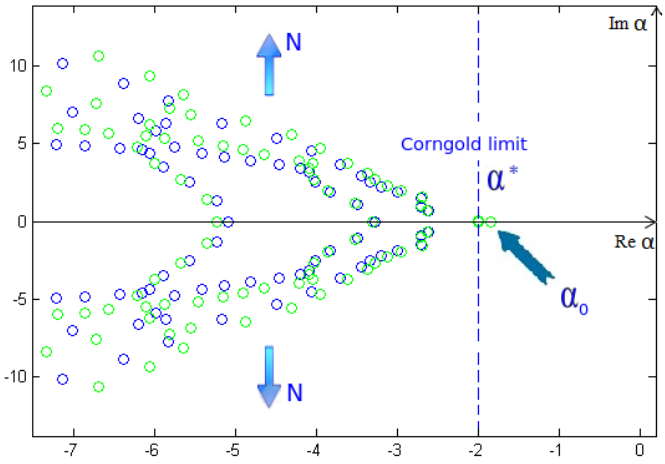

Fig. 5.11: α-eigenvalue spectrum (obtained by the deterministic solver) for the neutron thermalization in a bounded moderating medium with $L > L^*$

With these parameters, we run the α-static code and we obtain the α convergence as a function of the generations; we can see in figure 5.12 the result of the simulation. The α_0 eigenvalue averaged over the last 50 generations (after discarding the first 50) is plotted as a green line in figure 5.12 and we see that it is in very good agreement with the discrete value given by the deterministic solver.

As usual, if at least one discrete eigenvalue exists, after a transient, the neutron density $n(v,t)$ can be represented by the separable form $n(v,t) = n_0(v)e^{\alpha_0 t}$, where $n_0(v)$ is the eigenfunction associated to α_0 and physically represents the asymptotic velocity distribution of the neutrons.

To assess the behaviour of the neutron population in time, we run the reference dynamic Monte Carlo code. Then, we compare the asymptotic time behaviour ($e^{\alpha_0 t}$) and neutron density $n(v)$ provided by the α-static code to the results of the dynamic code.

Figure 5.13(a) shows that the time behaviour of the neutron population obtained by the dynamic code (green), after a transient, is well fitted by an

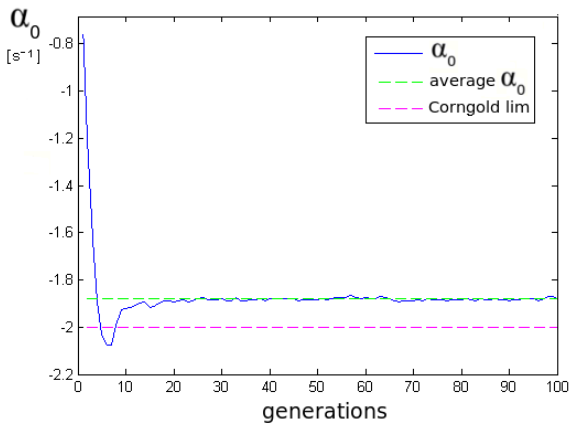

Fig. 5.12: Neutron thermalization in a bounded medium with $L > L^*$: the fundamental eigenvalue α_0 provided by the α-static code plotted as a function of the generations.

exponential decay whose rate is α_0 (blue). There is a good agreement also in the neutron velocity distribution provided by the static (blue) and dynamic (green) code, as shown in figure 5.13(b). We notice that again the velocity distribution of the α static code is much less *dispersed* than that of the dynamic code.

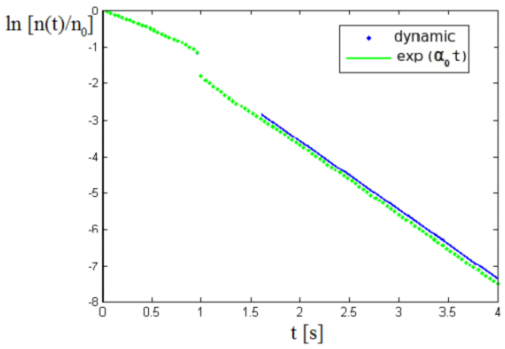

(a) The time decay of the neutron population in a bounded medium with $L > L^*$.

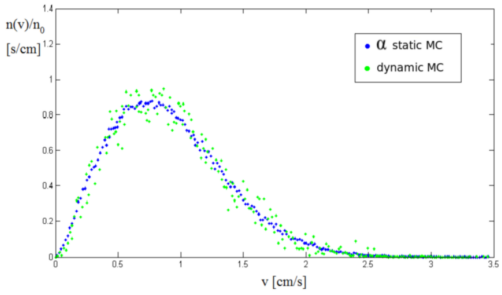

(b) The asymptotic velocity distribution of the neutron population in a bounded medium with $L > L^*$.

Fig. 5.13: α-static results (blue) compared to Dynamic Monte Carlo results (green).

Simulation 2 ($L < L^*$)

We reduce the rod size to a dimension smaller than L^*. We summarize the parameters adopted for the simulation in the following table:

L	1.2 cm
Σ_s	1.0 s^{-1}
Σ_s^0	0 cm^{-1}
Σ_a	1.0 s^{-1}
Σ_a^0	0 cm^{-1}
v_T	1.0 $cm\ s^{-1}$

The deterministic solver shows the absence of a discrete eigenvalue set, as shown in figure 5.14.

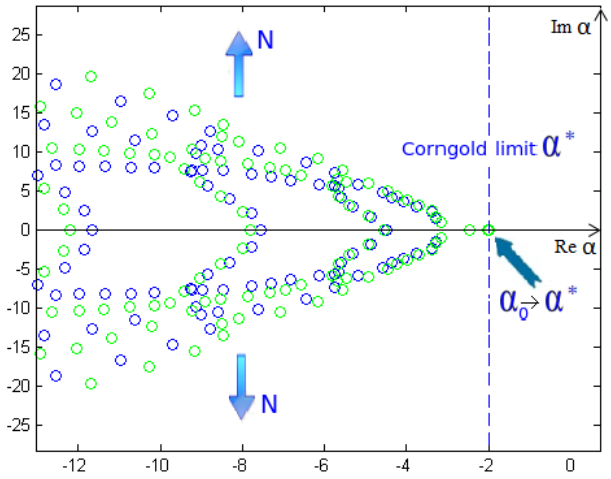

Fig. 5.14: α-eigenvalue spectrum (obtained by the deterministic solver) for the neutron thermalization in a bounded moderating medium with $L < L^*$.

Which is the α-static code behaviour in this case? We run the α-static code and we obtain the α convergence as a function of the generations, which

is shown in figure 5.15. We see that the α-static code converges to the Corngold limit, even if there are some fluctuations toward lower values, similarly as observed in the second simulation of subsection 5.2.1.

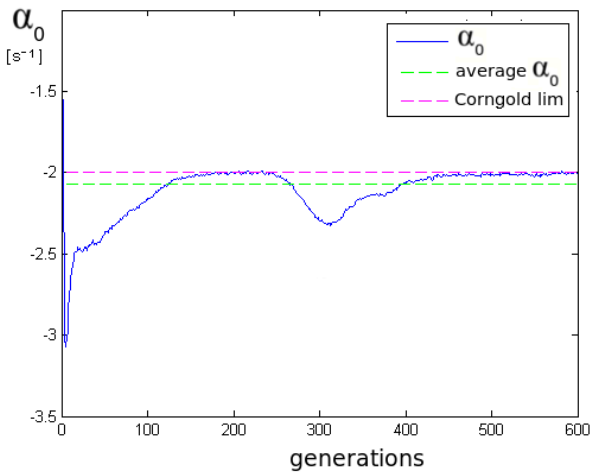

Fig. 5.15: Neutron thermalization in a bounded moderating medium with $L < L^*$: the fundamental eigenvalue α_0 provided by the α-static code plotted as a function of the generations.

We wonder again if the α_0 and the associated eigenfunction found by the α-static code have a physical meaning (respectively the inverse of the time constant and the neutron velocity distribution) like in the previous case. To answer the question, we explore the time behaviour of the neutron population by resorting to the reference results of the dynamic Monte Carlo code. Figure 5.16(a) shows that the neutron time decay (blue) is no more fitted by an exponential with rate α_0. Indeed, the Corngold theory (see subsection 4.2.2) shows that the exponential factorization is no more valid; for this case, Corngold has proposed an empirical formula [12, 13]:

$$n(x, v, t) \simeq n(x, v) \frac{e^{\alpha_0 t}}{t^2}, \tag{5.18}$$

which agrees with the time behaviour observed in the dynamic Monte Carlo (the purple fitting). Moreover, in figure 5.6(b), we see that also the neutron velocity distribution given by the α-static curve (blue) is different from the neutron velocity distribution of the dynamic Monte Carlo code (green). We remark again that the neutron density is characterized by a singular $\delta(v)$ term, which is represented by the peaks at $v = 0$ of figure 5.16(b).

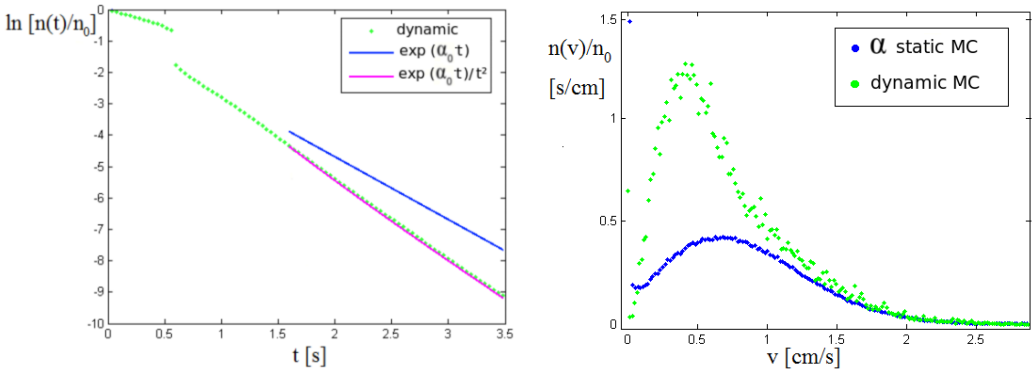

(a) The time decay of the neutron population in a bounded medium with $L < L^0$ *.

(b) The asymptotic velocity distribution of the neutron population in a bounded medium with $L < L^0$ *.

Fig. 5.16: The α-static results (blue) compared to the Dynamic Monte Carlo results (green).

Like in the infinite medium case of simulation 2 discussed in paragraph 5.2.1, we can conclude that it is no more possible to find the fundamental eigenvalue by the α-static code simply because a discrete eigenvalue does not exist anymore.

5.3 Thermalization with Bragg scattering

In paragraph 4.3, we have discussed the Bragg scattering features and the α spectrum of a bounded medium with Bragg scattering. A qualitative picture of the spectrum is provided in figure 4.5 and we summarize here the basics results:

1. the Corngold limit is

$$\alpha^* = -\min_{v\epsilon[0,\infty)}[v\Sigma_t(v)]; \tag{5.19}$$

2. there is a discrete eigenvalue set for $\alpha > \alpha^*$ (possibly empty);

3. a vertical line (or a narrow area) at $\alpha = \alpha^*$ constitutes the sub-Bragg continuum Γ_{SB};

4. an horizontal line for $\alpha \leq \alpha_{el}(B^2, v_B)$ constitutes the elastic continuum Γ_{el};

5. a discrete eigenvalue set may exist in the gap between the sub-Bragg continuum and the elastic continuum;

6. for $\alpha < \alpha_A$, where $\alpha_A = -\min_{v\epsilon[v_b^+,\infty)}[v\Sigma_T(v)]$, there is a continuum area;

7. the system is characterized by two critical sizes: L^* and L^{**}; for $L \leqslant L^*$ the discrete eigenvalue set $[\alpha > \alpha^*]$ is empty; for $L \leq L^{**} < L^*$ there are no discrete eigenvalues.

We emphasize that the starting point of the elastic continuum α_{el} changes as a function of the rod length, contrary to the moderators seen until now, where only the discrete eigenvalues decrease as decreasing the system size

and the continuum set does not depend on the system dimension. Conn and Corngold [10] have shown that the equation $\Gamma_e(B, v, \alpha) = 0$ satisfied by the elastic continuum set, for fixed v, has the form of a one-velocity dispersion relation law; this is due to the one-speed nature of the Bragg-scattered neutrons. They have also shown that α_{el}, i.e., the point of the elastic continuum set closest to the origin, is obtained for $v = v_B$. Then, we can use the one-speed dispersion law of the rod model, given by Eq. (4.19), to compute α_{el}; we just have to substitute $\Sigma_t = \Sigma_t(v_B) = \dfrac{v_B}{\Sigma_s} + \Sigma_B$. Then, we obtain:

$$\cosh\left(L\Sigma_t(v_B)\sqrt{\frac{\alpha_{el}}{v_B\Sigma_t(v_B)}\left(\frac{\alpha_{el}}{v_B\Sigma_t(v_B)}-1\right)}\right)+ \\ +\frac{\left(\dfrac{\alpha_{el}}{v_B\Sigma_t(v_B)}-\dfrac{1}{2}\right)\sinh\left(L\Sigma_t(v_B)\sqrt{\dfrac{\alpha_{el}}{v_B\Sigma_t(v_B)}\left(\dfrac{\alpha_{el}}{v_B\Sigma_t(v_B)}-1\right)}\right)}{\sqrt{\dfrac{\alpha_{el}}{v_B\Sigma_t(v_B)}\left(\dfrac{\alpha_{el}}{v_B\Sigma_t(v_B)}-1\right)}}=0 \tag{5.20}$$

that allows finding α_{el}, once the parameters of the system are fixed .

We now search for an analytical expression of L^*: the critical length such that $\alpha_0 \to \alpha^*$. We re-write the stationary equations for the rod model in the presence of the Bragg scattering:

$$+ v\frac{\partial}{\partial x}n^+(x,v) + v\Sigma_t n^+(x,v) + \alpha n^+(x,v) =$$
$$\frac{\beta}{2}v\Sigma_s(v)M(v)\int_0^\infty v'\Sigma_s(v')[n^+(x,v') + n^-(x,v')]\mathrm{d}v' +$$
$$+\int_0^\infty \frac{1}{2}\Sigma_B(v')v'\delta(v-v')[n^+(x,v') + n^-(x,v')]\mathrm{d}v' \quad (5.21)$$

$$- v\frac{\partial}{\partial x}n^-(x,v) + v\Sigma_t n^-(x,v) + \alpha n^-(x,v) =$$
$$\frac{\beta}{2}v\Sigma_s(v)M(v)\int_0^\infty v'\Sigma_s(v')[n^+(x,v') + n^-(x,v')]\mathrm{d}v' +$$
$$+\int_0^\infty \frac{1}{2}\Sigma_B(v')v'\delta(v-v')[n^+(x,v') + n^-(x,v')]\mathrm{d}v' \quad (5.22)$$

together with the usual boundary conditions:

$$n^+(0,v) = 0 \quad (5.23)$$

$$n^-(L,v) = 0. \quad (5.24)$$

We recall that the Bragg scattering is a threshold process. We take into account this feature and choose a simple piecewise constant cross section for the Bragg scattering:

$$\Sigma_B(v) = \begin{cases} 0 & v < v_B \\ \Sigma_B & v \geqslant v_B \end{cases} \quad (5.25)$$

Moreover, to simplify the calculation, we neglect the absorption and we choose a $1/v$ form for the thermalization scattering contribution:

$$\Sigma_s(v) = \frac{\Sigma_s}{v}. \quad (5.26)$$

The cross sections characterizing the medium are shown in figure 5.17.

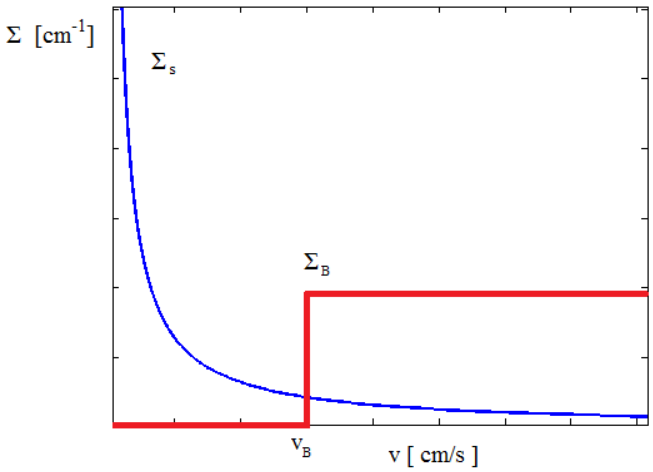

Fig. 5.17: Scattering cross section modeling for a medium with Bragg scattering

The Corngold limit in this case is $\alpha^* = -\min_{v\epsilon[0,\infty)}[v\Sigma_t(v)] = -\Sigma_s$. In order to compute the critical length L^*, we substitute $\alpha = \alpha^*$ into equations (5.21) and (5.22) and we re-write them by explicitly plugging the chosen cross sections. We separately consider the two cases $v < v_B$ or $v > v_B$.

For $n(x,v)$ with $v\epsilon[0, v_B)$:

$$+ \; v\frac{\partial}{\partial x}n^+(x,v) \quad = \quad \frac{\beta}{2}\Sigma_s M(v)\int_0^\infty \Sigma_s[n^+(x,v') \; + \; n^-(x,v')]\mathrm{d}v' \quad (5.27)$$

$$- \; v\frac{\partial}{\partial x}n^-(x,v) \quad = \quad \frac{\beta}{2}\Sigma_s M(v)\int_0^\infty \Sigma_s[n^+(x,v') \; + \; n^-(x,v')]\mathrm{d}v'. \quad (5.28)$$

For $n(x,v)$ with $v\epsilon[v_B, \infty)$:

$$+v\frac{\partial}{\partial x}n^{+}(x,v)+v\Sigma_B n^{+}(x,v)=\frac{\beta}{2}\Sigma_s M(v)\int_0^{\infty}\Sigma_s[n^{+}(x,v')+n^{-}(x,v')]\mathrm{d}v'+$$
$$+\int_{v_B}^{\infty}\frac{1}{2}\Sigma_B v'\delta(v-v')[n^{+}(x,v')+n^{-}(x,v')]\mathrm{d}v' \quad (5.29)$$

$$-v\frac{\partial}{\partial x}n^{-}(x,v)+v\Sigma_B n^{-}(x,v)=\frac{\beta}{2}\Sigma_s M(v)\int_0^{\infty}\Sigma_s[n^{+}(x,v')+n^{-}(x,v')]\mathrm{d}v'+$$
$$+\int_{v_B}^{\infty}\frac{1}{2}\Sigma_B v'\delta(v-v')[n^{+}(x,v')+n^{-}(x,v')]\mathrm{d}v'. \quad (5.30)$$

We now define:

$$\tilde{n}^{\pm}(x)=\int_0^{v_B}n^{\pm}(x,v) \quad (5.31)$$

$$\bar{n}^{\pm}(x)=\int_{v_B}^{\infty}n^{\pm}(x,v). \quad (5.32)$$

To keep notation simple, in the following we will not explicitly show the space variable.

Then, we divide by v and integrate equations (5.27) and (5.28) between 0 and v_B and equations (5.29) and (5.30) between v_B and ∞. Carrying out the calculation and using the definitions of equations (5.31) and (5.32), we obtain:

$$\frac{\mathrm{d}}{\mathrm{d}x}\tilde{n}^{+} = \frac{\tilde{\Gamma}}{2}\Sigma_s(\tilde{n}^{+} + \tilde{n}^{-} + \bar{n}^{+} + \bar{n}^{-}) \tag{5.33}$$

$$-\frac{\mathrm{d}}{\mathrm{d}x}\tilde{n}^{-} = \frac{\tilde{\Gamma}}{2}\Sigma_s(\tilde{n}^{+} + \tilde{n}^{-} + \bar{n}^{+} + \bar{n}^{-}) \tag{5.34}$$

$$\frac{\mathrm{d}}{\mathrm{d}x}\bar{n}^{+} = \frac{\bar{\Gamma}}{2}\Sigma_s(\tilde{n}^{+} + \tilde{n}^{-} + \bar{n}^{+} + \bar{n}^{-}) + \frac{\Sigma_B}{2}(\bar{n}^{+} + \bar{n}^{-}) \tag{5.35}$$

$$-\frac{\mathrm{d}}{\mathrm{d}x}\bar{n}^{-} = \frac{\bar{\Gamma}}{2}\Sigma_s(\tilde{n}^{+} + \tilde{n}^{-} + \bar{n}^{+} + \bar{n}^{-}) + \frac{\Sigma_B}{2}(\bar{n}^{+} + \bar{n}^{-}) \tag{5.36}$$

where

$$\tilde{\Gamma} = \int_0^{v_B} \beta M(v)\frac{\Sigma_s}{v}\mathrm{d}v \tag{5.37}$$

$$\bar{\Gamma} = \int_{v_B}^{\infty} \beta M(v)\frac{\Sigma_s}{v}\mathrm{d}v. \tag{5.38}$$

Equations (5.33), (5.34), (5.35), (5.36) form a system of four coupled ordinary differential equations, with the boundary conditions given by equations (5.23) and (5.24). Searching for non-trivial solutions leads to an implicit relation for L^*:

$$F(L^*) = (1+e^{-\frac{v_B^2}{v_T^2}})\cos(kL^*) + \sqrt{\frac{2e^{-\frac{v_B^2}{v_T^2}}}{\pi\Sigma_B\Sigma_s(v_T)}}\sin(kL^*) + e^{-\frac{v_B^2}{v_T^2}} - 1 = 0 \tag{5.39}$$

where

$$k = \sqrt{\frac{2}{\sqrt{\pi}}\Sigma_B\Sigma_s(v_T)e^{-\frac{v_B^2}{v_T^2}}}. \tag{5.40}$$

We will now discuss two simulations: in the former, we shall choose a rod length greater than L^*, expecting to find at least one discrete eigenvalue above α^*; in the latter, we will choose a rod length smaller than L^*, in order to investigate the possible existence of discrete eigenvalues below α^* and their effect on the time behaviour of the neutron population.

The source used for both simulations is still a burst of neutrons with $v = 1\ cm/s$ injected at $t = 0$.

Simulation 1 ($L > L^*$)

We summarize the parameters adopted for the simulation in the following table:

L	13 cm
Σ_s	0.05 s^{-1}
Σ_s^0	0 cm^{-1}
Σ_B (only for $v > v_B$)	1 cm^{-1}
$\Sigma_a(v)$	0 cm^{-1}
v_T	1 $cm\ s^{-1}$
v_B	0.4 $cm\ s^{-1}$

Considering these data, using equations (5.19) and (5.39) we find that the Corngold limit is characterized by:

α^*	-0.05 s^{-1}
L^*	$\simeq$ 12.031 cm

Thanks to the deterministic solver, we find the eigenvalue spectrum of this case, which is shown in figure 5.18.

The spectrum has been obtained by using an energy discretization with M meshes and a space discretization with N meshes. The discussion about the space and energy discretization made in paragraph 5.2.2 is still valid: increasing M the continuum regions are progressively filled; increasing N the

two-dimensional continuum below α_a grows, filling a plane. Taking into account these considerations, we remark the similarity between the spectrum of figure 5.18 and the spectrum predicted by the theory, shown in figure 4.5. Finally, we observe that there exists a discrete eigenvalue to the right of α^*.

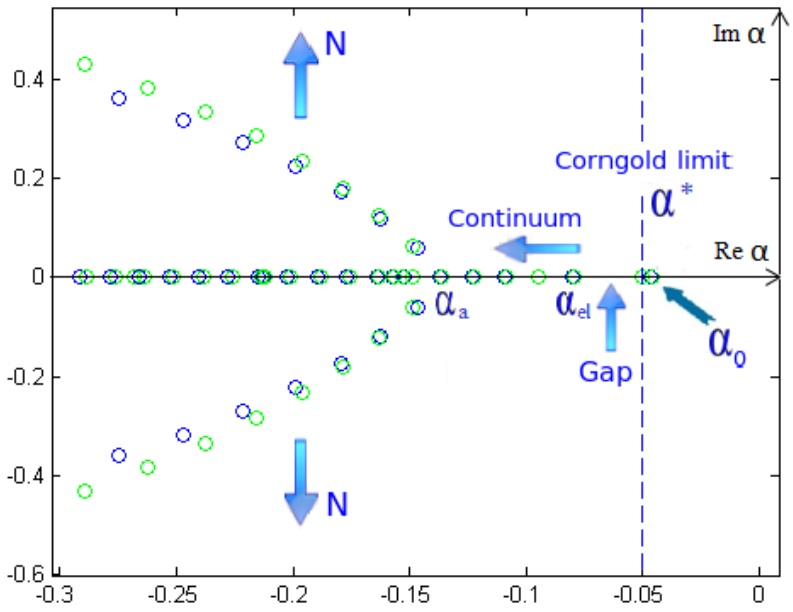

Fig. 5.18: α-eigenvalue spectrum (obtained by the deterministic solver) for the neutron thermalization in a moderating medium with Bragg scattering ($L > L^*$).

Following this analysis of the spectrum, we run the α-static code for this case and we obtain the α_0 convergence as a function of the generations; we see in in figure 5.19 the result of the simulation. The α_0 eigenvalue averaged over the last 50 generations (after discarding the first 50) is plotted as a green line in figure 5.19 and we see that it is in good agreement with the discrete eigenvalue given by the deterministic solver.

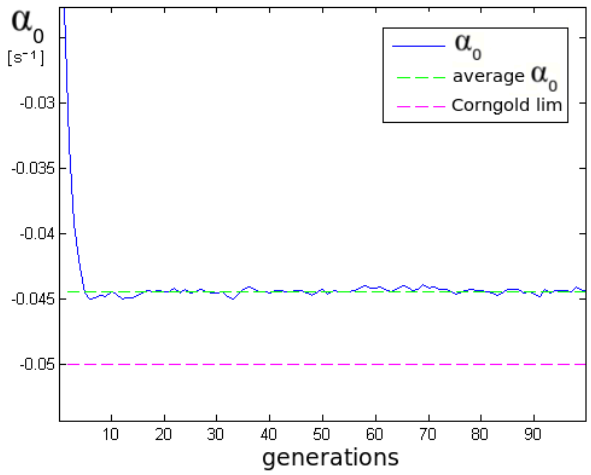

Fig. 5.19: Neutron thermalization in a medium with Bragg scattering ($L > L^*$): the fundamental eigenvalue α_0 provided by the α-static code plotted as a function of the generations.

As usual, if at least one discrete eigenvalue exists, after a transient, the neutron density $n(v,t)$ can be represented by the separable form $n(v,t) = n_0(v)e^{\alpha_0 t}$, where $n_0(v)$ is the eigenfunction associated to α_0 and physically represents the asymptotic velocity distribution of the neutrons.
To assess the behaviour of the neutron population in time, we run the reference dynamic Monte Carlo code. Then, we compare the asymptotic time behaviour ($e^{\alpha_0 t}$) and neutron density $n(v)$ provided by the α-static code to the results of the dynamic code.

Figure 5.20(a) shows that the time behaviour of the neutron population, after a transient, is well fitted by an exponential decay with rate equal to the eigenvalue α_0 given by the α-static code. There is a very good agreement also in the neutron velocity distribution provided by the static (blue) and dynamic (green) code, as shown in figure 5.20(b).
Observing figure 5.20(b), we note that the neutron velocity distribution of this case is different from the others seen until now: there is a discontinuity

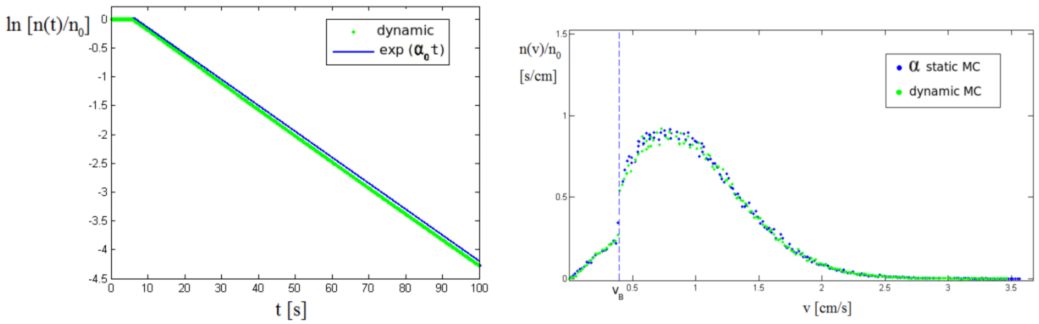

(a) The time decay of the neutron population in a medium with Bragg scattering ($L > L^*$).

(b) The asymptotic velocity distribution of the neutron population in a medium with Bragg scattering ($L > L^*$)

Fig. 5.20: α-static results (blue) compared to Dynamic Monte Carlo results (green).

in $v = v_B$. This feature is related to the Bragg scattering that, as said, is a threshold process: the discontinuous form of the Bragg cross section induces a discontinuity also in the neutron density $n(v)$.

Simulation 2 ($L < L^*$)

We reduce the rod size to a dimension smaller than L^*. We summarize the parameters adopted for the simulation in the following table:

L	11.5 cm
Σ_s	0.05 s
Σ_s^0	0 cm^{-1}
Σ_B (only for $v > v_B$)	1 cm^{-1}
$\Sigma_a(v)$	0 cm^{-1}
v_T	1 $cm\ s^{-1}$
v_B	0.4 $cm\ s^{-1}$

We use the deterministic solver to obtain a picture of the spectrum, shown in figure 5.21.

The deterministic solver shows the presence of a single discrete eigenvalue in the gap between α^* and α_{el}, that is between the sub-Bragg continuum and the elastic continuum.

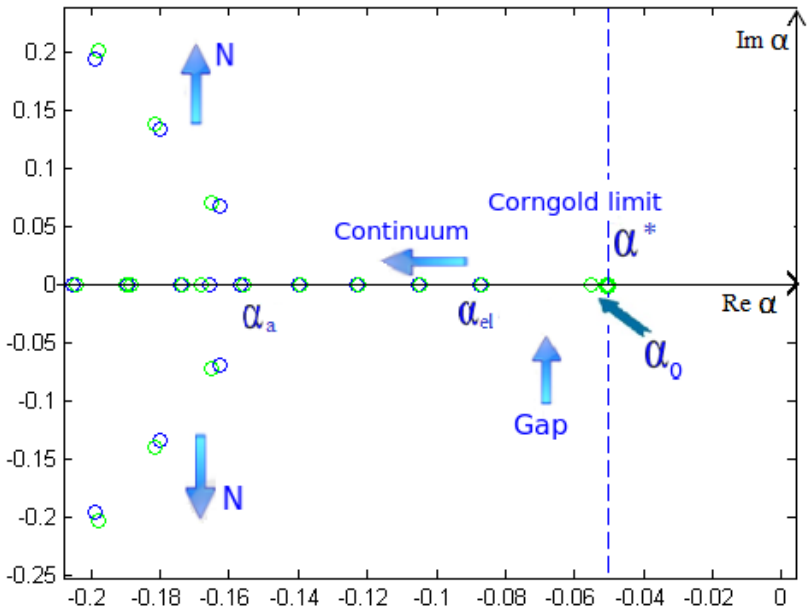

Fig. 5.21: α-eigenvalue spectrum (obtained by the deterministic solver) for the neutron thermalization in a moderating medium with Bragg scattering ($L < L^*$). It is possible to observe a single discrete eigenvalue in the gap between two continuum regions.

We wonder whether the α-static code is able to find a discrete eigenvalue below the Corngold limit α^*. Therefore, we run the α-static code for this case and obtain the α convergence as a function of the generations, which is shown in figure 5.22. We see that the α-static converges without difficulty to an eigenvalue α_0 smaller than the Corngold limit, in agreement with the value of the deterministic solver.

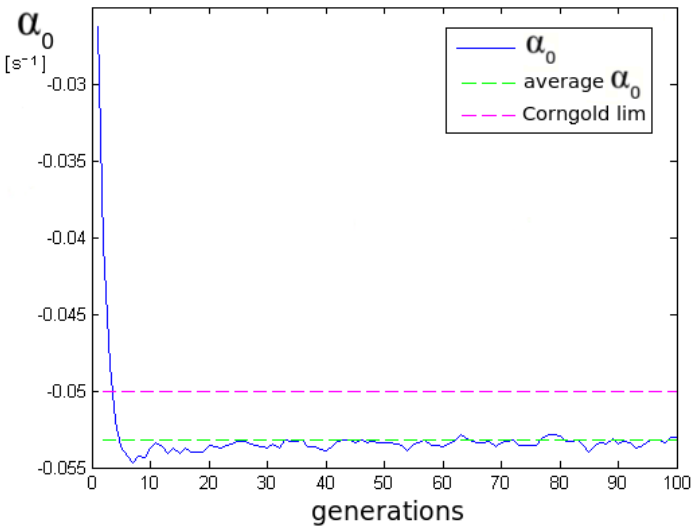

Fig. 5.22: Neutron thermalization in a medium with Bragg scattering ($L < L^*$): the fundamental eigenvalue α_0 provided by the α-static code plotted as a function of the generations.

What is the physical meaning of this discrete eigenvalue? To answer this question, we need to assess the behaviour of the neutron population in time: for this reason, we first run the dynamic Monte Carlo code.
In figure 5.23(a) we compare the reference neutron time decay obtained by the dynamic Monte Carlo code (green) to an exponential function with rate α_0 given by the α-static code (blue). We see that, after a transient, the two curves have the same slope. There is a good agreement also in the neutron velocity distribution provided by the α-static code (blue) and the dynamic code (green), as shown in figure 5.23(b).

However, we know from theory that the discrete eigenvalue found in the gap is not a fundamental eigenvalue, as explained in paragraph 4.3. In fact, it can be shown [10] that the eigenfunction associated with a discrete eigenvalue $\alpha_0 < \alpha^*$ cannot be everywhere positive and thus the asymptotic behavior of

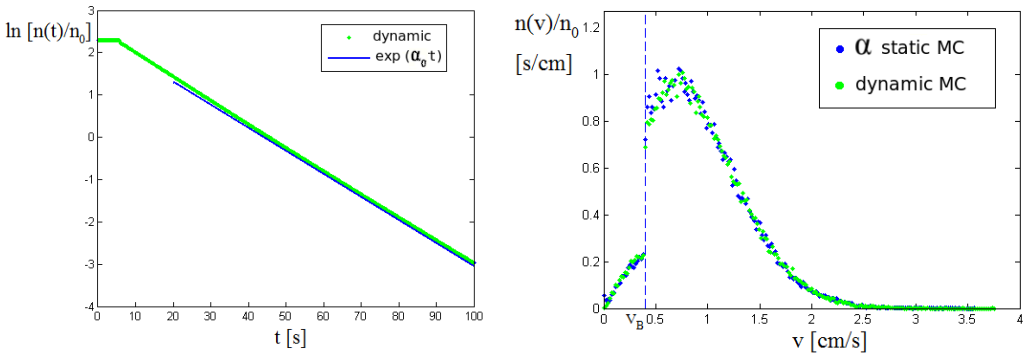

(a) The time decay of the neutron population in a medium with Bragg scattering ($L < L^*$).

(b) The asymptotic velocity distribution of the neutron population in a medium with Bragg scattering ($L < L^*$)

Fig. 5.23: The α-static results (blue) compared to the Dynamic Monte Carlo results (green).

the neutron density cannot be described by this eigenfunction alone: there must be a continuum contribution. Actually, as explained in chapter 4.3, to describe the neutron density we should take into account three contributions: the discrete eigenvalue, the sub-Bragg continuum contribution and the elastic continuum contribution. However, for dimensions only slightly smaller than L^*, the discrete eigenvalue is very "close" to α^* and "far" from α_{el}, so that the elastic continuum contribution can be neglected. In this case, an exponential decay can be observed but this must be followed, at very long times, by a non-exponential behaviour, due to the sub-Bragg continuum Γ_{SB}. We conjecture that this is the case in our simulation. To check this hypothesis, we compute α_{el} by using Eq. 5.20 and summarize the situation in the following table:

α^*	-0.05 s^{-1}
α_0	$\simeq$ -0.053 s^{-1}
α_{el}	$\simeq$ -0.073 s^{-1}

Note that the value α_{el} obtained using Eq. 5.20 is in good agreement with the spectrum of figure 5.21.
We conclude that in this system the elastic continuum contribution is negligible and that the exponential decay that we observe is transient: it must be followed, at very long times, by non-exponential behaviour. Unfortunately, it is difficult to "follow" the neutrons for such long times with the dynamic Monte Carlo code because we should simulate too many particles in order to have good statistical data.

5.4 Slowing down and thermalization

In paragraph 4.4, we have discussed the properties of the slowing down integral operator S_{SD} and we have seen that its spectrum is composed only of the point at $-\infty$. For this reason, if we add the slowing down process to the neutron transport cases studied in paragraph 5.2 (we neglect the Bragg scattering for simplicity) we do not expect changes in the spectrum features: the slowing down operator does not add other discrete eigenvalues or continuum intervals to the spectrum. However, we expect to find quantitative differences with respect to the previous cases. For instance, the presence of the operator S_{SD} will probably modify the asymptotic velocity distribution: in particular, we expect to find a lower average velocity. Does the slowing down process affect also the time behaviour? To verify our hypotheses, we propose now a study of the effects of the neutron slowing down operator on the α eigenvalue spectrum.
We reconsider the cases for the infinite medium and the rod model, presented in paragraph 5.2, introducing the slowing down. For this reason, we add to the $1/v$ thermalization scattering and absorption cross sections a constant

slowing down scattering cross section, like shown in figure 5.24.

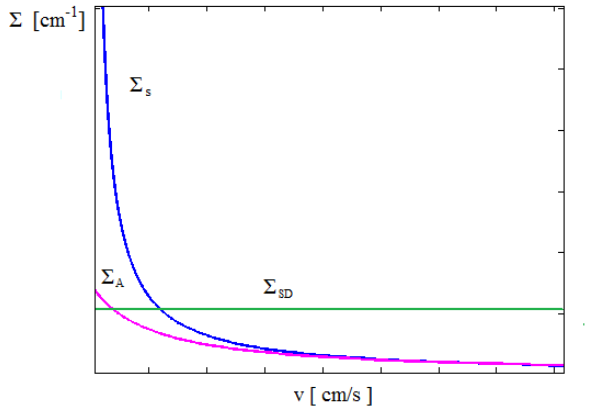

Fig. 5.24: Cross section modeling for slowing down and thermalization

Note that this model is quite "artificial": as explained in paragraph 4.4, the properties of the slowing down operator are stem from considering fast neutrons transport, with speed several orders larger than the speed of the background atom motion. For this reason, in order to have a more realistic model, we should separate the range of thermalization scattering from that of slowing down. Then, we should use a speed source much greater than that used for the precedent simulations. Note that the distribution source does not affect the α-static code: the asymptotic behaviour, that is the fundamental eigenvalue and the associated eigenmode, and the whole spectrum, do not dependent on the initial condition. The choice of the source influences only the time transient provided by the Monte Carlo code. Unfortunately, adopting this scheme we would have some "practical" problems:

- in order to properly treat a large speed range, we should increase the energy discretization mashes of the deterministic solver: this is quite problematic for our simple deterministic solver developed in MATLAB;
- we have seen that for our systems characterized by negative α_0, it is

difficult to obtain good statistical data by the dynamic Monte Carlo code: simulating fast particles, this problem is emphasized. In fact, all particles would be absorbed or would escape before reaching the asymptotic regime.

Note that the α-static code can easily handle the simulation of fast particles. However, in order to have the possibility to compare the α-static code results to those of the other codes, we prefer to treat the simple model described above and a source speed only slightly larger than the previous one ($v_{source} = 5\ cm/s$ in the following simulations).

5.4.1 Infinite medium

We re-consider the first simulation of paragraph 5.2.1: for this case we had chosen $\Sigma_a^0 < \Sigma_a^{0*}$ and so we had found a discrete eigenvalue ($\alpha_0 \simeq -1.28\ s^{-1}$). We now add the slowing down scattering; the parameters adopted are:

L	infinite
Σ_s	1.0 s^{-1}
Σ_s^0	0.1 cm^{-1}
Σ_a	0.5 s^{-1}
Σ_a^0	0.8 cm^{-1}
Σ_{sd}	1 cm^{-1}
v_T	1 cm/s

We use the deterministic solver to obtain a picture of the spectrum, shown in figure 5.25. We observe that the spectrum is qualitatively similar to that of the case without slowing down, in figure 5.4; as previewed, there are no

additional discrete eigenvalues and the continuum is unchanged. However, we note that the discrete eigenvalue is larger than that previously found.

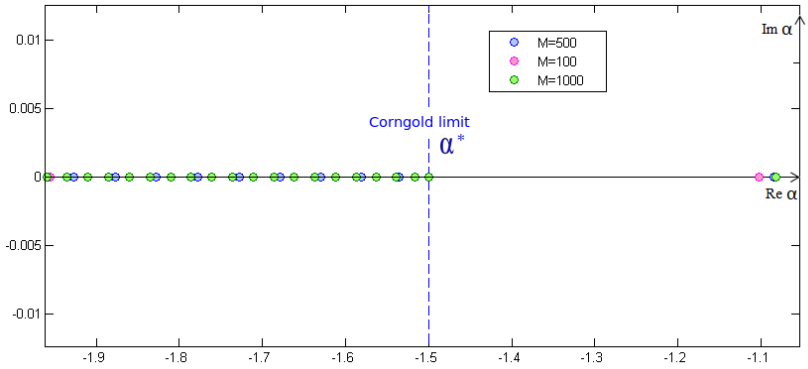

Fig. 5.25: α-eigenvalue spectrum (obtained by the deterministic solver) for the neutron slowing down and thermalization in an infinite moderating medium with $\Sigma_a^0 < \Sigma_a^{0\,*}$.

We run the α-static code and obtain the α_0 convergence as a function of the generations shown in figure 5.26; the result agrees with the deterministic code: the fundamental eigenvalue is above the previous one.

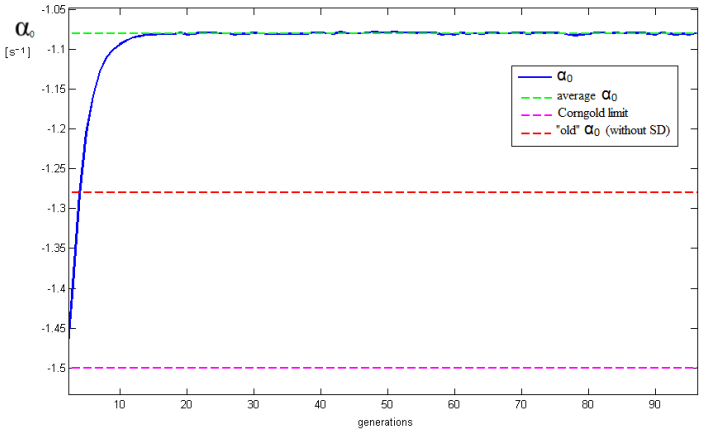

Fig. 5.26: Neutron slowing down and thermalization in an infinite medium with $\Sigma_a^0 < \Sigma_a^{0\,*}$: the fundamental eigenvalue α_0 provided by the α-static code plotted as a function of the generations.

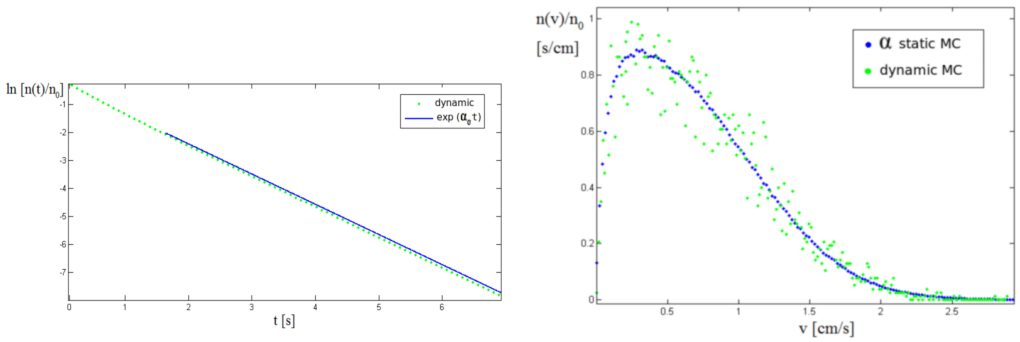

(a) The time decay of the neutron population in an infinite medium with $\Sigma_a^0 < \Sigma_a^{0\,*}$ (with slowing down scattering).

(b) The asymptotic velocity distribution of the neutron population in an infinite medium with $\Sigma_a^0 < \Sigma_a^{0\,*}$ (with slowing down scattering)

Fig. 5.27: The α-static results (blue) compared to the Dynamic Monte Carlo results (green).

Finally, we run the dynamic Monte Carlo code to assess the complete time behaviour of the neutrons.
Figure 5.27(a) confirms that the time decay of the neutron population obtained by the dynamic code (green), after a transient, is well fitted by an exponential with rate α_0. In figure 5.27(b), we see that there is also an agreement in the neutron velocity distribution provided by the static (blue) and dynamic (green) code, even if the dynamic data are very dispersed.

We use the good statistical α-static data to compare the velocity distribution of the two cases with and without slowing down. We can observe this comparison in figure 5.28, which shows that the velocity distribution is shifted toward lower velocities, as expected.

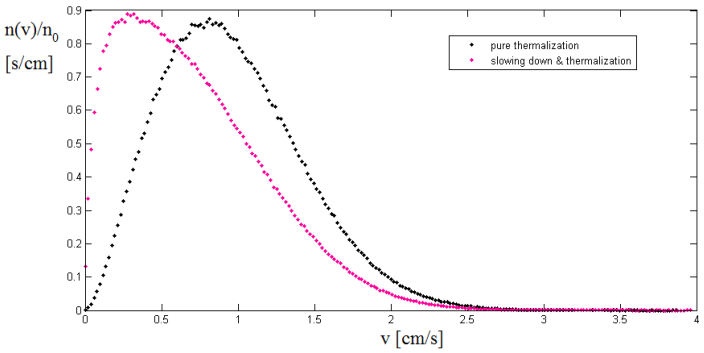

Fig. 5.28: The asymptotic velocity distribution in the pure thermalization case (black) and in the slowing down + thermalization case (red). (Infinite medium with $\Sigma_a^0 < \Sigma_a^{0\,*}$*)*

Summarizing, the introduction of the slowing down has produced a change in the velocity distribution form and in the average velocity, which is smaller than the average velocity without slowing down; it has also induced a shift of the fundamental eigenvalue: in other words, the slowing down operator removes the fundamental eigenvalue from the Corngold limit.

We wonder whether the disappearance of the discrete eigenvalue into the continuum is still possible. To answer the question, we have run the α-static code with different values Σ_a^0, leaving unchanged the other parameters. The α_0 (averaged over the last generations) provided by the α-static code is plotted as a function of Σ_a^0 in figure 5.29(a). We see that the Corngold limit is achieved for an absorption rate considerably larger ($\Sigma_a^{0*} \simeq 1.88\ cm^{-1}$) than that of the case without slowing down ($\Sigma_a^{0*} \simeq 1.104\ cm^{-1}$). This result is confirmed also by the deterministic solver, as shown in figure 5.29(b), where we see that the discrete eigenvalue moves toward the continuum with increasing Σ_a^0.

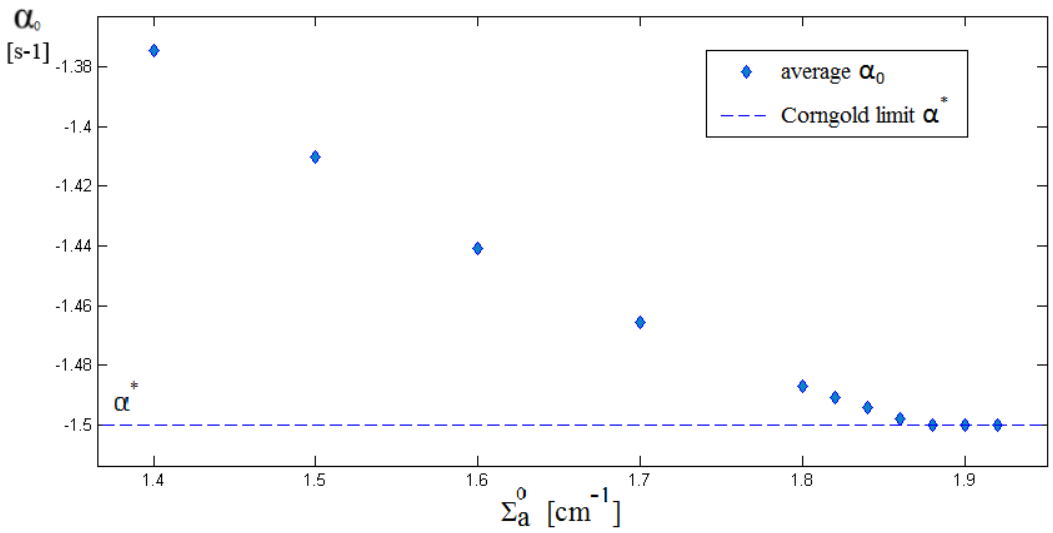

(a) The average α_0 obtained by the α-static code plotted as a function of Σ_a^0.

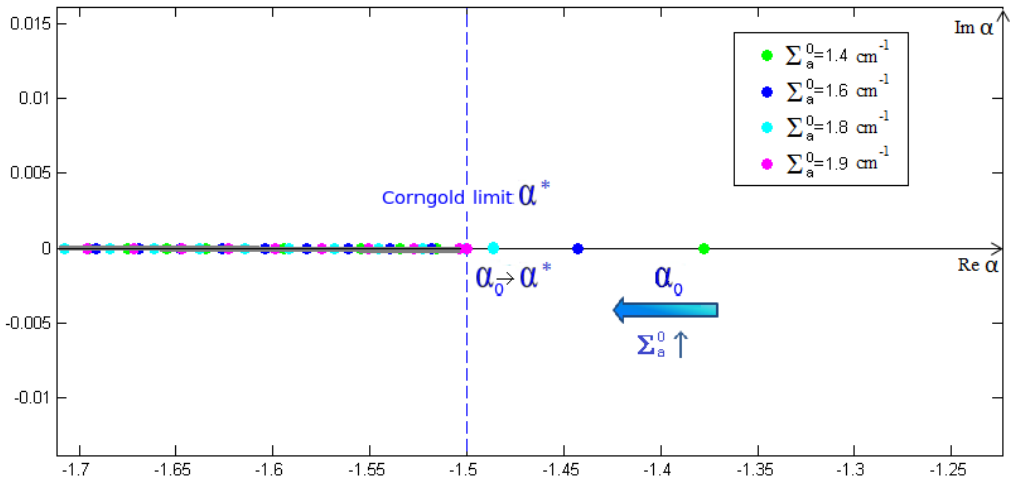

(b) The single discrete eigenvalue in the spectrum decreases with increasing Σ_a^0.

Fig. 5.29: The discrete eigenvalue α_0 as a function of Σ_a^0 for the neutron slowing down and thermalization in an infinite medium.

5.4.2 The rod model

We re-consider the first simulation of paragraph 5.2.2: for this case we had chosen a length $L > L^*$ and so we had found a discrete eigenvalue ($\alpha_0 \simeq -1.882\ s^{-1}$). We now add the slowing down scattering; the adopted parameters are:

L	2 cm
Σ_s	1.0 s^{-1}
Σ_s^0	0 cm^{-1}
Σ_a	1.0 s^{-1}
Σ_a^0	0 cm^{-1}
Σ_{sd}	1.0 cm^{-1}
v_T	1.0 cms^{-1}

We use the deterministic solver to obtain the spectrum, which is shown in figure 5.30. We observe that it is qualitatively similar to the spectrum of the rod without slowing down, in figure 5.11. The spectrum confirms that there are no additional discrete eigenvalues and the continuum is unchanged; moreover, comparing 5.30 to 5.11 we note again that the discrete eigenvalue is larger than that of the case without slowing down (the discrete eigenvalue on the spectrum of figure 5.30 is approximately $\alpha_0 \simeq -1.48$).

We run the α-static code and obtain the α_0 convergence as a function of the generations shown in figure 5.31; the result agrees with the deterministic code: the fundamental eigenvalue is above the previous one.

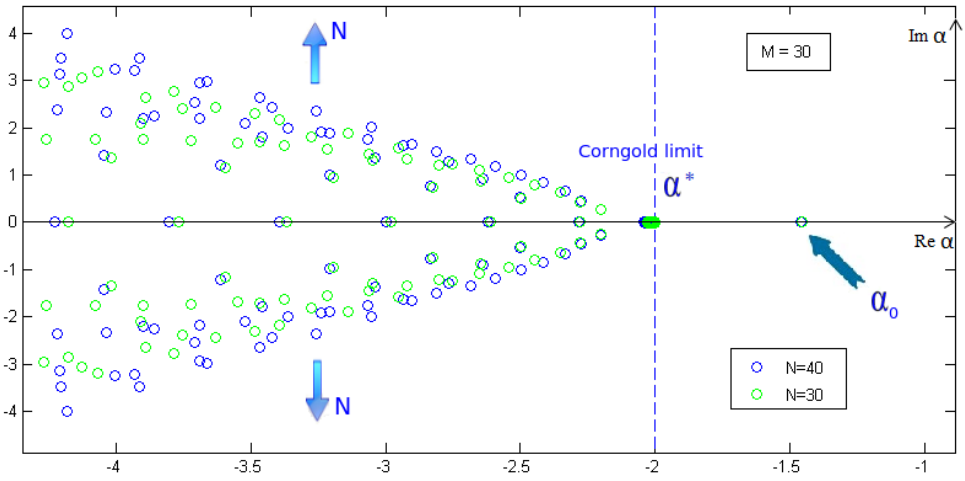

Fig. 5.30: α-eigenvalue spectrum (obtained by the deterministic solver) for the neutron slowing down and thermalization in a bounded moderating medium with $L > L^*$.

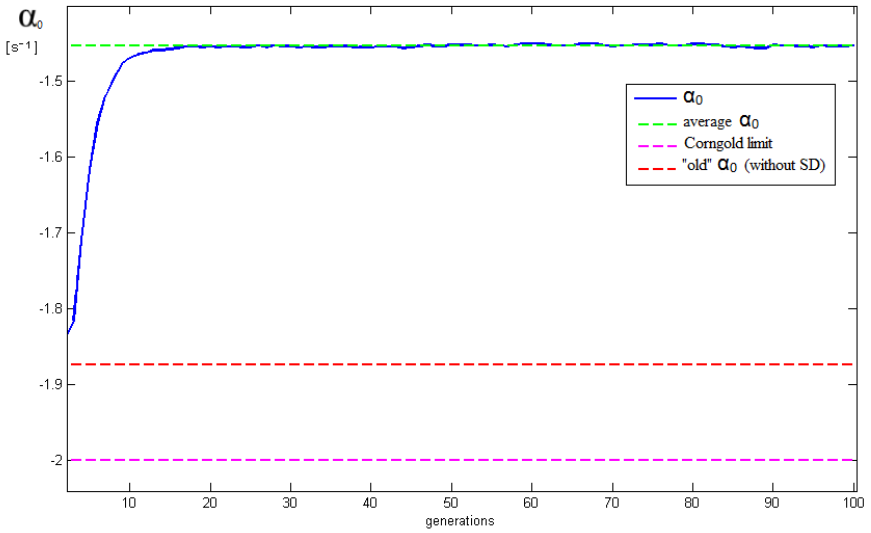

Fig. 5.31: Neutron slowing down and thermalization in a bounded medium with $L > L^*$: the fundamental eigenvalue α_0 provided by the α-static code plotted as a function of the generations.

We use now the α-static code (whose data are statistically better then those of the dynamic code) to compare the velocity distribution of the two cases with and without slowing down. Figure 5.32 shows that also for a bounded medium the velocity distribution is shifted toward lower velocities.

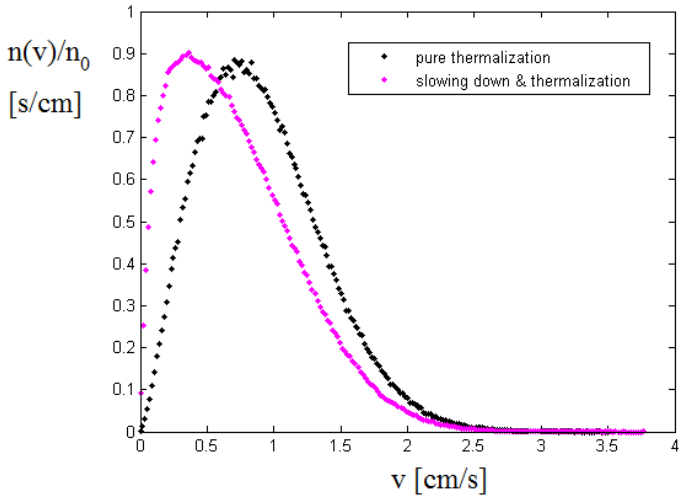

Fig. 5.32: The asymptotic velocity distribution in the pure thermalization case (black) and in the slowing down + thermalization case (red). (Bounded medium with $L > L^*$)

We conclude that also in a bounded medium the introduction of the slowing down has induced a change in the velocity distribution form and in the average velocity, which is smaller than the average velocity without slowing down; it has also induced a shift of the fundamental eigenvalue: the slowing down operator removes the fundamental eigenvalue from the Corngold limit. In order to test the possible disappearance of the discrete eigenvalue into the continuum, we have run the α-static code with different rod length values, leaving unchanged the other parameters. The α_0 (averaged over the last generations) provided by the α-static code is plotted as a function of L in figure 5.33(a). We see that the Corngold limit is achieved in correspondence

of a rod length considerably smaller ($L \simeq 0.89\ cm$) than that of the case without slowing down ($L^* \simeq 1.77\ cm$). This result is confirmed also by the deterministic solver, as shown in figure 5.33(b), where we see that the discrete eigenvalue moves toward the continuum with decreasing L.

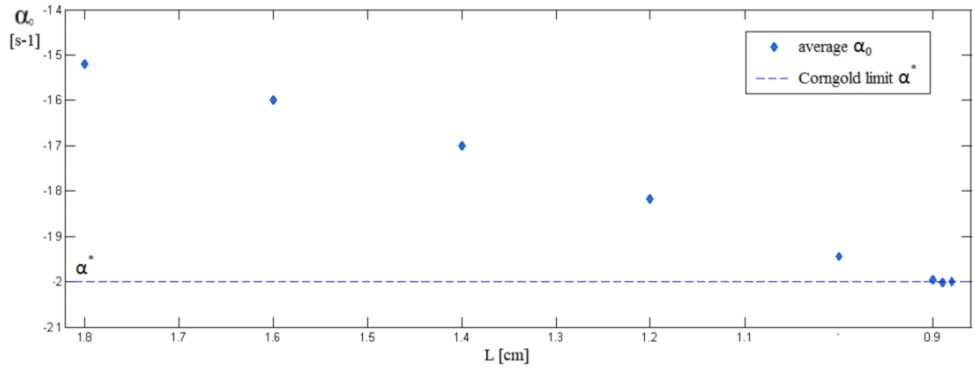

(a) The average α_0 obtained by the α-static code plotted as a function of L

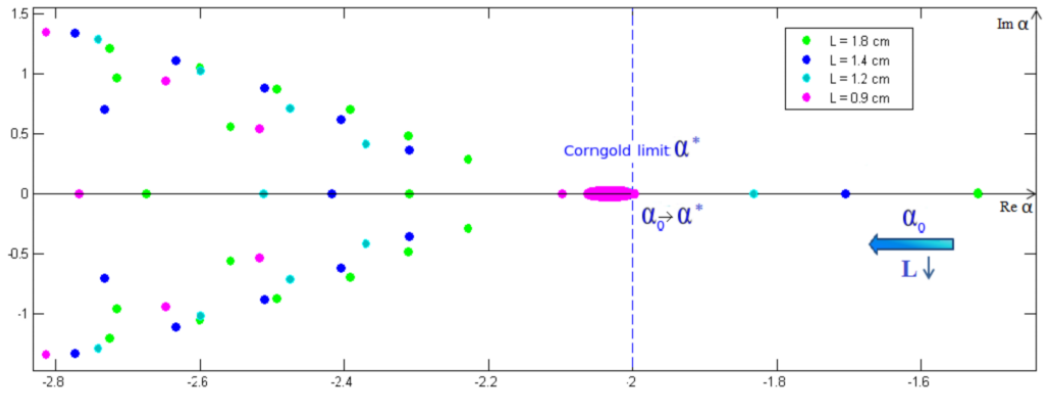

(b) The single discrete eigenvalue in the spectrum decreases with decreasing L

Fig. 5.33: The discrete eigenvalue α_0 as a function of L for the neutron slowing down and thermalization in a bounded medium

In summary, we have found the same effects for infinite and bounded media. The introduction of the slowing down causes a shift of the fundamental eigenvalue and a change in the neutron velocity distribution.
We observe that the model adopted to describe the slowing down and thermalization of fast neutrons is quite simplified, as explained at the beginning of section 5.4. However, this analysis of the slowing down effects on the neutron behaviour is a good example of the α-static method capability in the study of moderator properties.

Chapter 6

Conclusions

The Monte Carlo method is a powerful tool to solve transport problems, as neutron transport, because it is very accurate, since introduces a minimal amount of approximations. The Monte Carlo method has been adopted to determine the stationary behaviour of nuclear systems, i.e., to solve the stationary Boltzmann equation, since the beginning of the nuclear technology development. These "static calculations" neglect the time evolution.

In recent years, the interest toward numerical methods that allow assessing the time behaviour of neutron transport has grown. This interest has been raised on one hand by the improved computer power and on the other hand by the concerns about reactor safety. In fact, knowledge of the neutron time behaviour is important in nuclear engineering both for normal scenarios (start-up, power transients) and accidental situations [8, 22]. Until now, the analysis of transient dynamics of a neutron population has been mainly carried out by resorting to deterministic methods by solving the time-dependent Boltzmann equation; unfortunately, these latter introduce several approximations and in some situations it is desirable to have a higher-fidelity tool for transient analysis. In this respect, Monte Carlo methods including the

time dependence have been recently proposed: the Dynamic Monte Carlo methods, which allow assessing the complete time evolution of the neutron population [22]. However, a non-negligible drawback of Monte Carlo methods is that they suffer from slow convergence and are more time-consuming than deterministic methods; these drawbacks are accentuated for the dynamic Monte Carlo methods. If one is interested in the asymptotic (long time) behaviour of the system, instead of the full time dynamics, a possible solution is to resort to the α-static Monte Carlo method [48, 50], which is very accurate and less time-consuming than dynamic methods. This latter method is the subject of this thesis.

We have shown that the α-static Monte Carlo method allows determining the asymptotic time behaviour of the neutron population by transforming the time-dependent Boltzmann equation into an eigenvalue problem (the so called α eigenvalue), where the time dependence is not explicit (for this reason the method is called "static"). In particular, in chapter 3 we have shown that the mathematical assumption at the basis of the method is the possibility of decomposing the neutron density $n(\vec{r}, v, \hat{\Omega}, t)$ in a separate variable form with exponential time behaviour [3, 17, 44] of the kind

$$n(\vec{r}, v, \hat{\Omega}, t) = \sum_i n_{\alpha_i}(\vec{r}, v, \hat{\Omega}) e^{\alpha_i t}, \tag{6.1}$$

so that for long time we have

$$n(\vec{r}, v, \hat{\Omega}, t) \simeq n_{\alpha_0}(\vec{r}, v, \hat{\Omega}) e^{\alpha_0 t}, \tag{6.2}$$

where α_0 is the algebraically largest value among all α_i of the expansion. If $\alpha_0 < 0$, the neutron population decays in time; if $\alpha_0 > 0$, the neutron population grows in time. Note that the latter case is possible only if there are fissile materials in the system.

Substituting the solution given by Eq. (6.2) into the time-dependent Boltzmann equation leads to

$$L\, n_{\alpha_0}(\vec{r}, v, \hat{\Omega}, t) = \alpha_0 n_{\alpha_0}(\vec{r}, v, \hat{\Omega}, t) \tag{6.3}$$

where L is the linear Boltzmann operator introduced in chapter 2. The equation (6.3) is formally an eigenvalue problem; for this reason α_0 is named the *fundamental eigenvalue* and the associated n_{α_0} is the *fundamental eigenmode*. We note that the fundamental eigenvalue physically represents the rate of variation of the neutron population and that the fundamental eigenmode is the asymptotic neutron distribution in space, direction and velocity. An algorithm to solve the eigenvalue problem defined by Eq. 6.3 has been recently proposed by the LTSD laboratory of the CEA/Saclay [48, 49, 50]. In particular, the α-static algorithms are historically known to be numerically unstable when $\alpha_0 < 0$; the proposed algorithm has solved this problem thanks to a mathematical trick. Further details can be found in chapter 3.

We have also shown that the α-static method depends on the features of the spectrum of the Boltzmann operator, which is rather complicate. Indeed, generally speaking, the spectrum does not consist only of discrete eigenvalues. In fact, for negative α, below a limit value α^*, the spectrum contains a continuum interval [3, 12, 13, 17, 28, 44]. We know from literature [12, 13, 28] that, for some moderating systems, the fundamental eigenvalue can disappear in the continuum if the system size is too small or the absorption rate is too strong. For this reason, we have decided to focus our attention on moderating materials, in order to test the α-static method behaviour in such particular situations and also to better understand some interesting moderator properties.

To this aim, we have developed an α-static Monte Carlo code, based on the

α-static algorithm explained in chapter 3, which provides the fundamental eigenvalue α_0 and the associated fundamental eigenmode n_{α_0}. We have also developed a dynamic Monte Carlo code, which can be used as reference to assess the time behaviour of the system. Finally, we have developed a deterministic solver which can provide a picture of the entire spectrum of the Boltzmann operator.
We have used these codes to extensively study the diffusion of *thermal neutrons* in moderating materials. The physical models we have dealt with have been described in chapter 4. In summary:

- we have studied the neutron transport in infinite media and in one-dimensional bounded media (the rod model);
- we have considered two different kinds of moderators: hydrogen-based moderators and crystalline moderators. In the former, a single shock is sufficient to thermalize the neutron; in the latter, also an elastic coherent scattering (or Bragg scattering) can occur for neutrons with large enough velocities. The Bragg scattering is a threshold process that leaves unchanged the neutron speed.

The key results of the simulations have been presented in chapter 5.
First of all, we have performed several simulations in hydrogen-based moderator systems. Whenever a fundamental discrete eigenvalue exists, the α-static code has been able to correctly provide a value α_0, as confirmed by the dynamic Monte Carlo code and by analytical results (when available). In fact, the α-static code has been able to provide the asymptotic time decay and the asymptotic velocity distribution of the neutron population. For this kind of asymptotic analysis, we have also observed that the α-static code gives data statistically better than those of the dynamic Monte Carlo code. For

hydrogen-based moderators, in agreement with the theory reported in chapter 4, we have found that the fundamental discrete eigenvalue α_0 disappears in the continuum for system dimensions smaller than a critical dimension L^* or for absorption rates that strongly increase with increasing neutron speed. In this case, the α-static code converges to the continuum limit α^*: the code can not find the fundamental eigenvalue, because this does not exist anymore. In these cases, the exponential expansion of Eq. (6.1) at the basis of the α-static method is no more valid; in fact, by using the dynamic Monte Carlo code, we have observed that the time behaviour is no more exponential. However, the behaviour of the α-static code in these situations is not really troubling: the disappearance of the discrete eigenvalues is a pathological and quite uncommon behaviour.

Following the results about the hydrogen-based moderators, we have addressed the thermalization of neutrons in crystalline moderators. We have found again a very good agreement between the α-static code and the dynamic Monte Carlo code for the cases where the fundamental eigenvalue α_0 exists. Moreover, the α-static code has been able to detect a peculiarity of these moderators. As explained in section 4.3, the Bragg scattering induces the presence of several continuum regions in the spectrum; in particular, two of these regions are separated by a gap. For system dimensions slightly smaller than the critical dimension Ł*, it is possible to find a discrete eigenvalue in this gap, below the (sub-Bragg) continuum limit α^* but above the beginning of the other continuum region (the elastic continuum). As explained in section 4.3, a discrete eigenvalue α_0 smaller than α^* can not be a true fundamental eigenvalue: this means that the asymptotic time behaviour is not exponential and the neutron asymptotic density is not given only by the eigenfunction associated to this α_0, but also by a continuum contribu-

tion. However, as shown in section 4.3, in this case it is possible to observe an exponential time behaviour with rate α_0 during a very long transient. Our simulations agree with the theory: the α-static code is able to find the discrete eigenvalue in the gap and the velocity distribution of the neutron population during the long transient, as confirmed by the dynamic Monte Carlo code.
Finally, in chapter 5 we have presented some simulations concerning a very simple model of neutron slowing down. As stressed also in section 5.4, the adopted model is too approximated to give a physical meaning to the obtained results, but provides an example of the α-static code capability in the study of the moderator properties.

We conclude with an important final remark. In this thesis, we have applied the α-static method only to moderating systems. However, as said in chapter 3, the proposed algorithm can be applied also to multiplying systems and furthermore includes both the prompt and delayed neutrons. Several tests have been performed for fissile materials by the LTSD-laboratory (before and during this work of thesis) and they have provided very good results [50].
We know that, when fissile materials are present, the fundamental eigenvalue α_0 can be positive (supercritical system) or negative (subcritical system). In this respect, it would be interesting to perform other simulations with our codes in subcritical systems to investigate the consequent change of the Boltzmann operator spectrum and to understand if the disappearance of the fundamental eigenvalue into the continuum is still possible in presence of fissile materials.

Bibliography

[1] Akcasu, Z., Lellouche, G., Shotkin, L.M., *Mathematical methods in nuclear reactor dynamics*, Academic Press (1971).

[2] Albertoni, S., Montagnini, B., "On the spectrum of neutron transport equation in finite bodies," *J. Math. Anal. and Appl.*, **13**: pp. 19-48 (1966).

[3] Bell, G.I., Glasstone, S., *Nuclear reactor theory*, Van Nostrand Reinhold Company (1970).

[4] Beauwensen, R., Mika, J., *Transport theory stat. Phys.*, **2**, (1971).

[5] Borysiewicz, M., Mika, J., *Proceedings symposium on neutron thermalization and reactor spectra*, (IAEA, Vienna, 1967), **1**, p. 45.

[6] Brockway, D., Soran, P., Whalen, P., "Monte Carlo eigenvalue calculation," LA-UR-85-1224 (1985).

[7] Betzler, B.R., et al., "Calculating alpha eigenvalues in a continuous-energy infinite medium with Monte Carlo," LA-UR-12-24472 (2012).

[8] Cao.,Y., "Space-time kinetics and time-eigenfunctions", *University of Michigan*, (2008).

[9] Cohen, E. R., "Some topics in reactor kinetics", In *Proceedings of the 2nd UN conference of the peaceful uses of atomic energy*, P/629, Geneva, Switzerland (1958).

[10] Conn R., Corngold N., "A theory of pulsed neutron experiments in polycristalline media" In *Nuclear science and engineering*, **37**: pp. 85-93 (1969).

[11] Conn R., Corngold N., "Analysis of pulsed neutron experiments in polycristalline media using a model kernel" In *Nuclear science and engineering*, **37**: pp. 94-103 (1969).

[12] Corngold N., "Quasi-exponential decay of neutron fields", In *Advances in nuclear science and technology*, **8**: pp. 1-46 (1975).

[13] Corngold, N., Kuscer, I., "Discrete Relaxation Times in Neutron Thermalization", In *Physical Review*, **139**(3A) (1965)

[14] Corngold, N., *Nucl. Sci. Eng.*, **37**(85) (1969)

[15] Cullen, D.E., et al., "Static and dynamic criticality: are they different?," UCRL-TR-201506 (2003).

[16] De Saussure, "A note on the measurement of diffusion parameters by pulsed-neutron source technique", In *Nuclear science and engineering*, (1961).

[17] Duderstadt, J.J., Martin, W.R., *Transport theory*, J. Wiley and sons, New York (1979).

[18] Hansen, G.E., "Rossi alpha method," LA-UR-85-4176 (1985).

[19] Henry, A. F., "The application of inhour modes to the description of nonseparable reactor transients," *Nucl. Sci. Eng.*, **20**: pp. 338-351 (1964).

[20] HÃ©bert, A., *Applied reactor physics*, Presses Internationales Polytechnique (2009).

[21] Hill, T.R., "Efficient Methods for Time Absorption (α) Eigenvalue Calculations," LA-9602-MS (UC-32) (1983).

[22] Hoogenboom, J.E., "Numerical calculation of the delayed-alpha eigenvalue using a standard criticality code," In: *Proceedings of the PHYSOR conference*, Seoul, Korea (2002).

[23] Kaper, H. G., "The initial-value transport problem for monoenergetic neutrons in an infinite slab with delayed neutron production," *J. Math. Anal. and Appl.*, **19**: pp. 207-230 (1967).

[24] Keepin, G.R., *Physics of Nuclear Kinetics*, Addison-Wesley, Reading, UK (1965).

[25] Kiedrowski, B. C., "Analytic, infinite-medium solutions for point reactor kinetics parameters and reactivty perturbations," LA-UR-10-01803 (2010).

[26] Koblinger, L., Lux, I., *Monte Carlo Transport Methods: neutron and photon calculations*, Boca Raton:CRC (1991).

[27] Kothari, L.S, "Decay constant(of a neutron pulse inside finite solid moderator assembly", In *Nuclear science and engineering*, **23**: pp. 402-405 (1965).

[28] Larsen, E.W., Zweifel, P. F., "On the spectrum of the linear transport operator," *J. Math. Phys.*, **15**: pp. 1987-1997 (1974).

[29] Lehner, *J. Math. Mech.*, **11**, p.173, (1962).

[30] Montagnini, B., Pierpaoli, V., "The time-dependent rectilinear transport equation," *Transp. Theory and Stat. Phys.*, **1**: pp. 59-75 (1971).

[31] Nauchi, Y., "Attempt to estimate reactor period by natural mode eigenvalue calculation," To appear in *Proceedings of the SNA+MC 2013 conference*, Paris, France (2014).

[32] Nelkin, M., "Asymptotic solutions of the transport equation for thermal neutrons" *Physica*, **29**: pp. 261-273 (1963).

[33] Nikolaenco, B., Zweifel, P.F., "Neutron thermalization and Reactor spectra", *International Atomic Energy Agency*, Vienna, 1967

[34] Nolen, S.D., Adams, T.R., Sweezy, J.E., "Integral Criticality Estimators in MCATK(U)," LA-UR-12-25458 (2012).

[35] Pázsit, I., Pál, L., *Neutron Fluctuations: A Treatise on the Physics of Branching Processes*, Elsevier, Oxford (2008).

[36] Persson, C.M., et al., "Pulsed neutron source measurements in the subcritical ADS experiment YALINA-Booster," *Ann. Nucl. En.*, **35**: pp. 2357-2364 (2008).

[37] Pfeiffer, W., Brown, J.R., Marshall, A.C., "Fort St. Vrain startup test A-3: pulsed-neutron experiments," GA-A13079 (1974).

[38] Schmeidler, W., *Linear operators in Hilbert spaces*, Academic Press, New York (1965).

[39] Singh, K.P., Modak, R.S., Degweker, S.B., Singh, K., "Iterative schemes for obtaining dominant alpha-modes of the neutron diffusion equation," *Ann. Nucl. En.*, **36**: pp. 1086-1092 (2009).

[40] Singh, K.P., Modak, R.S., Degweker, S.B., Singh, K., "Iterative method for obtaining the prompt and delayed alpha-modes of the diffusion equation," *Ann. Nucl. En.*, **38**: pp. 1996-2004 (2011).

[41] Spanier, J., Gelbard, E.M., *Monte Carlo principles and neutron transport problems*, Dover Publications, INC., Mineola, New York (2008).

[42] TRIPOLI-4 Project Team, "TRIPOLI-4 ® User guide," Rapport CEA-R-6169 (2008).

[43] Weinberg, A. M., "Current status of nuclear reactor theory," *Am. J. Phys.*, **20**: pp. 401-412 (1952).

[44] Williams M.M.R. *The slowing down and thermalization of neutrons*, North-Holland, Amsterdam (1966).

[45] Yamamoto, T., "Higher order alpha mode eigenvalue calculation by Monte Carlo power iteration," *Progr. Nuc. Sci. Tech.*, **2**: pp. 826-835 (2011).

[46] Zoia, A., Dumonteil, E., Mazzolo, A., Mohamed, S., "Branching exponential flights: travelled lengths and collision statistics," *J. Phys. A: Math. Theor.*, **45**: pp. 425002 (2012).

[47] Zoia, A., Dumonteil, E., Mazzolo, A., "Properties of branching exponential flights in bounded domains," *Europhys. Lett.*, **100**: pp. 40002 (2012).

[48] Zoia, A., Brun, E., Malvagi, F., "Alpha eigenvalue calculations with TRIPOLI-4 ®," *Ann. Nucl. En.*, **63**: pp. 276-284 (2014).

[49] Zoia, A., Dumonteil, E., Mazzolo, A., "Residence time and collision statistics for exponential flights: the rod problem revisited," *Phys.Rev.*, E**84** 021139 (2011).

[50] Zoia, A., Brun, E., Malvagi, F., "A Monte Carlo method for prompt and delayed *alpha* eigenvalue calculations", *PHYSOR 2014- The Role of Reactor Physics toward a Sustainable Future*, (2014)

Appendix A

Spectral theory of operators

We here define the concept of an *eigenvalue* of an operator A. We usually refer to α as an eigenvalue of A if there exist nontrivial solutions to

$$A\,\psi_\alpha = \alpha\psi_\alpha. \tag{A.1}$$

Before talking about the eigenvalues α, it is necessary to decide just what class of functions are going to be allowed as eigenfunctions. This specification must usually be determined from the physics of the problem. When $\psi_\alpha(v)$ is going to be used in the calculation of a particle density $n(v,t)$, almost the only physical restriction we can demand is that the corresponding detector response is bounded and non-negative

$$0 \leq \int_0^\infty v\Sigma_d(v)\psi_\alpha(v)dv < \infty. \tag{A.2}$$

This specific class of functions is referred to as Banach class or space L^P. However, most authors [17] prefer to use the class of all square-integrable functions $f(v)$ such that

$$\int_0^\infty |f(v)|^2 dv < \infty. \tag{A.3}$$

This class is the Hilbert space of functions or space L^2. Hence even though physics demands a general function space such as a Banach space, mathematical convenience demands that we study instead the eigenvalues of operators A defined on a Hilbert space of functions. We trust that most of the results we obtain for such a function space will not be altered appreciably for a more general class of functions.

Now we study the spectral theory of operators that act on functions contained in the Hilbert space.

Linear operators on Hilbert space

A Hilbert space L^2 is (i) a linear vector space over the complex field, (ii) a metric space whose metric is defined from an inner product: $||f|| = [\int_0^\infty f(v) * f(v) dv]^{1/2}$, and (iii) a complete space (containing the limits of all Cauchy sequences).

Operators defined on a Hilbert space of functions

1. An operator A is a mapping of the function space L^2 into L^2;

2. the domain of an operator A, *D(A)*, is defined to be the class of all functions for which $A\,f$ is defined;

3. the range of an operator A, *R(A)*, is the set of functions generated by letting A act on all functions $f \in D(A)$;

4. we define the norm of an operator as $||A|| = \max\{||Af||/||f|| : f \in D(A)\}$; an operator is *bounded* if $||A|| < c$.

5. we define the *adjoint* $A^\dagger$ of an operator A by requiring that

$$(A^\dagger f, g) = (f, A\, g) \text{ for all } f \in D(A),\ g \in D(A^\dagger).$$

   An operator is *self-adjoint* if $A^\dagger = A$;

6. we denote with f_n a sequence of functions that converges to f, $f_n \to f$; an operator is *completely continuous* or *compact* if for f_n, $f \in D(A)$, $f_n \to f \Longrightarrow A\, f_n \to A\, f$;

7. to define the inverse of an operator A, consider the equation $A\, f = g$. Then we say that the inverse A^{-1} exists if for any g contained in the range $R(A)$, there exists a unique f such that $A\, f = g$, that is, we can solve $A\, f = g$ uniquely for f for any $g \in R(A)$.

With this background involving operators defined on a Hilbert space, we can proceed to study the eigenvalue problem $A\,\psi_\alpha = \alpha\psi_\alpha$.

The spectral theory of operators defined on a Hilbert space

The spectral theory of operators is approached in an indirect manner by considering the inhomogeneous problem

$$(A - \alpha)f = g \tag{A.4}$$

and looking for the values of α for which we have trouble inverting $(A - \lambda)$ to solve for f. The values of α for which this inhomogeneous problem is "singular" make up the eigenvalue "spectrum" of the operator A. First consider those values of α for which everything is well behaved, that is, the set of all α for which we can invert $(A - \alpha)$ to find f with no difficulty. This set of "nice" α is called the *resolvent set* and is defined as the set of all α for which:

1. $(A-\alpha)^{-1}$ exists;

2. $(A-\alpha)^{-1}$ is a bounded operator;

3. the closure of the range of $(A-\alpha)$, $R(A-\alpha) \equiv L^2$.

All the rest of the complex α-plane is defined to be in the *spectrum* of the operator A. From the three conditions necessary for α to be in the resolvent set, we can see that there are three possible types of spectrum:

- the *point spectrum* $\sigma_p(A)$. Those α for which $(A-\alpha)^{-1}$ does not exist;
- the *continuous spectrum* $\sigma_c(A)$. Those α for which $(A-\alpha)^{-1}$ exists, but $(A-\alpha)^{-1}$ is an unbounded operator;
- the *residual spectrum* $\sigma_r(A)$. Those α for which $(A-\alpha)^{-1}$ exists, but $R(A-\alpha)$ is a proper subset of the Hilbert space.

The point spectrum corresponds to what we have been calling discrete or point eigenvalues. The existence of a point spectrum implies that there must be some nontrivial ψ_α such that $A\,\psi_\alpha = \alpha\psi_\alpha$.

The continuous spectrum does not corresponds to the condition $A\,\psi_\alpha = \alpha\psi_\alpha$ and, indeed, reflects the unboundedness of $(A-\alpha)^{-1}$. It is more correct to say that, for $\alpha \in \sigma_c(A)$ there are no solutions ψ_α that are in the Hilbert space. However, there are solutions to this equation that lie outside the space but involve singularities such as delta functions or weak divergences.
Finally, we observe that the terms "point" and "continuous" are misleading because the concept of a point or continuous set does not enter into their definition. In fact, it is possible to have a point eigenvalue in the midst of a continuous spectrum (an "embedded" eigenvaue) and a $\alpha \in \sigma_c(A)$ that is

an isolated point (e.g., an eigenvalue of infinite multiplicity). Most of the time, however, $\sigma_p(A)$ corresponds to a point set and $\sigma_c(A)$ corresponds to a continuous set.
The residual spectrum $\sigma_r(A)$ usually does not arise in the transport theory applications. Our transport operators usually possess "enough symmetry" to avoid having a residual spectrum [17].

We conclude this discussion with some useful properties of the operators defined on the Hilbert space [38]

- a self-adjoint operator possesses a real spectrum $\sigma = \sigma_p + \sigma_c$;
- a completely continuous (compact) operator has only a point spectrum. (In this sens, the compact operator is the direct analogue to a matrix);
- a completely continuous self-adjoint operator possesses only a point spectrum, and it is also characterized by a complete, orthonormal set of eigenfunctions;
- adding a compact, self-adjoint operator B to another operator A does not change the continuous spectrum: $\sigma_c(A+B) = \sigma_c(A)$.